



Molluscan aminostratigraphy of the US Mid-Atlantic Quaternary coastal system: Implications for onshore-offshore correlation, paleochannel and barrier island evolution, and local late Quaternary sea-level history

John F. Wehmiller^{a,*}, Laura L. Brothers^b, Kelvin W. Ramsey^c, David S. Foster^b, C.R. Mattheus^c, Christopher J. Hein^d, Justin L. Shawler^d

^a Dept. of Earth Sciences, University of Delaware, Newark, DE, 19716, USA

^b U. S. Geological Survey, Coastal and Marine Science Center, Woods Hole, MA, 02543, USA

^c Delaware Geological Survey, University of Delaware, Newark, DE, 19716, USA

^d Virginia Institute of Marine Science, William & Mary, P.O. Box 1346, Gloucester Point, VA, 23062, USA

ARTICLE INFO

Keywords:

Quaternary sea-level
Delmarva peninsula
US Mid-Atlantic shelf
Paleovalley
Amino acid racemization
Geochronology
Age-mixing
Seismic stratigraphy
Mollusks

ABSTRACT

The Quaternary record of the US Mid-Atlantic coastal system includes onshore emergent late Pleistocene shoreline deposits, offshore inner shelf and barrier island units, and paleovalleys formed during multiple glacial stage sea-level lowstands. The geochronology of this coastal system is based on uranium series, radiocarbon, amino acid racemization (AAR), and optically stimulated luminescence (OSL) methods. We report over 600 mollusk AAR results from 93 sites between northeastern North Carolina and the central New Jersey shelf, representing samples from both onshore cores or outcrops, sub-barrier and offshore cores, and transported shells from barrier island beaches. AAR age estimates are constrained by paired ¹⁴C analyses on specific shells and associated U-series coral ages from onshore sites. AAR data from offshore cores are interpreted in the context of detailed seismic stratigraphy. The distribution of Pleistocene-age shells on the island beaches is linked to the distribution of inner shelf or sub-barrier source units. Age mixing over a range of time-scales (~1 ka to ~100 ka) is identified by AAR results from onshore, beach, and shelf collections, often contributing insights into the processes forming individual barrier islands. The regional aminostratigraphic framework identifies a widespread late Pleistocene (Marine Isotope Stage 5) aminozone, with isolated records of middle and early Pleistocene deposition. AAR results provide age estimates for the timing of formation of the three major paleochannels that underlie the Delmarva Peninsula: Persimmon Point paleochannel ≥800 ka; Exmore paleochannel ~400–500 ka (MIS 12); and Eastville paleochannel > 125 ka (MIS 6). The results demonstrate the value of synthesizing abundant AAR chronologic data across various coastal environments, integrating multiple distinct geologic studies. The ages and elevations of the Quaternary units are important for current hypotheses about relative sea-level history and crustal dynamics in the region, which was likely influenced by the Laurentide ice sheet, the margin just ~400 km to the north.

1. Introduction

The Quaternary units of the Delmarva Peninsula (Delaware, Maryland, and Virginia) on the US Mid-Atlantic margin (~37° to ~39.5°N) (Figs. 1–3) consist of multiple estuarine, open-bay, fluvial, barrier island and lagoonal deposits that have formed during multiple cycles of Quaternary sea-level change. Although ~400 km south of the Laurentide ice sheet, this region was influenced not only by glacial-interglacial sea

level changes but also by glacial isostatic adjustment (e.g., Potter and Lambeck, 2004; Pico et al., 2017), colder climate (e.g., French et al., 2009; Litwin et al., 2013), and fluvial drainage from the Laurentide (e.g., Reusser et al., 2004) and other rivers that constitute the Chesapeake Bay drainage.

The Virginia portion of the peninsula is underlain by four major paleochannels, formed during glacial stage low sea levels, whose positions track the southward progradation of the peninsula during the Quaternary (Colman et al., 1990; McFarland and Beach, 2019). These

* Corresponding author.

E-mail addresses: jwehm@udel.edu (J.F. Wehmiller), lbrothers@usgs.gov (L.L. Brothers), kwramsey@udel.edu (K.W. Ramsey), dfoster@usgs.gov (D.S. Foster), mattheus@illinois.edu (C.R. Mattheus), hein@vims.edu (C.J. Hein), jshawler@vims.edu (J.L. Shawler).

<https://doi.org/10.1016/j.quageo.2021.101177>

Received 1 December 2020; Received in revised form 19 February 2021; Accepted 8 March 2021

Available online 18 May 2021

1871-1014/Published by Elsevier B.V. This is an open access article under the CC BY license (<http://creativecommons.org/licenses/by/4.0/>).

Abbreviations

| | |
|-----------------|--|
| AAR | amino acid racemization |
| ¹⁴ C | carbon-14 or radiocarbon |
| GC | gas chromatography |
| IE | ion-exchange chromatography |
| RP | reverse-phase chromatography |
| D/L | the ratio of “dextro” (right-handed) to “levo” (left handed) amino acids |
| Delmarva | the peninsula of the US mid-Atlantic, including Delaware, Maryland, and Virginia |
| ka | kiloanno, age in thousand years or duration in thousand years |
| OSL | optically stimulated luminescence |
| U–Th | Uranium-thorium dating method |
| U-series | Uranium-thorium dating method |
| ASP | Aspartic acid, an abundant amino acid in most mollusk samples |
| GLU | Glutamic acid, an abundant amino acid in most mollusk samples |
| ALA | Alanine, a common amino acid in many mollusk samples |
| ILC | Interlaboratory comparison (refers to samples shared and analyzed by many AAR labs) |
| SER | Serine, an amino acid whose presence in large relative amounts is often indicative of sample contamination |

paleochannels, their filling units, and associated Pleistocene interfluvial and shoreline deposits, form the antecedent geology that has influenced the Quaternary history of the eastern Delmarva barrier islands, particularly those in Virginia (Oertel and Foyle, 1995; Oertel et al., 2008). The origin and age of sediments found within the barriers, back-barriers, and lagoons of Delmarva have significant implications for the late Quaternary relative sea-level history of the region (Colman et al., 1989; Finkelstein, 1992; Finkelstein and Kearney, 1988, 1989; Pico et al., 2017; Scott et al., 2010; Toscano, 1989). Prior offshore studies with relevant chronologic results include Toscano et al. (1989), Toscano (1992), Toscano and York (1992), Chen et al. (1995), and Williams (1999). Onshore stratigraphic and geomorphic studies include those of Mixon (1985), Colman and Mixon (1988), Colman et al. (1990), Powars and Bruce (1999), all reviewed by Krantz et al. (2016). Onshore Delmarva sites with chronologic data are described in Belknap (1979), Belknap and Wehmiller (1980), Wehmiller et al. (1988), Groot et al. (1990), York (1990), and Toscano and York (1992).

The present study seeks to refine the Quaternary geochronology of this coastal system, using amino acid racemization (AAR) results for mollusk samples from onshore (outcrop or subsurface units), barrier island and inner shelf vibracores, and transported beach shell samples. Data for each sample type establish a broad regional aminostratigraphic framework that is useful for offshore-onshore correlation, characterization of sediment transport processes and barrier island evolution, and establishing the timing of formation of the major paleochannels underlying the peninsula. The Delmarva paleochannels form a major component of the region's Quaternary stratigraphy because their formation and preservation involved glacial-stage low sea-level incision into older units and subsequent filling and transgression during interglacial-stage high sea levels. They are mapped throughout the Chesapeake Bay, onshore, and along the adjacent continental shelf where several coeval paleodrainage systems have been identified (Colman and Mixon, 1988; Oertel and Foyle, 1995; Brothers et al., 2020) (Fig. 3). Better constraints on the timing of the formation of Delmarva paleochannels would clarify the geochronology for a significant portion of the Mid-Atlantic Bight.

AAR data from beach shells collected from six barrier islands are used to assign either Pleistocene or Holocene ages to these shells (e.g., Wehmiller et al., 1995, 2015, Wehmiller et al., 2019a, 2019b). Shelly deposits on beaches are created by multiple interacting processes, such as sediment source variations and delivery rates, beach erosion and migration rates, storm frequency, and relative sea-level history (Freya and Dorjes, 1988; Rojas and Martínez, 2020 and references therein). The AAR results identify age-mixing at onshore, offshore and beach sites on time scales (~10³–10⁵ yrs) comparable to, and greater than, those observed in other coastal environments (Murray-Wallace et al., 1996; Kidwell et al., 2005; Nicholas et al., 2011; Kowalewski et al., 1998, 2000, 2018; Olszewski and Kaufman, 2015; Ryan et al., 2020). The large dataset created here helps to quantify the magnitude of age-mixing processes, which can otherwise be a serious issue if samples for geochronology are limited in number. In particular, the AAR data for beach shells are useful for understanding the role of sub-barrier units in barrier island evolution. The history of the eastern Delmarva barrier islands, particularly those in Virginia, has been reviewed by McBride et al. (2015), with more recent contributions by Deaton et al. (2017), Raff et al. (2018), and Shawler et al. (2019, 2020).

AAR age estimates are calibrated with associated coral uranium-series ages or paired ¹⁴C analyses on individual mollusks. More than 600 previously unreported AAR results, 35 ¹⁴C ages, and two uranium-series ages are reported, and we build upon and confirm the early work of Toscano et al. (1989) who used AAR to compare onshore data from the peninsula with offshore data from the Maryland inner shelf. Additionally, we incorporate newer AAR analytical methods into the study area to evaluate and, in some cases, reinterpret the earliest AAR results for onshore sites in the region (Belknap, 1979; Belknap and Wehmiller, 1980). With these newer methods we report multiple analyses from inner shelf vibracores that are linked to detailed seismic stratigraphy (Brothers et al., 2020).

In following sections, we combine beach and onshore AAR and ¹⁴C results to identify major aminozones (clusters of similar amino acid D/L values) for *Mercenaria* and *Spisula*, the taxa most commonly collected at these sites. We then link these aminozones to offshore AAR results that are based primarily on the taxon *Mulinia*, the most common mollusk found in the offshore cores. The intergeneric relative racemization rates for these three taxa are known from multiple field studies, particularly for *Mercenaria-Mulinia* (York et al., 1989; York, 1990; Wehmiller et al., 1988; 2010). Age estimates for the combined onshore/offshore aminozones are based on limiting ¹⁴C ages in selected cores, associated U-series coral ages (~75–85 ka) from onshore sites in Virginia and North Carolina, and age modeling that extends the AAR time scale for the region to the early Quaternary. Finally, we propose an age estimates for the major paleochannel systems that underlie the peninsula, testing the proposed chronology of Colman and Mixon (1988) and comparing AAR age estimates with existing U-series and optically-stimulated luminescence (OSL) ages. The results presented here refine our understanding of the earliest Delmarva AAR studies (Belknap, 1979; Belknap and Wehmiller, 1980) in the context of these paleochannels (Colman and Mixon, 1988; Colman et al., 1990; Hobbs, 2004; Powars, 2011; Krantz et al., 2016). These collective results provide insights into the AAR method itself, the reliability of shell radiocarbon ages, processes of shelf, shoreface and beach sediment transport, and the regional history of Quaternary sea-level change.

2. Sites and collection history

Samples used in this study were collected during early research on AAR geochronology of onshore units in the Delmarva-Chesapeake region (summary in Wehmiller et al., 1988; Groot et al., 1990; Wehmiller, 2013a) and, more recently, during offshore (core) and beach sampling efforts in the region. The offshore sites have been sampled as part of several projects, focused on understanding the regional geologic framework (Brothers et al., 2020; Mattheus et al., 2020a, b) and offshore

sand resources (Toscano et al., 1989; BOEM/ASAP). The collections and relevant sites are listed in Table 1 and plotted in Figs. 1–3; sample numbers from Table 1 are referred to in all subsequent text and are identified in Figs. 1–3. Beach collections were made between 1991 and 1994 on Parramore (60) and Wallops (42) islands and the first Parramore results, supplemented here, indicated a significant abundance of Pleistocene shells (Wehmiller et al., 2015). Subsequent beach collections were made on Cedar (57, 59) and Metompkin (46, 50) islands in 2006 and 2011, and finally on Wreck (71) and Smith (74) islands in 2015 and 2016. None of these islands experienced any artificial sand nourishment prior to the dates of our collections [PSDS, 2020]. Because of the remoteness of the Virginia Barrier Islands, beach shell collections were made by “volunteers” involved with other field projects, hence the collections do not represent an effort to collect at all sites at a single time or even to collect a time-series at a single site. Beach sample collections were usually made by gathering all whole shells within a 10 m × 10 m area of shell concentration. This approach is inherently biased toward those shells that are robust enough to survive intact within the nearshore environment, and it does not attempt to document faunal assemblages. Our emphasis is on the ages of the analyzed shells and their possible sources, rather than relating apparent age to taphonomic characteristics as in other studies (i.e., Davies et al., 1989; Powell et al., 1989; Wehmiller et al., 1995; Martin et al., 1996). Photographs of most of the beach shells used in this study are available in Appendix A. Because the

samples relevant to this study have been analyzed over a period of several decades (1992–2018), different analytical methods have been employed (Table 1). In a few cases, only results for the early analyses are reported, as no newer results are available, hence these earlier results are used to supplement our regional aminostratigraphic interpretations.

Many of the Delmarva subsurface samples re-analyzed here are from early collections made by colleagues at the U. S. Geological Survey (Belknap, 1979; Mixon, 1985). AAR results from five sites, CW-4 (38), Mathews Field (39), Exmore (66), Eyreville (69), and Cheriton East (94), constrain the ages of the Persimmon Point, Exmore and Eastville paleochannels. The Cheriton East samples are from a drill site whose location is not precisely known (other than being within the USGS Cheriton 1:24,000 quadrangle), but the site can be related to a published stratigraphic section (Mixon, 1985: fig. 18 and inset, Fig. 3). Samples from the original Maryland shelf project of Toscano et al. (1989) remained available for the current analytical effort. A few results for samples from the New Jersey shelf (sites 1–6) (Uptegrove et al., 2012; some re-interpreted by Miller et al., 2013a), although outside our primary study area, are relevant for regional comparisons of AAR data. All core and onshore samples are archived at the Delaware Geological Survey, and beach samples are archived at the Paleontological Research Institution, Ithaca NY.

Numerous stratigraphic terms have been applied to the sedimentary units sampled for this study, as summarized in Fig. 4. The purpose of this

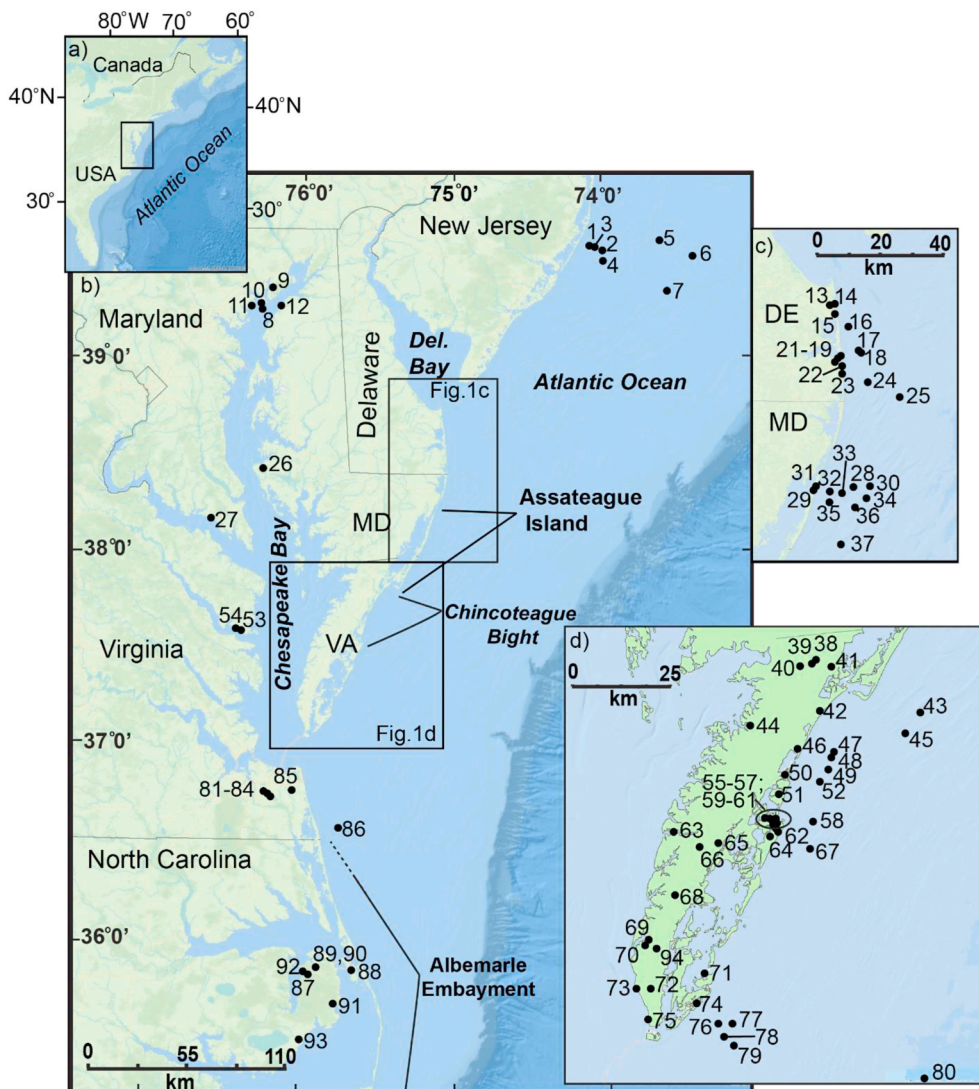


Fig. 1. Map of the Mid-Atlantic, USA with collection sites for samples discussed here labeled with dots (1b). Numbers on map refer to the site numbers listed in Table 1. Inset map a) shows study area location on the US Atlantic Margin. Inset maps c) and d) show closer views of the Delmarva Peninsula where samples were collected onshore, on beaches and on the continental shelves. Delaware and Maryland are shown in 1c and Virginia is shown in 1d. Land imagery and bathymetry are from World Base Ocean from ESRI, Garmin, GEBCO, NOAA, NGDC and other contributors.

figure is to present stratigraphic terminology as it is used in mapping local or regional sedimentary successions, rather than placing all these named units on a common time scale. Citations are included for available published stratigraphic sections, or for other relevant studies of the named units. Where possible, we include in Fig. 4 the identity of collection sites that represent the named stratigraphic unit.

3. Methods and results

The beach shells analyzed in this study are either *Mercenaria* or *Spisula* (Table 1). For purposes of age estimation, results for these two taxa are compared with results for the same taxa from either offshore or onshore sites. Because these taxa are not present at all sites (onshore or offshore), we also include AAR data from *Rangia*, *Astarte*, and *Mulinia* when appropriate. Data for these latter two taxa are particularly useful for discussion of the broader regional ¹⁴C-AAR dataset and its relation to offshore geophysical studies (Pendleton et al., 2015; Sweeney et al., 2015; Brothers et al., 2020). Only one site with ¹⁴C data (25) has AAR data for all four taxa. All AAR results are presented in Appendices B and C. Graphical presentations of the AAR data appear in following sections to demonstrate the relation of AAR results to specific stratigraphic sequences.

AAR samples were prepared using routine preparative methods involving mechanical and chemical (dilute HCl) cleaning to remove at least 20% of the shell carbonate, dissolution, hydrolysis (22 h), and

instrumental analysis using one of three methods: high-pressure ion-exchange liquid chromatography (IE), gas chromatography (GC), or reverse-phase liquid chromatography (RP). These methods are reviewed in (Wehmiller and Miller, 2000) for IE and GC and (Kaufman and Manley, 1998) for RP. In a few cases, samples were hydrolyzed for 6 instead of 22 h, so results from the analysis using the shorter hydrolysis time must be converted for comparison (Appendix B). For a variety of reasons, the three methods yield D/L values with varying reliabilities for different amino acids, hence numerical results from the three methods for a specific amino acid may differ (Wehmiller, 1984; 2013b). Results for several individual shells analyzed by multiple AAR methods are available (Appendix B).

Selected beach and offshore samples have associated radiocarbon ages (paired AAR and ¹⁴C analyses conducted on the same shell). Samples for ¹⁴C analysis were selected after AAR results became available so that a range of D/L values could be compared with the anticipated range in ¹⁴C ages. All samples submitted for ¹⁴C were fragments cut from the original shell after AAR analysis; fragments were cleaned with dilute acid and distilled water prior to submission for ¹⁴C analysis. One *Mercenaria* sample (JW2017-306, site 48) was subjected to a serial ¹⁴C analysis on progressive carbonate dissolution extracts of a single shell following removal of outer shell material to evaluate the possible effects of ¹⁴C contamination (incorporation of younger carbon) on Pleistocene-age samples. ¹⁴C results are cited below as they relate to ages inferred from AAR results obtained on the ¹⁴C-dated samples.

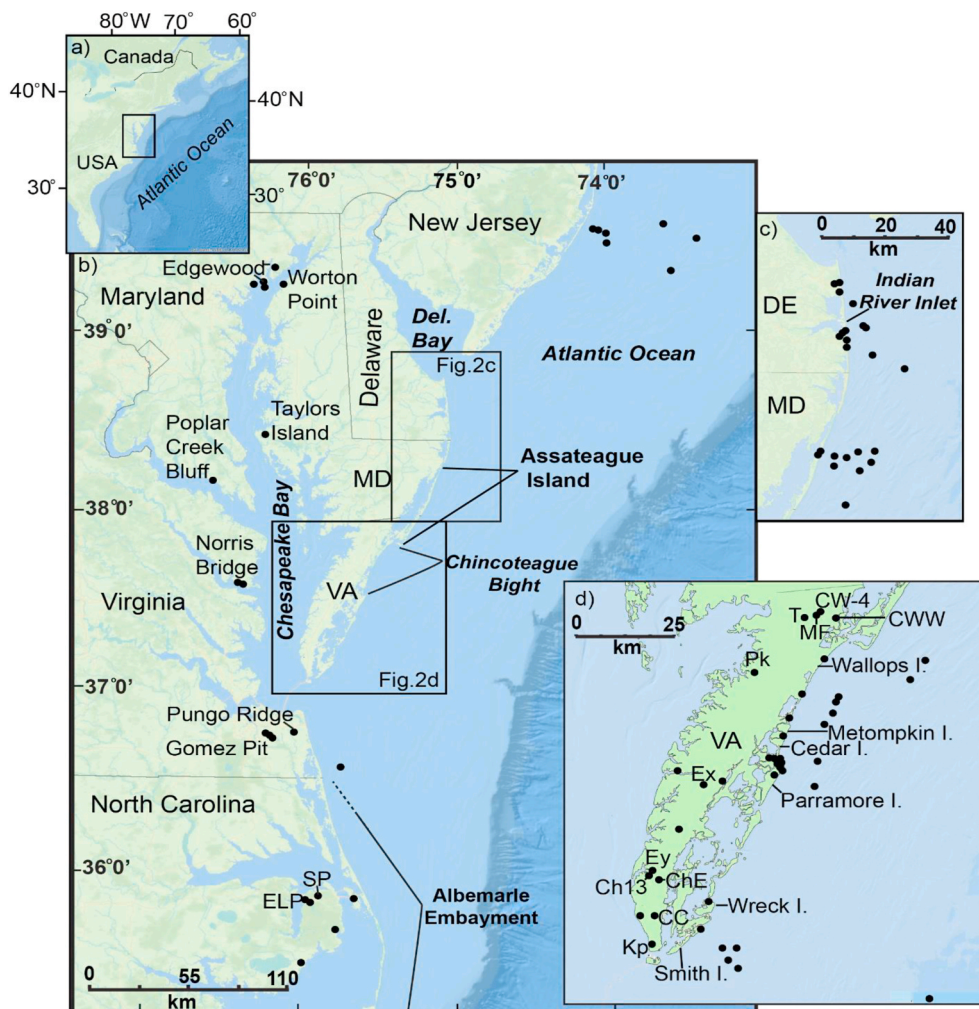


Fig. 2. Location map showing onshore collection sites and Virginia barrier islands (2d) referred to in the text. Labels are for selected onshore sites; dots represent all other sites. DE = Delaware, MD = Maryland, VA = Virginia, SP = Stetson Pit, ELP = East Lake Pit, CWW = Chincoteague Water Well, T = T's Corner, Pk = Parksley, Ex = Exmore, Ey = Eyreville, ChE = Cheriton East, Kp = Kiptopeake.

Two coral samples, from East Lake Pit, NC (site 87) were analyzed for their Uranium-series ages; data are shown in Table 2b. Coral samples were prepared, analyzed and interpreted using procedures described in Thompson et al. (2003); ages reported in Table 2b are based on half-lives reported in Cheng et al. (2013). The two coral samples are typical of those found in Coastal Plain sites (*Astrangia* and *Septastrea*), and photographs of the two analyzed corals are available in Appendix A. Cleaning of these samples can be challenging (Wehmiller et al., 2004; W. Thompson, pers. comm., 2012) because the samples are usually found buried in fine-grained muds, and the results in Table 2b show that even with careful cleaning the ²³²Th concentrations indicate significant levels of detrital contamination. The East Lake Pit coral ages fall in the late MIS 5 range, similar to many prior U-series coral results from northeastern North Carolina and southeastern Virginia, as summarized in Wehmiller et al. (2004; 2010). The U-series results for East Lake Pit are discussed below for their role as calibration for the regional aminostratigraphy.

The emphasis in this paper is on the AAR results obtained using the RP method; in almost all cases, conclusions about relative ages derived from prior IE or GC results are verified by the newer RP data. Quantitative results from the RP method are found in Appendix C for shell material and Appendix D for Interlaboratory Comparison Samples. Because different taxa not only have different racemization rates, but also have significant differences in the relative abundances of individual amino acids (examples in Appendix E), some D/L values are considered

more useful than others. Aspartic acid (hereafter ASP) is always the most abundant amino acid of those reported in this study (and ASP D/L values are well-resolved chromatographically by the RP method: Kaufman and Manley, 1998), so it is the primary focus for many discussions (especially involving *Mulinia*), supplemented with D/L data for glutamic acid (GLU), usually the next most abundant amino acid. The coefficients of variation for the D/L values of the two amino acids are almost always smaller (5–8%) than those for the other amino acids (see examples of *Mulinia* data, Appendix B). Trace amounts of asparagine and glutamine can decompose to ASP and GLU during diagenesis or sample preparation (Kaufman, 2006), potentially introducing some scatter in the D/L values observed for these two amino acids. Alanine (ALA) is abundant in most samples, but because ALA D/L values can be affected by the decomposition (to ALA) from other amino acids (e.g., Westaway, 2009; Miller et al., 2013b), this amino acid may be less useful for aminostratigraphic studies. Prior discussions of GC and IE results from this study area emphasized data for D/L leucine, D/L valine, and A/I (D-alloisoleucine/L-isoleucine). In those cases where multiple methods have been applied to individual samples, the earlier results from GC or IE were used to guide selection of the samples for later RP analysis. Appendix B also includes values for L-serine/L-aspartic acid concentrations (L-SER/L-ASP) (as determined by RP) as a measure of potential shell contamination with “young” (low D/L value) amino acids (Kaufman, 2006; Simonson et al., 2013). In the rare cases when samples are thought to be

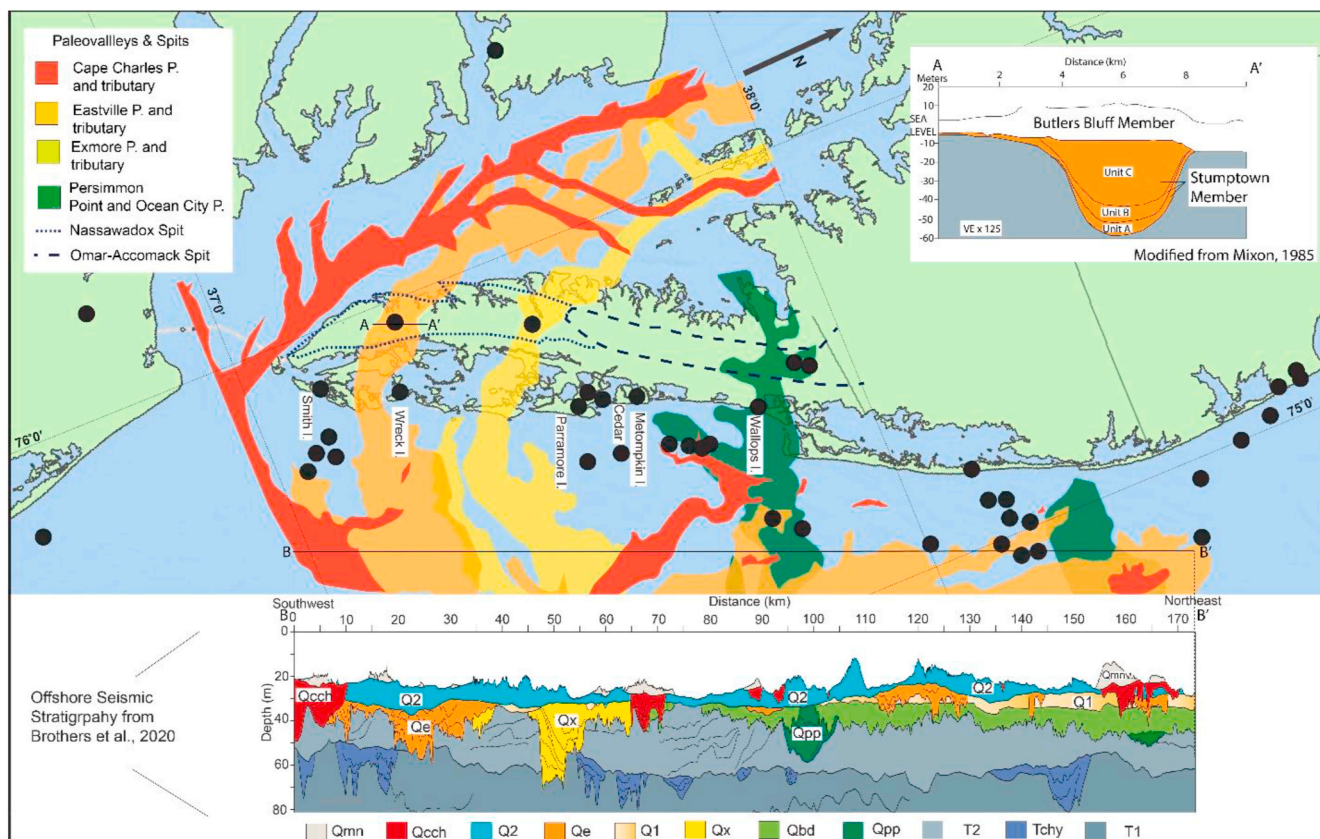


Fig. 3. Large spits and paleovalleys of the southern Delmarva Peninsula. Dots are collection sites for AAR analyses. Locations of the Persimmon Point, Exmore, Eastville, and Cape Charles paleovalleys or paleochannels and associated tributaries are from Mixon (1985), Colman et al. (1990), Oertel and Foyle (1995), Powars (2011), McFarland and Beach (2019), and Brothers et al. (2020). Cross-section A-A' depicts the Eastville Paleochannel as reported by Mixon (1985: Fig. 18), filled with the Stumptown member of the Nassawadox Formation and transgressed by the Butlers Bluff member of the Nassawadox Formation. Cross-section B-B' shows the offshore seismic stratigraphic section of Brothers et al. (2020: Fig. 5). The locations of the Omar-Accomack and Nassawadox spits, which form the upland spine of the Peninsula, are outlined by dashed lines as mapped by Mixon (1985) without the subdivisions proposed by Oertel and Foyle (1995). The Omar-Accomack extends from ~38° N south to the Exmore paleovalley and is younger than both the Persimmon Point and Exmore paleovalleys. The Nassawadox spit extends nearly to the southern end of the Peninsula, and is younger than the Eastville Paleochannel. Paleovalley margins mapped in Chesapeake Bay and offshore correspond to the ~30 m depth contour, or in the case of the deepest offshore channels the shallowest contour on the subaerial unconformities that define the paleochannels. Depth scale for the offshore section is related to mean sea level. All paleovalley delineations are limited by data availability.

Table 1

Sample collection sites. Site numbers in first column are plotted in Figs. 1 and 2. Columns 2, 3, and 4 list identifications used by the Delaware Geological Survey, informal names, and AAR database locality designations (AARDB: Wehmiller and Pellerito, 2015). Analytical methods used in this or prior studies of each site are listed, as are the number of individuals of each taxon analyzed, the rationale for using data from the specific site, and prior publications related to the site. Method abbreviations: RP = Reverse-phase liquid chromatography; GC = Gas chromatography; IE = Ion-exchange liquid chromatography (often identified as “HPLC” for high-pressure liquid chromatography). “This work” refers to the RP data not previously published. RP* = GC and/or IE data already published and not included here unless necessary. Appendix F contains core logs and detailed discussion for sites 25, 32, 33, 37, 47–49, 52, and 76. Numerous collections have been made at Gomez Pit, Virginia Beach, VA (sites 81–84); these are summarized in the cited references and with maps and photographs at the University of Delaware Institutional Repository.

| Map # | DGSID | Site name | AARDB ID | Lat | Lon | Surface Elev., m | Collection type | Analytical methods | 14C | Astarte | Mercenaria | Mulinia | Spisula | Rangia | Other | Reference | Rationale for inclusion in paper |
|-------|----------------------|------------------------------|----------|--------|---------|------------------|---------------------|--------------------|-----|---------|------------|---------|---------|--------|-------|--------------------------------|---|
| 1 | Du15-01 | New Jersey shelf Core 12 | 05166 | 39.652 | -74.084 | -20.6 | Offshore core | RP* | | 1 | | | 3 | | | Uptegrove et al. (2012) | Regional comparison of AAR data |
| 2 | Dv22-01 | New Jersey shelf Core 17a/R2 | 05168 | 39.645 | -74.051 | -19.6 | Offshore core | RP* | | | | | 1 | | | Uptegrove et al. (2012) | Regional comparison of AAR data |
| 3 | Dv11-01 | New Jersey shelf Core 13 | 05169 | 39.652 | -74.073 | -15.46 | Offshore core | RP* | | | | | 1 | | | Uptegrove et al. (2012) | Regional comparison of AAR data |
| 4 | Dv53-01 | New Jersey shelf Core 18 | 05170 | 39.598 | -74.039 | -18.63 | Offshore core | RP* | | | | | 1 | | | Uptegrove et al. (2012) | Regional comparison of AAR data |
| 5 | na | 313 site 27 | 05291 | 39.634 | -73.622 | -33.5 | Offshore core | GC | | | 1 | | 1 | | | (Miller et al., 2013a) | Regional comparison of AAR data |
| 6 | na | 313 site 29 | 05292 | 39.520 | -73.413 | -35.9 | Offshore core | GC | 1 | 2 | 1 | | 1 | | 2 | (Miller et al., 2013a) | Regional comparison of AAR data |
| 7 | Zz63-137 | AMCOR 6020 | 06080 | 39.424 | -73.594 | -39 | Offshore core | IE RP | | 1 | | | | | 1 | Sheridan et al. (2000) | Regional comparison of AAR data |
| 8 | Zz63-555 | Edgewood Arsenal #81 | 05095 | 39.301 | -76.290 | 3.05 | Excavation/Exposure | IE RP | | | | | | 5 | | This work; Dunbar et al., 2001 | Paleochannel discussion |
| 9 | Zz63-ai | Edgewood APG pit | 05140 | 39.397 | -76.243 | 2 | Excavation/Exposure | IE | | | | | | 2 | | This work; Dunbar et al., 2001 | Paleochannel discussion |
| 10 | Zz63-550 | Edgewood-OE-3 | 05145 | 39.325 | -76.292 | 10.6 | Inland core | IE RP | | | | | | 5 | | This work; Dunbar et al., 2001 | Paleochannel discussion |
| 11 | | Carroll Island | 05096 | 39.320 | -76.346 | 1 | Inland core | IE | | | | | | 2 | | This work; Dunbar et al., 2001 | Paleochannel discussion |
| 12 | Zz63-595, -596, -597 | Worton Pt | 05009 | 39.309 | -76.177 | 4 | Inland core | GC | | | | | | 4 | | Belknap (1979) | Paleochannel discussion; indirect 14C control |
| 13 | Oj11-05 | REB-1 | 05227 | 38.737 | -75.081 | 2.12 | Inland core | GC RP (6) | | | | 5 | | | | Ramsey (2011) | Lynch Heights Formation |
| 14 | Oi25-39 | REB-6 | 05228 | 38.733 | -75.092 | 6.1 | Inland core | GC RP (6) | | | | 5 | | | | Ramsey (2011) | Lynch Heights Formation |
| 15 | Oj31-14 | Silver Lake SB1 | 05212 | 38.708 | -75.081 | 3.05 | Inland core | GC RP | | | | 4 | | | | Ramsey (2011) | Lynch Heights Formation |
| 16 | Oj53-02 | DGS07-17 | 05268 | 38.671 | -75.038 | -12.2 | Offshore core | GC | 1 | | 1 | | | | | (Mattheus et al., 2020a,b) | Shoal deposits |
| 17 | Pj45-01 | DGS92-02 | 05119 | 38.607 | -75.008 | -12.5 | Offshore core | IE RP | 1 | | | 2 | 2 | | 1 | | Sheet sand deposits |

(continued on next page)

Table 1 (continued)

| Map # | DGSID | Site name | AARDB ID | Lat | Lon | Surface Elev., m | Collection type | Analytical methods | 14C | Astarte | Mercenaria | Mulinia | Spisula | Rangia | Other | Reference | Rationale for inclusion in paper |
|-------|----------|---------------------|----------|--------|---------|------------------|----------------------|--------------------|-----|---------|------------|---------|---------|--------|-------|---|--|
| 18 | Pj42-a | Indian River Inlet | 05107 | 38.605 | -75.006 | -1 | Beach | IE | | | 6 | | | | | Williams, 1999; (Mattheus et al., 2020a,b) Wehmiller et al. (1995) | prior data; no new data; for discussion only |
| 19 | Qj22-06 | KAM-NOV-80 | 05018 | 38.559 | -75.058 | 1.5 | Inland core | RP* | | | | 3 | | | | Ramsey and Tomlinson (2012) | Sinepuxent Formation |
| 20 | Qj32-27 | Bethany Beach Core | 05297 | 38.549 | -75.063 | 1.4 | Inland core | RP (6) | | | | 3 | | | | McLaughlin et al. (2008) | Sinepuxent Formation |
| 21 | Qj 31-20 | BEB-17 | 05309 | 38.543 | -75.074 | 0.6 | Inland core | RP | | | | 10 | | | | Ramsey (2010) | Sinepuxent Formation |
| 22 | Qj32-10 | Bethany #3 | 05296 | 38.538 | -75.059 | -35.9 | Inland core | RP (6) | | | | 3 | | | | Ramsey and Tomlinson (2012) | Sinepuxent Formation |
| 23 | Qj42-07 | KAM-MB-80-8 | 05020 | 38.525 | -75.054 | 3 | Inland core | RP (6)* | | | | 6 | | | | Ramsey and Tomlinson (2012) | Sinepuxent Formation |
| 24 | Qk53-03 | Qk53-03 | 05183 | 38.514 | -74.960 | -14.76 | Offshore core | RP | 1 | | | 3 | | | | McLaughlin et al. (2020a,b) | Sheet sand deposits |
| 25 | Rl25-01 | DGS92-16 | 05130 | 38.475 | -74.840 | -23 | Offshore core | IE GC RP | 4 | 12 | 4 | 8 | 3 | | | Williams (1999); McLaughlin et al. (2020a,b) | Marine shelf deposits |
| 26 | Zz63-548 | DCMD Taylors Island | 05007 | 38.479 | -76.277 | 1 | Inland core | GC RP | | | | | | 4 | | Jacobs, 1980; Groot et al., 1990; Genau et al., 1994; this work | Paleochannel discussion |
| 27 | Zz63-ag | Poplar Creek Bluff | 05001 | 38.212 | -76.586 | 3.7 | Excavation/ Exposure | GC IE RP | | | | | | 2 | | Belknap, 1979; Wehmiller et al., 1988; this work | Paleochannel discussion |
| 28 | Uj35-03 | MD-BOEM-15-03A | 05380 | 38.207 | -75.011 | -21 | Offshore core | RP | 1 | 1 | 4 | | | | | This work | |
| 29 | Ui31-01 | ASSGO2 | 06286 | 38.204 | -75.153 | 1.74 | Barrier island core | RP | | | | 5 | | | | Shawler et al., 2019; this work | Sinepuxent Formation ? |
| 30 | Uk33-01 | MGS-16-1002 | 05056 | 38.203 | -74.952 | -21 | Offshore core | IE RP | 1 | 2 | | | 1 | | | Toscano et al., 1989; York, 1990 | previous AAR work; multiple samples |
| 31 | Ui41-01 | Tingles Island | 05004 | 38.194 | -75.158 | 1.5 | Barrier island core | RP* | | | | 3 | | | | Toscano et al., 1989; York, 1990 | sub-barrier comparison site; Sinepuxent Fm? |
| 32 | Uj45-01 | MGS-18-1248 | 05063 | 38.187 | -75.098 | -16.5 | Offshore core | IE RP | | | | 14 | 5 | 1 | | Toscano et al., 1989; York, 1990 | prior evidence of two aminozones (IE data) |
| 33 | Uj42-01 | MGS-18-1230 | 05062 | 38.184 | -75.056 | -19.5 | Offshore core | IE RP | | | 1 | 11 | 4 | 2 | | Toscano et al., 1989; York, 1990 | prior evidence of two aminozones (IE data) |
| 34 | Uk53-01 | MGS-18-1142 | 05060 | 38.174 | -74.961 | -18.9 | Offshore core | IE RP | 2 | | 1 | | 2 | 3 | | Toscano et al., 1989; York, 1990 | previous AAR work; multiple samples |
| 35 | Vi14-01 | Vi14-01 | 05393 | 38.161 | -75.107 | -13.2 | Offshore core | RP | | | | 5 | | 1 | | This work | |
| 36 | Vk21-01 | MGS-20-1430 | 05065 | 38.148 | -74.999 | -18.9 | Offshore core | IE RP | 1 | 2 | | 5 | 2 | 1 | | Toscano et al., 1989; York, 1990 | previous AAR work; multiple samples |
| 37 | Wj32-01 | MGS-27-1520 | 05075 | 38.035 | -75.055 | -16.8 | Offshore core | IE RP | | 1 | | 20 | 1 | | | Toscano et al., 1989; York, 1990 | |

(continued on next page)

Table 1 (continued)

| Map # | DGSID | Site name | AARDB ID | Lat | Lon | Surface Elev., m | Collection type | Analytical methods | 14C | Astarte | Mercenaria | Mulinia | Spisula | Rangia | Other | Reference | Rationale for inclusion in paper |
|-------|----------|-------------------------------|----------|--------|---------|------------------|---------------------|--------------------|-----|---------|----------------|---------|---------|--------|-------|--|--|
| 38 | Xe31-01 | CW-4 | 06009 | 37.955 | -75.492 | 6.71 | Inland core | GC RP* | | | (2gc)1 (rp) | | | | | Belknap, 1979; Belknap and Wehmiller, 1980; Mixon et al., 1982, Fig. 5; Mixon, 1985: ~ H27 | previous AAR work; multiple samples prior data; relates to Delmarva paleochannel history |
| 39 | Xd45-01 | MF | 06004 | 37.949 | -75.500 | 4.57 | Inland core | GC RP* | | | (3 gc) 3 (rp) | | | | | Mixon, 1985: H-27; Mixon et al., 1982, Fig. 5; Belknap, 1979; Belknap and Wehmiller, 1980 | prior data; relates to Delmarva paleochannel history |
| 40 | Xd43-01 | Ts Corner (T's) | 06002 | 37.946 | -75.541 | 7.5 | Inland core | GC RP* | | | (20 gc) 3 (rp) | | | | | Mixon, 1985: H-8; Mixon et al., 1982, Fig. 5; Belknap, 1979; Belknap and Wehmiller, 1980 | prior data; relates to Delmarva paleochannel history |
| 41 | Xe43-01 | CWW - Chincoteague Water Well | 06007 | 37.944 | -75.453 | 7 | Inland core | GC | | | 1 | | | | | Belknap, 1979; Belknap and Wehmiller, 1980 | prior data; relates to Delmarva paleochannel history; Tertiary age beach collection |
| 42 | Ye51-a | Wallops June 1994 | 06203 | 37.839 | -75.483 | ~1 | Beach | IE | | | 11 | | | | 2 | This work | |
| 43 | Yh54-01 | VA-BOEM-2017-03 | 06270 | 37.839 | -75.199 | -20.8 | Offshore core | RP | | | | 1 | 3 | | 1 | This work | |
| 44 | Zb24-01 | Parksley (Pk) | 06008 | 37.808 | -75.684 | 0.91 | Inland core | GC RP* | | | (2 gc) (2 rp) | | | | | Mixon, 1985: P-11; Belknap, 1979 | prior data; relates to Delmarva paleochannel history |
| 45 | Zh31-01 | VA-BOEM-2015-08 | 06254 | 37.793 | -75.245 | -20.67 | Offshore core | RP | 1 | | | 1 | 3 | | | This work | |
| 46 | Zz82-dw | Metompkin 2 May 2011 | 06234 | 37.752 | -75.548 | ~1 | Beach | RP | | | 15 | | | | | This work | beach collection |
| 47 | Zz82-68 | VA-BOEM-2016-11 | 06262 | 37.744 | -75.443 | -14.51 | Offshore core | RP | 1 | 2 | | 12 | | | 1 | This work | 82-68 and 82-69 multiple samples; evidence of multiple ages |
| 48 | Zz82-69 | VA-BOEM-2016-02 | 06263 | 37.736 | -75.448 | -15 | Offshore core | RP | 1 | 4 | | 21 | | | | This work | |
| 49 | Zz92-92 | VA-BOEM-2017-14 | 06281 | 37.710 | -75.459 | -13.1 | Offshore core | RP | | | 2 | 7 | | | | This work | |
| 50 | Zz82-dx | Metompkin 1 May 2011 | 06233 | 37.694 | -75.584 | ~1 | Beach | RP | | | 15 | | | | | This work | beach collection |
| 51 | Zz82-102 | CEDGO1 | 06287 | 37.655 | -75.596 | 2.26 | Barrier island core | RP | | | | 4 | | | | Shawler et al., 2019; this work | |
| 52 | Zz82-71 | VA-BOEM-2016-04 | 06265 | 37.677 | -75.483 | -15.7 | Offshore core | RP | 1 | 3 | | | 2 | | | This work | Merc-Spis-Ast comparison |
| 53 | Zz82-e | Norris Bridge (NB) | 06000 | 37.632 | -76.408 | 9.15 | Excavation/Exposure | RP* | | | 5 | | | | 1 | Belknap, 1979; Mixon et al., | Prior data; onshore |

(continued on next page)

Table 1 (continued)

| Map # | DGSID | Site name | AARDB ID | Lat | Lon | Surface Elev., m | Collection type | Analytical methods | 14C | Astarte | Mercenaria | Mulinia | Spisula | Rangia | Other | Reference | Rationale for inclusion in paper |
|-------|----------|--|----------|--------|---------|------------------|-------------------------|--------------------|-----|---------|------------|---------|---------|--------|-------|---|--|
| 54 | Zz82-f | RRB | 06018 | 37.638 | -76.414 | 3.96 | Excavation/ Exposure | RP* | | | | | | 1 | | 1982, Fig. 4; Mirecki, 1985; Wehmiller et al., 1988 Belknap, 1979; Wehmiller et al., 1988 | comparison site; includes 06107 RRB-E Zz82-t prior data |
| 55 | Zz82-103 | CEDVO3 | 06288 | 37.600 | -75.641 | 0.52 | Barrier island core | RP | | | | 4 | | | | Shawler et al., 2019; this work | |
| 56 | Zz82-104 | CEDGO4 | 06289 | 37.595 | -75.620 | -0.06 | Barrier island core | RP | | | | 8 | | | | Shawler et al., 2019; this work | |
| 57 | Zz82-dy | Cedar Island shell 1: October 2006 | 06228 | 37.594 | -75.614 | ~1 | Beach | RP | | | 15 | | | | | This work | beach collection |
| 58 | Zz82-94 | VA-BOEM- 2017-16 | 06283 | 37.590 | -75.502 | -9.6 | Offshore core | RP | | 1 | | 3 | | | | This work | |
| 59 | Zz82-dz | Cedar Island Oyster: October 2006 | 06227 | 37.582 | -75.612 | ~1 | Beach | RP | | | 13 | | 2 | | | This work | beach collection |
| 60 | Zz82-r | North Parramore April 1991 | 06196 | 37.581 | -75.612 | ~1 | Beach | IE GC RP | 1 | | 1 | | | 1 | | This work; Wehmiller et al., 2015; cited in Miller et al., 2013b | beach collection |
| 61 | Zz82-s | North Parramore November 1993 | 06202a | 37.577 | -75.610 | ~1 | Beach | IE RP | | | 16 | | | | | This work; Wehmiller et al., 2015; cited in (Miller et al., 2013a) | beach collection |
| 62 | Zz82-dr | North Parramore November 1993 | 06202c | 37.572 | -75.600 | ~1 | Beach | RP | | | 25 | | 4 | | | This work; Wehmiller et al., 2015; cited in (Miller et al., 2013a) | beach collection |
| 63 | Zz82-34 | SN (Mixon J- 24) | 06012 | 37.566 | -75.900 | 2.7 | Inland core | RP* | | | 1 | | | | | Belknap, 1979; Mixon, 1985; Wehmiller et al., 1988; Toscano et al., 1989; Groot et al., 1990; this work | onshore reference site; Delmarva paleoshoreline unit |
| 64 | Zz82-100 | PARGO4 | 06285 | 37.559 | -75.624 | 0.5 | Barrier island core | RP | (x) | | | 6 | | | | This work; Raff et al., 2018 | sub-barrier comparison site |
| 65 | Zz82-33 | BN | 06013 | 37.544 | -75.771 | 0.9 | Inland core | GC, IE | | | | 3 | | 1 | | Belknap, 1979; Toscano et al., 1989; Groot et al., 1990 | Delmarva paleoshoreline unit |
| 66 | Zz82-111 | Exmore core | 05081 | 37.53 | -75.820 | 9 | Inland core | IE RP | | | | 17 | | | | Powars and Bruce, 1999; this work | mid-Pleistocene paleochannel fill |
| 67 | Zz82-87 | VA-BOEM- 2017-09 | 06276 | 37.527 | -75.514 | -9.1 | Offshore core | RP | 1 | | | | 1 | | | This work | Holocene 14C calibration |
| 68 | Zz82-35 | F-30 | 06010 | 37.416 | -75.898 | 9.8 | Inland core | GC RP | | | 1 | | | | | Belknap, 1979; Mixon, 1985; | onshore comparison site; |

(continued on next page)

Table 1 (continued)

| Map # | DGSID | Site name | AARDB ID | Lat | Lon | Surface Elev., m | Collection type | Analytical methods | 14C | Astarte | Mercenaria | Mulinia | Spisula | Rangia | Other | Reference | Rationale for inclusion in paper |
|-------|---------|-----------------------|----------|--------|---------|------------------|---------------------|--------------------|------|---------|------------|---------|---------|--------|-------|--|---|
| 69 | Zz82-21 | Eyreville cores C & D | 06261 | 37.321 | -75.975 | 2.4 | Inland core | RP | | | | 14 | | | 5 | Wehmiller et al., 1988; this work T. M. Cronin and R. Poirier (USGS), pers. comm; Browning et al., 2009 | prior data; Delmarva paleoshoreline unit Pleistocene paleochannel fill |
| 70 | Zz82-36 | Ch13 (Mixon Ch-13) | 06011 | 37.300 | -75.984 | 4.3 | Inland core | GC RP | | | 1 | 3 | | | | Belknap, 1979; Mixon, 1985; Wehmiller et al., 1988; this work | onshore comparison site; prior data; Delmarva paleoshoreline unit |
| 71 | Zz82-i | Wreck Island May 2015 | 06236 | 37.243 | -75.800 | -1 | Beach | RP | 2 | | | | 16 | | | This work | beach collection |
| 72 | Zz82-37 | CC (Mixon T-15) | 06014 | 37.211 | -75.966 | 11.6 | Inland core | RP* | | | 2 | | | | | Mixon, 1985; Wehmiller et al., 1988; Groot et al., 1990; this work | onshore comparison site; prior data |
| 73 | Zz82-38 | EC-1 (Mixon EC-1) | 06015 | 37.207 | -76.008 | 2.5 | Inland core | RP* | | | 1 | | | | | Mixon, 1985; Wehmiller et al., 1988; Groot et al., 1990; this work | onshore comparison site; prior data |
| 74 | Zz82-v | Smith Island May 2016 | 06251 | 37.175 | -75.835 | -1 | Beach | RP | 6 | | 15 | | 16 | | | This work | beach collection |
| 75 | Zz82-60 | Kiptopeake | 06204 | 37.138 | -75.965 | 7.6 | Inland core | IE RP | | | 2 | 8 | 3 | | | Powars and Bruce, 1999; this work | onshore comparison site; prior data |
| 76 | Zz82-85 | VA-BOEM-2017-07 | 06274 | 37.131 | -75.775 | -11.3 | Offshore core | RP | | | 1 | 6 | 2 | | | This work | |
| 77 | Zz82-86 | VA-BOEM-2017-08 | 06275 | 37.129 | -75.731 | -13.1 | Offshore core | RP | | | | 1 | 2 | | | This work | |
| 78 | Zz82-84 | VA-BOEM-2017-06 | 06273 | 37.103 | -75.756 | -12.3 | Offshore core | RP | | | | 6 | | | | This work | |
| 79 | Zz82-83 | VA-BOEM-2017-05 | 06272 | 37.079 | -75.730 | -14.9 | Offshore core | RP | 1 | | 1 | 2 | | | | This work | |
| 80 | Zz82-59 | USGS-1423 | 05225 | 37.009 | -75.180 | -39.6 | Offshore core | RP | 5 | 2 | 1 | | 8 | | | Leupke, 1990 | Holocene 14C calibration |
| 81 | Zz82-g | Gomez Pit | 06076a | 36.785 | -76.199 | 7 | Excavation/Exposure | IE GC RP | U-Th | | 2 | | | | | Mirecki et al., 1995; O'Neal et al., 2000 | onshore comparison site; prior data |
| 82 | Zz82-g | Gomez Pit | 06076b | 36.785 | -76.199 | 7 | Excavation/Exposure | IE GC RP | | | 2 | | | | | Mirecki et al., 1995; O'Neal et al., 2000 | onshore comparison site; prior data |
| 83 | Zz82-1 | Gomez Pit | 06058 | 36.783 | -76.198 | 7 | Excavation/Exposure | IE GC RP | | | | 2 | 2 | | | Mirecki et al., 1995; O'Neal et al., 2000 | onshore comparison site; prior data |
| 84 | Zz82-m | Gomez Sept 95 MS#2 | 06212 | 36.781 | -76.197 | 7 | Excavation/Exposure | IE GC RP | | | 2 | | 2 | | | Mirecki et al., 1995; O'Neal et al., 2000 | onshore comparison site; prior data |

(continued on next page)

Table 1 (continued)

| Map # | DGSID | Site name | AARDB ID | Lat | Lon | Surface Elev., m | Collection type | Analytical methods | 14C | Astarte | Mercenaria | Mulinia | Spisula | Rangia | Other | Reference | Rationale for inclusion in paper |
|-------|---------|--------------------|----------|--------|---------|------------------|---------------------|--------------------|-----|---------|------------|---------|---------|--------|-------|---|---|
| 85 | Zz82-ap | PR#1 | 06192 | 36.745 | -76.020 | 5.2 | Excavation/Exposure | IE GC RP | | | 14 | | 24 | | | Darby, 1983;(Darby and Evans, 1992) (Pungo Ridge) | onshore comparison site; prior data indicating age mixing |
| 86 | Zz82-63 | VA-BOEM-2015-01 | 06258 | 36.602 | -75.804 | -14.8 | Offshore core | RP | 1 | | | 1 | 1 | | | This work | |
| 87 | na | East Lake Pit | 07556 | 35.888 | -75.959 | 1 | Excavation/Exposure | RP* | | | | 7 | | | | Wehmiller et al., 2010; Parham et al., 2013 | onshore comparison site; prior data |
| 88 | Zz62-05 | CS80 | 07118 | 35.873 | -75.650 | 1 | Inland core | IE GC RP | 1 | | 1 | 3 | 1 | | | York, 1990; Riggs et al., 1992; this work | onshore comparison site; prior data |
| 89 | na | Stetson Pit core 1 | 07077 | 35.864 | -75.859 | -0.5 | Inland core | RP* | | | | 3 | | | | York et al., 1989; Riggs et al., 1992; Wehmiller et al., 2010 | onshore comparison site; prior data |
| 90 | na | Stetson Pit core 2 | 07127 | 35.864 | -75.859 | -0.5 | Inland core | RP* | | | | 9 | | | | York et al., 1989; Riggs et al., 1992; Wehmiller et al., 2010 | onshore comparison site; prior data |
| 91 | na | MLD-05 | 07572 | 35.698 | -75.771 | 1.8 | Inland core | RP* | | | | 3 | | | | Wehmiller et al. (2010) | onshore comparison site; prior data |
| 92 | na | MLD-06 | 07707 | 35.897 | -75.971 | 1.25 | Inland core | RP* | | | | 3 | | | | Wehmiller et al. (2010) | early Pleistocene reference loc |
| 93 | na | MLD-01 | 07534 | 35.509 | -76.001 | 0.22 | Inland core | RP* | | | | 3 | | | | Wehmiller et al. (2010) | early Pleistocene reference loc |
| 94 | na | Cheriton East | 06310 | 37.280 | -75.950 | -9.5 | Inland core | RP | | | | 12 | | | | Mixon, 1985: assumed = Ch-14 or Ch-15 | Paleochannel discussion |

Onshore lithostratigraphic units

Southeastern Virginia and northeastern North Carolina

| | | | |
|----------------------------|--|-------------------------------|--|
| | <i>Mixon et al., 1989; Mirecki et al., 1995 Scott et al., 2010; Mixon et al., 1982</i> | <i>Mallinson et al., 2008</i> | |
| Tabb Fm | Poquoson Mbr Lynnhaven Mbr Sedgefield Mbr (81-84) | | <i>York et al., 1989 Wehmiller et al., 2010 Mallinson et al., 2010 Culver et al., 2008; 2011; 2016 Parham et al., 2013 Multiple un-named units in superposition in the Albemarle Embayment (87-93)</i> |
| Shirley Formation (53, 54) | | | |

Virginia portion of Delmarva

| | | | |
|---|---|---|--|
| | <i>Mixon, 1985; Colman and Mixon, 1988 Mixon et al., 1982</i> | | |
| High-stand shoreline (various named scarps) | | | |
| Wachapreague Fm (51, 55, 56, 64, 65) | Kent Island Fm | | |
| High-stand shoreline (various named scarps) | | | |
| Joynes Neck Sand | Nassawadox Fm, Ocohanock Mbr | | |
| High-stand shoreline (various named scarps) | | | |
| Nassawadox Fm | Butler's Bluff Mbr Stumptown Mbr C Stumptown Mbr B Stumptown Mbr A | Overlying Eastville paleochannel (63,65,66,70,72,73,75) Eastville Paleochannel fill (69, 94) | |
| Incision of Eastville paleovalley | | Accomack member, Omar Fm (southern portion Omar-Accomack split) | |
| Incision of Exmore paleovalley | Exmore Paleochannel fill (66) <i>(Powars and Bruce 1999)</i> | Accomack member, Omar Fm (northern portion Omar-Accomack split) (38-40, 44) | |
| Incision of Persimmon Point paleovalley | Persimmon Point Paleochannel Fill <i>(Powars 2011)</i> | | |

Maryland and Delaware portion of Delmarva

| | | | |
|--|---|---|---|
| Maryland (<i>Owens and Denny, 1978</i>) | Delaware Atlantic Coast (<i>Ramsey, 2010</i>) | Delaware Bay and Atlantic inland bays (<i>Ramsey, 2010</i>) | Delaware Offshore (<i>Mattheus et al., 2020</i>) |
| | | | Incision of paleovalleys filled with Holocene sediments |
| Sinepuxent Fm (29, 31) | Sinepuxent Fm (19, 21-23) | Scotts Corner Fm (younger) | Sinepuxent Fm./Quaternary marine deposits |
| Ironshire Fm | Ironshire Fm | Scotts Corner Fm (older) | Quaternary marine deposits |
| Omar Fm | Omar Fm | Lynch Heights Fm (younger) | |
| <i>Omar Fm not subdivided in Maryland by Owens and Denny, 1978</i> | | | |
| Omar Fm | Omar Fm | Lynch Heights Fm (older) (13-15) | Omar Fm and Lynch Heights Fm paleovalley fill |
| Incision of Omar paleovalley | Incision of Omar paleovalley | Incision of Lynch Heights paleovalley | Incision of Omar and Lynch Heights paleovalleys |

Offshore Seismic Stratigraphic Units

| | | | |
|-----------------------------|-------------------------------|-------------------------------|--|
| <i>Toscano et al., 1989</i> | <i>Colman and Mixon, 1988</i> | <i>Foyle and Oertel, 1997</i> | <i>Brothers et al., 2020</i> |
| Q5 | Qhe | Seq I | Qmn:Modern (late Holocene) including coastal sand bodies, ridges and sandy shoreface |
| Q3 | Qc | Seq I | Qcch:Transgressive unit filling the Cape Charles paleochannel that formed during LGM (MIS2) |
| Q2 | Qe | Seq II and III | Q2:Shelf and estuarine sediments not related to paleochannel fill (30,34,36,37) |
| Q1 | | Seq IV | Qe: Unit filling the Eastville paleochannel |
| T1 | Qx | Seq V and VI | Q1: Shelf and estuarine sediments not related to paleochannel fills (32, 33) Qx: Exmore paleochannel fill |
| | | | Qbd: Low stand fluvial plain deposit, offshore equivalent of the Beaverdam Qpp: Persimmon Point paleochannel fill |

Fig. 4. Summary of stratigraphic terminology for three regions within the study area. References in italics contain published stratigraphic diagrams. Numbers in parentheses identify sites in Table 1 that can be related to the named stratigraphic unit. See section 4.5 for discussions of AAR data for individual stratigraphic units (Mixon et al., 1989).

Table 2a

Compilation of conventional and accelerator-mass-spectrometer (AMS) radiocarbon analyses and associated median calibration ages for all shells with paired amino acid racemization results (see Appendix B), and arranged in order of the AARDB ID number. Site and sample identifications are as in Table 1. Sample depths are in meters relative to MSL. ^{14}C ages were calibrated using OxCal 4.3 (Bronk Ramsey, 2009) and the Marine20 calibration curve (Heaton et al., 2020), corrected to a regional ΔR of 54 ± 74 years following Raff et al. (2018). All dates presented in the text are calibrated, 2-sigma (2σ) years before present (BP; present = 1950). Conv RC Age: Conventional Radiocarbon age; DGSID: Delaware Geological Survey site identifier; DGSRCDB: Delaware Geological Survey Radiocarbon Date Database identifier number. Laboratory code is identifier for the analyzing radiocarbon laboratory: OS = NOSAMS laboratory, Woods Hole MA; AA = University of Arizona, Tucson AZ; Beta = Beta Analytical, Miami Florida. Results are plotted in Fig. 5; results for samples with “greater than” ^{14}C ages are arbitrarily plotted as if their ages are 55 ka.

| Site # | DGSID | Local Site name | AARDB ID | SampleID | Mollusk Genus | Analysis | Pretreatment | Sample Elevation (m) | DGSRCDB ID # | Laboratory Code | Reported ^{14}C Age (yrs BP) | Calibrated median age (yrs BP) |
|--------|---------|----------------------------|----------|-----------------|-------------------|----------|-----------------|----------------------|--------------|-----------------|---------------------------------------|--------------------------------|
| 30 | Uk33-01 | MGS-16-1002 | 05056 | jw2015-140-001 | <i>Astarte</i> | C14 AMS | (HY) Hydrolysis | -23.8 | 489 | OS-124831 | 51600 ± 2500 | N/A |
| 34 | Uk53-01 | MGS-18-1142 | 05060 | jw2015-128-001 | <i>Spisula</i> | C14 AMS | (HY) Hydrolysis | -20.3 | 492 | OS-124834 | 695 ± 15 | 117 ± 137 |
| 34 | Uk53-01 | MGS-18-1142 | 05060 | jw2015-129-001 | <i>Spisula</i> | C14 AMS | (HY) Hydrolysis | -20.2 | 491 | OS-124833 | 37400 ± 450 | 41183 ± 666 |
| 36 | Vk21-01 | MGS-20-1430 | 05065 | jw2015-103-001 | <i>Astarte</i> | C14 AMS | (HY) Hydrolysis | -22.1 | 604 | OS-141999 | 48500 ± 1500 | 51087 ± N/A |
| 36 | Vk21-01 | MGS-20-1430 | 05065 | jw2015-103-003 | <i>Ensis</i> | C14 AMS | (HY) Hydrolysis | -22.1 | 493 | OS-124835 | 41400 ± 710 | 43568 ± 1037 |
| 36 | Vk21-01 | MGS-20-1430 | 05065 | jw2015-101c | <i>Mulinia</i> | C14 AMS | (HY) Hydrolysis | -20.8 | 484 | OS-124792 | 35200 ± 340 | 39370 ± 726 |
| 17 | Pj45-01 | DGS92-02 | 05119 | CW93-008-1 | <i>Spisula</i> | Conv C14 | acid etch | -13.4 | 496 | Beta-437604 | 720 ± 30 | 136 ± 149 |
| 17 | Pj45-01 | DGS92-02 | 05119 | CW93-009-1 | <i>Spisula</i> | Conv C14 | acid etch | -13.6 | 497 | Beta-437605 | 820 ± 30 | 221 ± 203 |
| 25 | Rl25-01 | DGS92-16 | 05130 | cw93-070-1 | <i>Astarte</i> | C14 AMS | (HY) Hydrolysis | -23.6 | 603 | OS-141998 | 48900 ± 1500 | 51518 ± N/A |
| 25 | Rl25-01 | DGS92-16 | 05130 | cw93-076-002 | <i>Astarte</i> | C14 AMS | unknown | -25.7 | 212 | AA-14749 | >49900 ± n/a | N/A |
| 25 | Rl25-01 | DGS92-16 | 05130 | cw93-070-3 | <i>Astarte</i> | C14 AMS | (HY) Hydrolysis | -23.6 | 602 | OS-141997 | 46300 ± 1100 | 48148 ± 2990 |
| 24 | Qk53-03 | DGS04-12 | 05183 | jw2005-164-1 | <i>Mulinia</i> | C14 AMS | (HY) Hydrolysis | -19.2 | 608 | OS-142003 | 1880 ± 20 | 1218 ± 203 |
| 24 | Qk53-03 | DGS04-12 | 05183 | jw2005-161-2 | <i>Spisula</i> | C14 AMS | (HY) Hydrolysis | -16.4 | 607 | OS-142001 | 580 ± 20 | 20 ± 21 |
| 80 | Zz82-59 | USGS-1423 | 05225 | jw2007-122-003 | <i>Astarte</i> | C14 AMS | (HY) Hydrolysis | -40.3 | 589 | OS-126619 | 3980 ± 25 | 3732 ± 250 |
| 80 | Zz82-59 | USGS-1423 | 05225 | jw2007-122-007 | <i>Mercenaria</i> | C14 AMS | (HY) Hydrolysis | -40.9 | 590 | OS-126620 | 5590 ± 25 | 5724 ± 213 |
| 80 | Zz82-59 | USGS-1423 | 05225 | jw2007-122-001 | <i>Spisula</i> | C14 AMS | (HY) Hydrolysis | -40.3 | 588 | OS-126618 | 6320 ± 25 | 6507 ± 218 |
| 80 | Zz82-59 | USGS-1423 | 05225 | jw2007-122-006 | <i>Spisula</i> | C14 AMS | (HY) Hydrolysis | -40.9 | 587 | OS-126065 | 6000 ± 30 | 6166 ± 220 |
| 16 | Oj53-02 | DGS07-17 | 05268 | jw2009-068-1 | <i>Mercenaria</i> | Conv C14 | acid etch | -15.5 | 302 | Beta-257231 | 4210 ± 40 | 4037 ± 279 |
| 28 | Uj35-03 | MD-BOEM-15-03A | 05380 | jw2016-017-002 | <i>Astarte</i> | C14 AMS | (HY) Hydrolysis | -25.8 | 605 | OS-142000 | 44800 ± 940 | 46480 ± 1946 |
| 60 | Zz82-r | North Parramore April 1991 | 06196 | LY92-015 | <i>Spisula</i> | C14 AMS | acid etch | 0 | 694 | Beta-53234 | >44600 ± n/a | N/A |
| 71 | Zz82-i | Wreck Island May 2015 | 06236 | ERT2015-100-004 | <i>Spisula</i> | C14 AMS | (HY) Hydrolysis | 0 | 495 | OS-125184 | 38000 ± 740 | 41541 ± 905 |
| 71 | Zz82-i | Wreck Island May 2015 | 06236 | ERT2015-100-016 | <i>Spisula</i> | C14 AMS | (HY) Hydrolysis | 0 | 494 | OS-125183 | 27600 ± 260 | 30845 ± 538 |
| 74 | Zz82-v | Smith Island May 2016 | 06251 | ERT2016-003-14 | <i>Mercenaria</i> | C14 AMS | (HY) Hydrolysis | 0 | 599 | OS-141994 | 4400 ± 25 | 4288 ± 261 |
| 74 | Zz82-v | Smith Island May 2016 | 06251 | ERT2016-003-3 | <i>Mercenaria</i> | C14 AMS | (HY) Hydrolysis | 0 | 601 | OS-141996 | 1870 ± 35 | 1208 ± 209 |
| 74 | Zz82-v | Smith Island May 2016 | 06251 | ERT2016-003-17 | <i>Spisula</i> | C14 AMS | (HY) Hydrolysis | 0 | 600 | OS-141995 | 35000 ± 340 | 39179 ± 722 |
| 74 | Zz82-v | Smith Island May 2016 | 06251 | ERT2016-003-25 | <i>Spisula</i> | C14 AMS | (HY) Hydrolysis | 0 | 596 | OS-141991 | 29500 ± 170 | 33058 ± 627 |
| 74 | Zz82-v | Smith Island May 2016 | 06251 | ERT2016-003-27 | <i>Spisula</i> | C14 AMS | (HY) Hydrolysis | 0 | 597 | OS-141992 | 29600 ± 180 | 33191 ± 597 |
| 74 | Zz82-v | Smith Island May 2016 | 06251 | ERT2016-003-29 | <i>Spisula</i> | C14 AMS | (HY) Hydrolysis | 0 | 598 | OS-141993 | 31400 ± 260 | 34945 ± 568 |
| 86 | | | 06258 | | <i>Spisula</i> | | | -17.9 | 610 | OS-142005 | 1760 ± 25 | 1100 ± 192 |

(continued on next page)

Table 2a (continued)

| Site # | DGSID | Local Site name | AARDB ID | SampleID | Mollusk Genus | Analysis | Pretreatment | Sample Elevation (m) | DGSRCD ID # | Laboratory Code | Reported ¹⁴ C Age (yrs BP) | Calibrated median age (yrs BP) |
|--------|---------|-----------------|----------|----------------|-------------------|------------|--------------------|----------------------|-------------|-----------------|---------------------------------------|--------------------------------|
| | Zz82-63 | VA-BOEM-2015-01 | | jw2016-039-001 | | C14 AMS | (HY) Hydrolysis | | | | | |
| 86 | Zz82-63 | VA-BOEM-2015-01 | 06258 | jw2016-038-005 | <i>Mulinia</i> | C14 AMS | (HY) Hydrolysis | -18.6 | 609 | OS-142004 | 31400 ± 220 | 34941 ± 496 |
| 48 | Zz82-69 | VA-BOEM-2016-02 | 06263 | jw2017-306 | <i>Mercenaria</i> | C14 AMS | (HY) Hydrolysis | -17.9 | 606 | OS-142002 | 42100 ± 730 | 44079 ± 1207 |
| 48 | Zz82-69 | VA-BOEM-2016-02 | 06263 | jw2017-306-1* | <i>Mercenaria</i> | C14 AMS | (HY) Hydrolysis | -17.9 | 696 | OS-149175 | 40500 ± 670 | 42950 ± 929 |
| 48 | Zz82-69 | VA-BOEM-2016-02 | 06263 | jw2017-306-2* | <i>Mercenaria</i> | C14 AMS | (HY) Hydrolysis | -17.9 | 697 | OS-149174 | 43000 ± 990 | 44909 ± 1878 |
| 48 | Zz82-69 | VA-BOEM-2016-02 | 06263 | jw2017-306-3* | <i>Mercenaria</i> | C14 AMS | (HY) Hydrolysis | -17.9 | 698 | OS-149173 | 46600 ± 1400 | 48757 ± 4370 |
| 79 | Zz82-83 | VA-BOEM-2017-05 | 06272 | JW2018-018 | <i>Mercenaria</i> | C14 AMS | (HY) Hydrolysis | -15.6 | 593 | OS-141988 | 6650 ± 30 | 6882 ± 240 |
| 67 | Zz82-87 | VA-BOEM-2017-09 | 06276 | JW2018-019-002 | <i>Spisula</i> | C14 AMS | (HY) Hydrolysis | -14.2 | 591 | OS-141986 | 740 ± 20 | 150 ± 157 |
| 88 | Zz62-05 | CS80 | 07118 | LY85-161A | <i>Mercenaria</i> | C14 AMS | acid etch | -8.2 | 695 | AA-7322 | >39700 ± n/a | N/A |

*successive leaches of second fragment of original sample.

1 = first 42.6%.

2 = second 37.7%.

3 = final 19.7%.

Table 2b

Uranium series age results for two corals from East Lake Pit, North Carolina (site 87, Table 1). Analyses performed by W. Thompson, Woods Hole Oceanographic Institution. Photos of the coral samples are available in Appendix A. Samples collected by Peter Parham, East Carolina University. The stratigraphic relation of the coral samples and associated AAR and OSL results is shown in Appendix F. The conventional U-series ages were corrected using the open-system conversion procedure of Thompson et al., 2003. Final U-series ages were calculated using the half-lives of Cheng et al., 2013. The high ²³²Th content of sample JW2004-147 is an indication of the high detrital content of many Coastal Plain samples (Wehmiller et al., 2004).

| Sample | ²³⁴ U/ ²³⁸ U | ²³⁰ Th/ ²³⁸ U | Apparent Excess ²³⁴ U | Model Slope | Open-System Age, ka | Conventional Age | Initial δ ²³⁴ U | [U] ppm | [²³² Th] ppb |
|------------|------------------------------------|-------------------------------------|----------------------------------|-------------|---------------------|------------------|----------------------------|-----------------|--------------------------|
| JW2004-146 | 1.118 ± 0.0006 | 0.576 ± 0.0016 | 0.998 | 0.272 | 77.95 ± 0.44 | 77.73 ± 0.32 | 146.4 ± 0.7 | 3.0844 ± 0.0004 | 131.788 ± 0.4 |
| JW2004-147 | 1.128 ± 0.0002 | 0.648 ± 0.0019 | 1.058 | 0.294 | 83.97 ± 0.35 | 91.13 ± 0.41 | 165.8 ± 0.4 | 1.9533 ± 0.0002 | 303.959 ± 1.5 |

altered based on L-SER/L-ASP or otherwise aberrant D/L values they are usually specimens of the thin-shelled taxa *Mulinia* or *Ensis*. The potential for shell alteration (and/or age mixing) underscores the importance of doing as many analyses as possible from each site or core interval; Table 1 lists the number of samples of each genus analyzed from each site.

4. Results and discussion

Clusters of D/L values observed at individual sites are defined as “local” aminozones but, if observed at multiple sites, they can be interpreted as “regional” aminozones. These aminozones are usually characteristic of specific lithologic units at outcrops or in cores, but for transported shells, the aminozone is defined solely on the basis of the numerical clusters. Although the typical precision of AAR analysis of an individual shell can be as small as 2% (see results for Interlaboratory Comparison Samples, Appendix D), numerous diagenetic and thermal factors, as well as age-mixing, can cause the precision of a single aminozone to be on the order of 10% (Wehmiller et al., 2000). Therefore, we use this qualitative guideline to define aminozones based on the RP results, with the caveat that a range of ages can be represented by a defined aminozone even if all the D/L values fall within this range. Similarly, in the discussion of radiocarbon results (and particularly for those samples with paired Pleistocene ¹⁴C-AAR results), we report ¹⁴C ages at “face value” even though there are reasons to suspect that some of these ages are minimum values only.

4.1. Paired ¹⁴C – AAR results

Paired ¹⁴C-AAR results demonstrate an expected trend of increasing D/L values with ¹⁴C age (Fig. 5). The paired results for *Astarte* and *Mercenaria* are limited, but there are enough paired results for *Spisula* to conclude that there is no clear relation between D/L values and ¹⁴C ages for the Pleistocene samples of this genus. The shapes of these curves are the combined consequence of the fundamental diagenetic pathway of racemization and the contrast in effective temperature between Holocene and Pleistocene samples (Wehmiller et al., 2010: Figs. 12 and 13). Other studies (e.g., Ryan et al., 2020) also confirm the general observation that ASP appears to racemize very quickly in young (Holocene) samples, with racemization rates then slowing significantly in older samples. Kaufman (2006) demonstrated this trend using controlled laboratory experiments, showing that incremental increases in D/L ASP and GLU get progressively smaller with increasing sample age. For natural samples, at some point the increase in D/L value will be equal to, or less than, the inherent variability of D/L values within a group of samples (e.g., Blakemore et al., 2015). The D/L ASP and GLU values for the Pleistocene samples in Fig. 5 fall within the ranges seen in *Mercenaria* and *Spisula* from onshore Pleistocene sites, including several samples from the Marine Isotope Stage (MIS) 5a (calibrated with U-series coral results) unit at Gomez Pit, VA (81–84)

4.2. Identification of Holocene and Pleistocene aminozones: beach and onshore comparison samples

Co-varying D/L values of ASP and GLU in *Mercenaria* and *Spisula* from five of the six islands, and for several onshore comparison sites, are

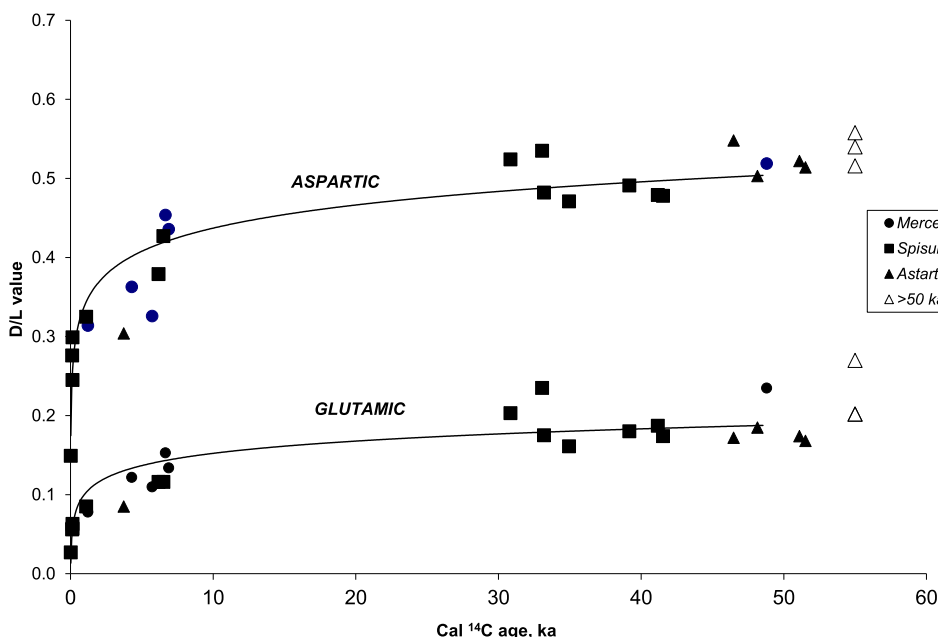


Fig. 5. Plots of D/L values of ASP and GLU vs. ^{14}C (calibrated) age for *Astarte*, *Mercenaria* and *Spisula* for samples of these taxa that have both AAR and ^{14}C results for the same sample (paired analyses). ^{14}C ages in Table 2a; D/L values in Appendix B. One paired *Mulinia* analysis is listed in Table 2 but not plotted here. The D/L ASP and GLU values for this sample are 0.46 and 0.22; the ^{14}C calibrated age is ~ 39.3 ka. The open symbols represent *Spisula* and *Astarte* with “greater than” ^{14}C results and are plotted with an assigned age of 55 ka. The plotted curves are logarithmic fits to all finite age results without distinction regarding genus.

shown in Fig. 6a and b. Only IE data for *Mercenaria* are available for Wallops Island, where no *Spisula* were collected. Four clusters of *Mercenaria* D/L values, designated M1, M2, M3, and M4 are observed (Fig. 6a), and two clusters of *Spisula* D/L values (designated S1 and S2) (Fig. 6b). For the beach and onshore samples only mean values (with ranges of $\pm 10\%$) are plotted. Co-variance plots such as these have been used to screen for aberrant or anomalous results (e.g., Kaufman, 2006); although some results in Fig. 6a and b might be considered suspect, no results have been excluded from these plots. Results for Interlaboratory Comparison Samples (ILC) are plotted in Fig. 6c; the ranges of D/L values for the ILC samples provide a useful comparison with the ranges seen in the different *Mercenaria* or *Spisula* clusters, as the ILC results are for homogeneous samples analyzed at different times during the course of this study. The ILC samples represent different ages and molluscan genera, but the D/L values are a qualitative indication of the age differences between the samples.

Clusters M1 and S1 in Fig. 6a and b represent Holocene ages based on a limited number of paired ^{14}C -AAR analyses of specific shells of each genus that fall within these clusters (Table 2a; Fig. 5). The actual range of D/L values for the M1 and S1 beach samples is variable depending on the island site and is as large as $\pm 20\%$ (Appendix B). Based on paired ^{14}C -AAR results for *Mulinia* (Simonson et al., 2013), the ranges of D/L values in clusters M1 and S1 likely represent the mid-to late Holocene. Clusters M2 and S2 include shells that are inferred to be of Pleistocene age based on paired ^{14}C -AAR results or stratigraphic association with units dated via U–Th. Clusters M2 and M3 at the Gomez sites (81–84) represent two distinct aminozones in the Sedgfield member of the Tabb Formation, in stratigraphic superposition. These two aminozones are identified in numerous exposures throughout the excavation (Wehmiller et al., 1988; Mirecki et al., 1995; Lamothe et al., 1998). Shells in the M2 zone are associated with corals with U-series ages of ~ 75 –80 ka (Wehmiller et al., 2004). The M2 and S2 clusters also include samples from several southern Delmarva onshore sites that represent the Nassawadox Formation (Mixon, 1985). The M2 and S2 clusters both contain results for two collection sites approximately 100 m apart within the same shell bed at Gomez Pit, providing examples of local variability within a single aminozone and lithostratigraphic unit. Clusters M2 and M3 include results for two *Mercenaria* shells from PR#1 (85), confirming the original GC and IE results.

Cluster M3 includes data for three sites (T’s, Pk, and NB) (40, 44, and 53) originally grouped (using GC data) with the M4 Omar-Accomack

samples from CW-4 (38) and MF (39) using GC or IE data. All but NB (53) are located in the northern Virginia portion of Delmarva. However, the newer results indicate that sites T’s, Pk, and NB (40, 44 and 53) are younger than the MF/CW-4 samples, with mixed ages possibly being inferred from the T’s data. The inferred clusters of RP ASP and GLU data for these samples conflict with the clusters based on GC data for leucine and valine, implying that some amino acids are more useful for aminozone distinctions, particularly with the more extensively racemized samples. T’s and Pk collection sites lie off the axis (Fig. 3) of the Omar-Accomack spit (Mixon, 1985), hence could be younger than the unit represented by the MF/CW-4 group. The question of the age difference between the MF/CW-4 and NB/T’s/P samples requires further study, including repeat GC/RP analyses on the same sample using current analytical methods. The implications of the MF/CW-4 results are discussed in section 4.5.5.

Cluster M4 includes results from the Accomack member of the Omar formation of Mixon (1985) (38–40, 44, Table 1). Original results from the M4 samples were interpreted to be mid-Pleistocene (>400 ka) in age (Belknap and Wehmiller, 1980; Wehmiller et al., 1988). One *Mercenaria* sample, from onshore site CWW (41, Tables 1 and 2), has D/L values at or near racemic equilibrium (D/L ~ 1.0), indicating it is more extensively racemized than all the others of this genus in the present study. The CWW sample is from a deep (~ 50 m) water well that penetrated the Yorktown Formation, a Neogene unit that underlies much of the central Delmarva Peninsula (Belknap, 1979; Belknap and Wehmiller, 1980; Mixon, 1985). Although the D/L values for beach shells in this study are not represented by clusters M3 or M4, these latter two clusters are important for the overall understanding of the regional aminostratigraphy because they constrain the ages of the Delmarva paleo-channel system. A limited number of samples with M3 or M4 D/L values are found in shelf cores (section 4.6).

The covariance of ASP and GLU D/L values for *Mercenaria* and *Spisula* is quite similar, as seen in Fig. 6a and 6b. D/L values for *Rangia* specimens (a brackish water mollusk) from several central and northern Chesapeake Bay sites (8–11), plot within the M2 and M3 clusters. The *Rangia* RP D/L values are consistent with previously obtained IE data identifying two clusters. At only one site (NB, site 53) are *Rangia* and *Mercenaria* found together in outcrop (Mixon, 1985; Fig. 4) but because they are in superposed units it cannot be proven that they are equal in age. Combining data for different taxa into a single D/L vs. D/L figure does not imply equivalent intergeneric racemization rates, rather it

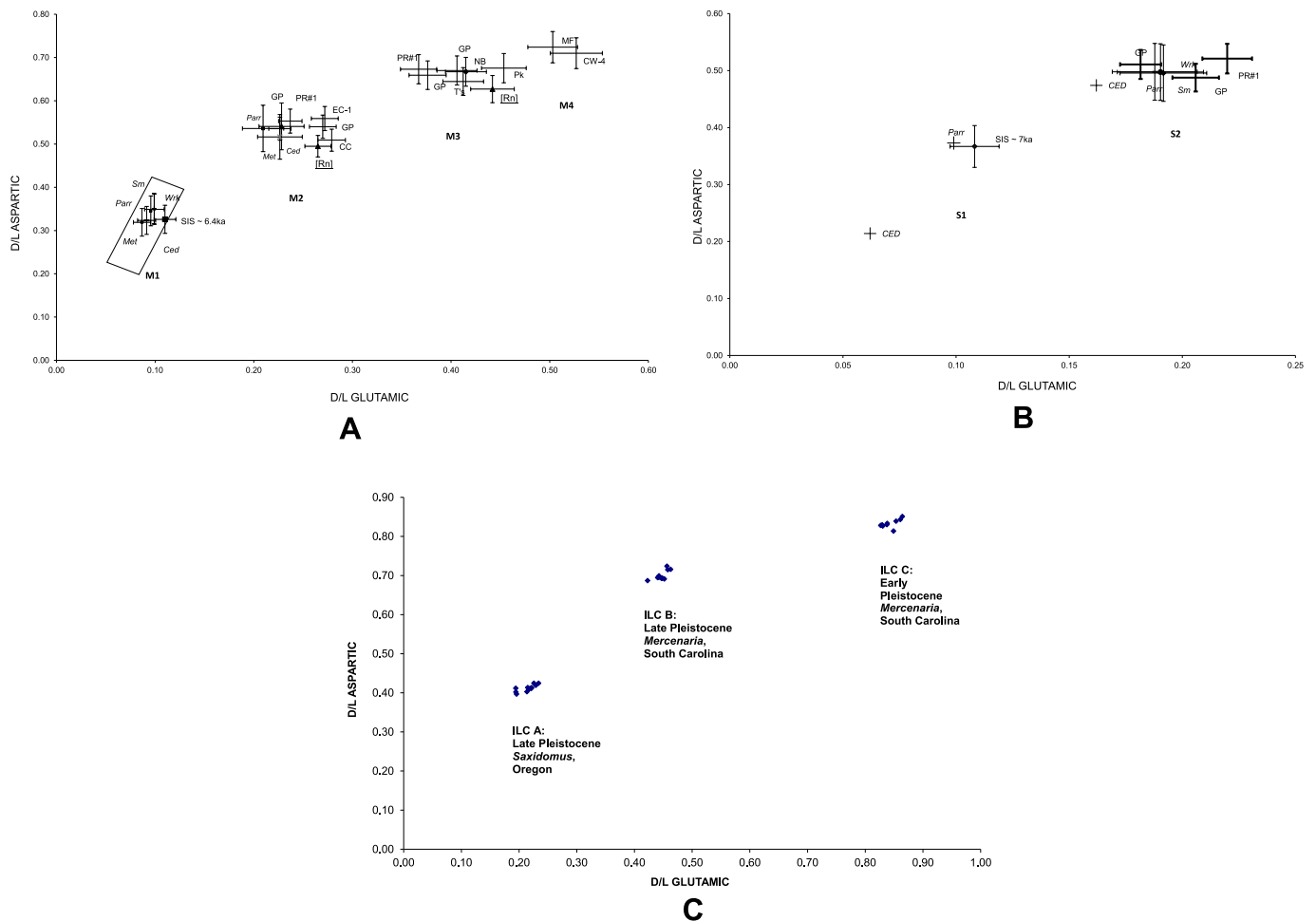


Fig. 6. RP data for D/L ASP vs D/L GLU in *Mercenaria* (6a) and *Spisula* (6b) from Metompkin, Cedar, Parramore, Wreck and Smith islands, Smith Island Shoal (SIS) (80), and onshore comparison sites as follows: NB (53,54); GP (81–84); CC (72) EC-1 (73); SN (63); MF (39); CW-4 (38); T's (40); Pk (44); PR#1 (85). Mean values for clusters from each island are plotted with a range of ±10%, although the actual ranges can be larger. Samples from SIS (80) have Holocene paired ¹⁴C-AAR results. Samples from Parramore (Parr), Smith (Sm), and Wreck (Wrk) have Pleistocene paired ¹⁴C-AAR results. Results for onshore sites are plotted as mean values with ranges of ±10%. D/L results for *Astarte* are more limited and fall within the M1 and M2 clusters (Appendix B). The two data points labeled Rn are for the two clusters of *Rangia* D/L values observed at sites in the central and northern Chesapeake Bay (8–11). M1, M2, M3, M4, S1, and S2 identify the general clusters of D/L values for *Mercenaria* and *Spisula*, as discussed in text. Fig. 6c shows comparable ASP-GLU D/L values by RP for Interlaboratory Comparison Samples (Wehmiller, 1984) (data in Appendix D), indicating the range of results for multiple analyses of individual homogeneous samples. ILC B and C are homogeneous powders of *Mercenaria* from late and early Pleistocene sites in South and North Carolina, respectively, and ILC A is a homogenous powder sample of *Saxidomus* from a late Pleistocene site on the US Pacific coast. The D/L values in ILC A and ILC B span the range of most of the values observed in the present study.

indicates a similarity in relative intrageneric rates. Comparison of the *Mercenaria* and *Spisula* data with *Astarte* is more limited because only one cluster of Pleistocene *Astarte* is observed (Appendix B), with mean D/L values of ~0.58 and ~0.23 for ASP and GLU, respectively.

The ranges of D/L values for each cluster in Fig. 6 represent a combination of factors: actual age differences within a given aminozone, intra-sample variability, differences in sample quality, and contrasting temperature histories for individual samples. The latter effect is significant, as the localities represented by these clusters include both offshore and onshore sites spanning a ~2° latitude range, representing a range of approximately 2.5 °C in mean annual temperature (Wehmiller et al., 2000). None of these possibilities is dismissed, but a Pleistocene age for the M2 and S2 clusters observed in shells from the island beaches is confirmed by the paired ¹⁴C-AAR results for these shells, which provide minimum ages of at least ~30 ka. A heating effect, in which long exposure on the beach surface leads to anomalously high D/L values, has been noted in earlier AAR studies of Holocene mollusk samples (Wehmiller, 1977; Wehmiller et al., 1995). Although the number of beach shell analyses reported here is limited, the AAR results indicate that only Holocene *Mercenaria* have been found on Wreck and Smith Islands, and

that only Pleistocene *Spisula* have been found on these two islands. Both Pleistocene and Holocene *Mercenaria* and *Spisula* are found on Parramore Island, and with a few exceptions, the shells from Wallops, Cedar and Metompkin islands appear to be primarily Holocene in age; these interpretations are summarized in Table 3.

4.3. Identification of Holocene and Pleistocene aminozones: offshore samples

Mulinia specimens are found much more frequently in the offshore cores than either *Spisula* or *Mercenaria*, hence data for *Mulinia* are particularly useful for developing a regional aminostratigraphic framework and linking offshore, beach, and onshore results. The *Mulinia* aminostratigraphy for the study area is shown in Figs. 7 and 8. Fig. 7 presents the D/L ASP-GLU relation for *Mulinia* samples from offshore and onshore sites, with four clusters identified as Mu1, Mu2, Mu3, and Mu4. As in the case of the clusters of D/L values observed for *Mercenaria* and *Spisula* (Fig. 6), the individual *Mulinia* clusters identified in Fig. 7 have ranges of D/L values that can represent both age and temperature differences, among other factors. The intrageneric ASP-GLU relation for

Table 3
Numbers and proportions of Delmarva island beach shells interpreted as being either Holocene or Pleistocene in age.

| Map # | Collection site | UDAMS | Holocene | | Pleistocene | | % Pleistocene | | % Pleistocene Combined** |
|-------|-----------------|--------------|-------------------|-----------------|-------------------|-----------------|-------------------|-----------------|--------------------------|
| | | | <i>Mercenaria</i> | <i>Spistula</i> | <i>Mercenaria</i> | <i>Spistula</i> | <i>Mercenaria</i> | <i>Spistula</i> | |
| 42 | Wallops Island | 06203 | 13* | nc | 0 | nc | 0 | na | 0 |
| 50 | Metompkin 1 | 06233 | 10 | nc | 5 | nc | 33 | na | 33 |
| 46 | Metompkin 2 | 06234 | 15 | nc | 0 | nc | 0 | na | 0 |
| 59 | Cedar Island O | 06227 | 13 | 1 | 0 | 1 | 0 | 50 | 7 |
| 57 | Cedar Island 1 | 06228 | 13 | nc | 2 | nc | 13 | na | 13 |
| 59–62 | North Parramore | 06196, 06202 | 14 | 1 | 9 | 7 | 40 | 88 | 52 |
| 71 | Wreck Island | 06236 | 16 | 0 | 0 | 16 | 0 | 100 | 50 |
| 74 | Smith Island | 06251 | 15 | 0 | 0 | 17 | 0 | 100 | 50 |

* including 2 *Noetia*
nc = none collected
na = not applicable
** = # Pleist/(#Hol + #Pleist)

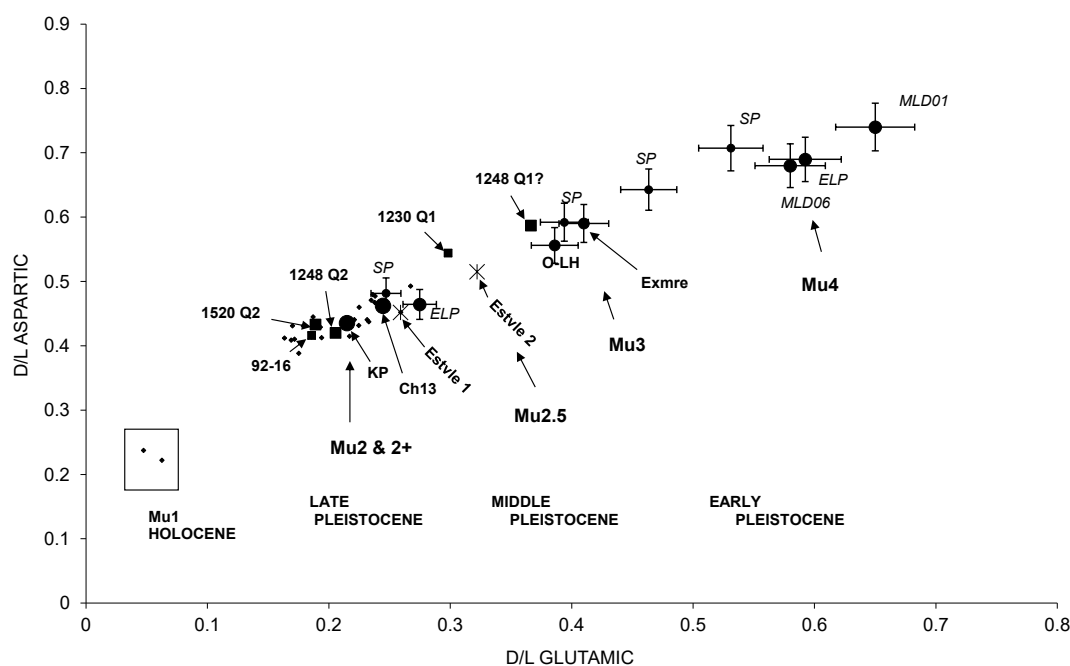


Fig. 7. D/L ASP vs. D/L GLU for *Mulinia* from onshore and offshore sites. Onshore sites are identified with large solid circles and identified by name. Offshore sites are identified by small solid circles and by solid squares, the latter identified by name. Each data point represents the mean value for each site with three or more analyses. Selected sites are identified for reference, as follows: 18–1230 (33); 18–1248 (32); 27–1520 (37); O-LH as the mean of three Omar/Lynch Heights (13–15), Exmore (Ex) (66); Kiptopeake (Kp) (75); Stetson Pit (SP) (89, 90); the plotted Eastville mean values (Estville 1 and Estville 2) represent two apparent groups of D/L values for Eyreville (69) and Cheriton East (94). The Stetson Pit results represent a superposed sequence from late to early Pleistocene (York et al., 1989). MLD01 and MLD06 (93, 92) are results for early Pleistocene samples from the Albemarle Embayment, NC (Wehmiller et al., 2010). Ranges of D/L values for late, middle, and early Pleistocene are based on the Albemarle data and U-series results (Table 2b). See Fig. 12 for further discussion. Data for only 22-h hydrolysis analyses are included.

Mulinia in Fig. 7 is similar to those for *Mercenaria* and *Spistula* (Fig. 6), but for any specified D/L GLU value the D/L ASP values in *Mulinia* are lower than in either *Mercenaria* or *Spistula*. Because Fig. 7 represents both offshore and onshore sites from a broad latitude range, we use Fig. 8 to show *Mulinia* ASP and GLU D/L values for the onshore and offshore sites listed in Table 1, demonstrating the latitude (temperature) effect on the range of D/L values for the Mu2 cluster. There is a clear trend of D/L values for both ASP and GLU increasing with decreasing latitude (which represents an increase in mean annual temperature of approximately 2.5°, cited above), although there is some scatter around both of these trends (not always in the same direction for the two amino acids). For simplicity, each data point in Fig. 8 is plotted with a ±5% precision, acknowledging that some results have either smaller or larger coefficients of variation. The solid lines are linear regressions on all the D/L ASP and D/L GLU site means for *Mulinia*, and the dashed lines depict a range of 10% above or below these regressions. These “envelopes”

represent simple guidelines for definition of a regional *Mulinia* aminozone, which represents the range of D/L values in cluster Mu2 in Fig. 7.

Cluster Mu2 (Figs. 7 and 8) includes results from offshore, onshore, and barrier island cores from southern Delmarva, southeastern Virginia and northeastern North Carolina excavations or subsurface sections. The onshore Mu2 sites include a superposed subsurface sequence at Stetson Pit NC (89, 90) (York et al., 1989; Riggs et al., 1992; Wehmiller et al., 2010), a superposed sequence at East Lake Pit (87) (Parham et al., 2013; this work) and the Lynch Heights/Omar Formation in southeastern Delaware (Ramsey, 2010), the latter with Mu3 D/L values (sites 13–15). Both the Stetson Pit and East Lake Pit superposed stratified sections also yield Mu4 values, the latter interpreted as early Pleistocene (Wehmiller et al., 2010, 2012). Also included are results for cores MLD-05, MLD-06, and MLD-01 (91–93), from the Albemarle Embayment study that includes detailed litho- and seismic stratigraphic information (Mallinson et al., 2010; Wehmiller et al., 2010). AAR results for East Lake Pit and

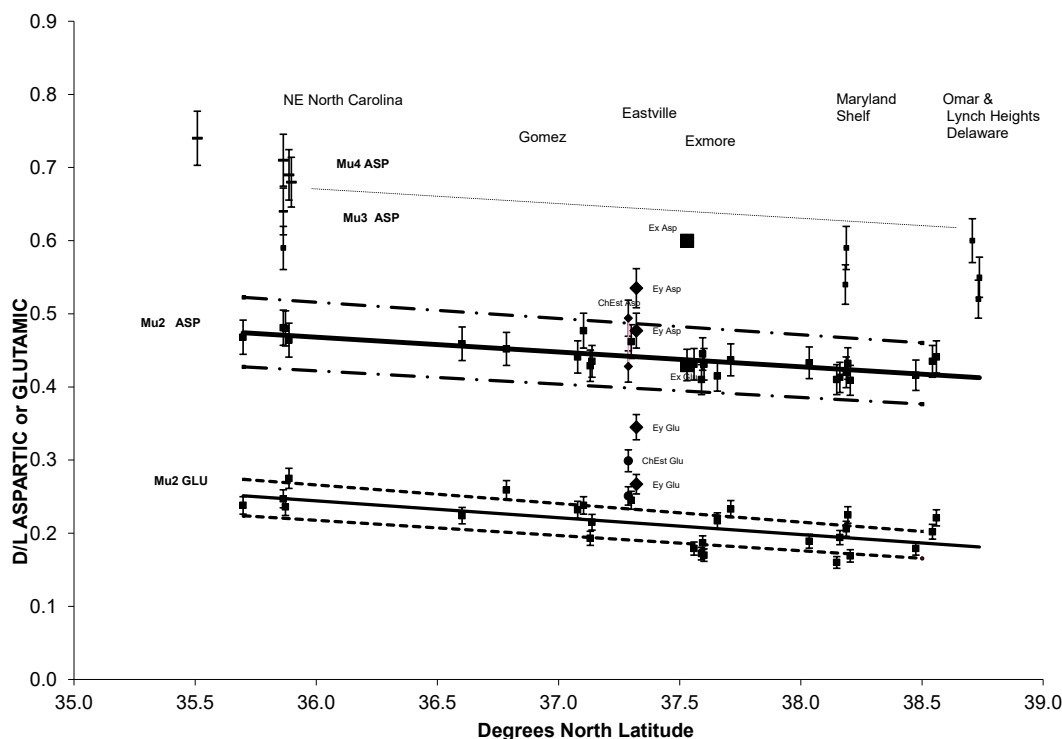


Fig. 8. Latitudinal distribution of mean D/L ASP and GLU values (RP method only) for *Mulinia* samples from all sites listed in Table 1. Each site mean is plotted with a range of 5%. The solid lines are linear regressions on the mean values for ASP and GLU; the dashed lines represent ranges of 10% above or below the linear regression. “Mu2 ASP” and “Mu2 GLU” represent the “Mu2 *Mulinia* aminozone” as discussed in text. For clarity, with the exception of the Eyreville, Cheriton East, and Exmore GLU D/L values, only ASP D/L values for Mu3 and Mu4 are plotted, as the GLU D/L values for these clusters overlap with the ASP values for Mu2. The dashed line between Mu3 points is qualitative and not an actual regression. See Fig. 7 for ASP and GLU D/L values for Mu3 and Mu4. Sites with either U-series or ^{14}C age control are SP (Stetson Pit, NC, sites 89, 90); ELP (East Lake Pit, NC (site 87) at latitude 35.8° and DGS92-16 (25) at latitude 38.5° (see Fig. 9). Other identified sites or groups of sites are: Ey = Eyreville (site 69); Ex = Exmore (site 66); ChE = Cheriton East (94); Md Shelf (sites 32, 33); Omar Fm (Lynch Heights) (sites 13–15). ASP and GLU D/L values for Holocene *Mulinia* are ~ 0.24 and 0.05 , respectively (Appendix B and Fig. 7). Data for only 22-h hydrolysis results are included. Regressions for Mu2 values as follows: ASP D/L = $1.1961 - 0.0202$ (Latitude) GLU D/L = $1.0734 - 0.0232$ (Latitude).

MLD-06 are discussed in greater detail in section 4.5.1. The Mu2 and Mu3 clusters are clearly separated; the intermediate D/L values for MGS18-1230 (33) and Eyreville/Cheriton East (69, 94) are interpreted as cluster Mu2.5.

A few *Mulinia* results in Fig. 8 plot below or above the Mu2 envelope but do not appear to fit in either the Mu1 or Mu3 clusters. The magnitude of these deviations from the Mu2 envelope is quantified in Table 4, where the ratio of observed to predicted ASP and GLU D/L values for all sites within the Mu2 envelope is listed. The reference regressions for the two amino acids are found in the caption for Fig. 8, and both predicted and observed site mean values are listed in Table 4. The averages of the deviations for ASP and GLU are used as guides to assignment of Mu2- or Mu2+ to each site, using an arbitrary threshold of 8% below or above the reference regression. In several cases the difference between the ASP and GLU deviations is quite large (Table 4), suggesting anomalous results likely related to diagenetic factors such as leaching or contamination (selective loss or gain of amino acids).

The constraints on the range of ages represented by the Mu2 envelope in Fig. 8 are based on both radiocarbon and U-series results for associated samples. The younger age limit is defined by the ^{14}C results (at or near detection limit) from offshore core DGS92-16 (25) that are stratigraphically above analyzed *Mulinia* from this core (Fig. 9a; Appendix F). A >52 ka ^{14}C -AAR result for *Astarte* with D/L values like those from DGS92-16 from the New Jersey shelf (site 6; Miller et al., 2013a) further supports this age constraint. Less direct calibration of this aminozone is discussed in section 4.5.3. The older age range is based on U-series results (\sim MIS 5a-5c) from two of the North Carolina sites (East Lake and Stetson: 87, 89, 90) that define the Mu2 aminozone to represent at least part of Marine Isotope Stage (MIS) 5, and we adopt as a

working model that this envelope represents the full range of MIS 5 from ~ 130 ka to ~ 75 ka. The combined results for the East Lake Pit, Stetson Pit, and DGS92-16 sites represent the best-controlled “end members” for the envelope of D/L values shown in Fig. 8. The detailed relation of AAR and independent chronologies for these sites are summarized in Fig. 9. Muhs et al. (2014; 2018) presented similar D/L envelopes for MIS 5 samples from United States Pacific coast marine terraces; although the data are for different taxa, the trends of D/L values are comparable, as are the ranges of D/L values ($\pm 10\%$) for samples of the same age within each envelope. Muhs et al. report GLU and VAL D/L values increasing by $\sim 30\%$ over a temperature range of ~ 2.5 °C, a range similar to that represented in Fig. 8, where GLU D/L values increase by $\sim 35\%$. Corresponding VAL D/L values in *Mulinia* (Appendix B) increase by $\sim 35\%$.

4.4. Linking offshore and onshore aminozones – intergeneric comparisons

Comparison of beach shell AAR results for *Mercenaria* and *Spisula* with results from potential offshore source units requires quantifying the intergeneric relation between the D/L values of these two taxa with those of *Mulinia*, the genus that dominates the results from offshore cores. This relation is shown in Fig. 10, where ASP and GLU D/L values for *Mulinia*, *Astarte*, *Mercenaria* and *Spisula* from offshore cores are plotted when any of the latter three taxa are found at the same core depth as *Mulinia* (Tables 1 and 2). Although no *Astarte* beach samples have been analyzed, the inclusion of *Astarte* results in this plot is important because several of the *Astarte* samples have ^{14}C results (Tables 1 and 2) that provide reference ages (~ 50 ka or greater) for the associated *Mulinia*. Fig. 10 demonstrates that *Mulinia* ASP D/L values

Table 4

Comparison of observed D/L values for ASP and GLU with those predicted by reference regression lines (Fig. 8). Ratio of observed to predicted (O/P) shown in right columns; average of the ASP and GLU O/P values is used as a guide for assigning Mu2, Mu2+, Mu2.5, or Mu2-to to the site cluster values. Included in this analysis are those sites where two or more specimens yielded “similar” results (avoiding sites with widely-divergent results, with the exception of GP, site #83). No results from the 6-h hydrolysis procedure are included.

| Site No. | UDAMS | Other Loc ID | Latitude | Predicted | | Observed | | Obs/Pred | | Avg dev | | Mu zone | Notes |
|---|-------|--------------|----------|-----------|-------|----------|-------|----------|-------|-----------|-------|-----------|-------|
| | | | | ASP | GLU | ASP | GLU | ASP | GLU | ASP & GLU | | | |
| 91 | 07572 | MLD05 | 35.698 | 0.475 | 0.245 | 0.468 | 0.238 | 0.985 | 0.971 | 0.978 | Mu2 | | |
| 89,90 | 07077 | Stetson | 35.864 | 0.472 | 0.241 | 0.481 | 0.247 | 1.020 | 1.023 | 1.022 | Mu2 | | |
| 88 | 07118 | CS80 | 35.873 | 0.471 | 0.241 | 0.480 | 0.236 | 1.018 | 0.979 | 0.998 | Mu2 | | |
| 87 | 07556 | ELP | 35.887 | 0.471 | 0.241 | 0.464 | 0.275 | 0.985 | 1.142 | 1.063 | Mu2 | 3 | |
| 86 | 06258 | VA-2015-01 | 36.602 | 0.457 | 0.224 | 0.459 | 0.224 | 1.005 | 0.999 | 1.002 | Mu2 | | |
| 83 | 06058 | Gomez | 36.785 | 0.453 | 0.220 | 0.452 | 0.259 | 0.998 | 1.177 | 1.088 | Mu2 | 3,4 | |
| 75 | 06204 | Kiptopke | 37.138 | 0.446 | 0.212 | 0.435 | 0.215 | 0.976 | 1.015 | 0.995 | Mu2 | | |
| 79 | 06272 | VA-2017-05 | 37.079 | 0.447 | 0.213 | 0.441 | 0.232 | 0.986 | 1.088 | 1.037 | Mu2 | | |
| 78 | 06273 | VA-2017-06 | 37.103 | 0.447 | 0.213 | 0.477 | 0.238 | 1.068 | 1.119 | 1.094 | Mu2 | | |
| 76 | 06274 | VA-2017-07 | 37.131 | 0.446 | 0.212 | 0.429 | 0.193 | 0.962 | 0.911 | 0.936 | Mu2 | | |
| 77 | 06275 | VA-2017-08 | 37.130 | 0.446 | 0.212 | 0.470 | 0.250 | 1.054 | 1.179 | 1.116 | Mu2+ | | |
| 69 | 06261 | Eyreville 1 | 37.320 | 0.442 | 0.208 | 0.477 | 0.267 | 1.079 | 1.286 | 1.182 | Mu2+ | 3 | |
| 69 | 06261 | Eyreville 2 | 37.320 | 0.442 | 0.208 | 0.535 | 0.345 | 1.210 | 1.658 | 1.434 | Mu2.5 | 3, 5, 7 | |
| 94 | 06310 | CherEst 1 | 37.288 | 0.443 | 0.208 | 0.428 | 0.251 | 0.966 | 1.205 | 1.086 | Mu2 | 3 | |
| 94 | 06310 | CherEst 2 | 37.288 | 0.443 | 0.208 | 0.494 | 0.299 | 1.115 | 1.438 | 1.277 | Mu2.5 | 3, 5, 7 | |
| 70 | 06011 | Ch-13 | 37.300 | 0.443 | 0.208 | 0.462 | 0.245 | 1.044 | 1.178 | 1.111 | Mu2+ | 3 | |
| 64 | 06285 | PARGO4 | 37.559 | 0.437 | 0.202 | 0.431 | 0.179 | 0.985 | 0.886 | 0.936 | Mu2 | 2 | |
| 58 | 06283 | VA-2017-16 | 37.590 | 0.437 | 0.201 | 0.410 | 0.172 | 0.939 | 0.854 | 0.897 | Mu2- | 2 | |
| 56 | 06289 | CEDGO4 | 37.595 | 0.437 | 0.201 | 0.445 | 0.187 | 1.019 | 0.929 | 0.974 | Mu2 | | |
| 55 | 06288 | CEDVO3 | 37.600 | 0.437 | 0.201 | 0.431 | 0.170 | 0.987 | 0.845 | 0.916 | Mu2- | 2, 3 | |
| 51 | 06287 | CEDGO1 | 37.656 | 0.435 | 0.200 | 0.415 | 0.217 | 0.953 | 1.086 | 1.020 | Mu2 | 3 | |
| 43 | 06281 | VA-2017-14 | 37.711 | 0.434 | 0.199 | 0.437 | 0.233 | 1.006 | 1.174 | 1.090 | Mu2 | 3 | |
| 48 | 06263 | VA-2016-02 | 37.736 | 0.434 | 0.198 | 0.464 | 0.247 | 1.070 | 1.248 | 1.159 | Mu2+ | 1,3 | |
| 47 | 06262 | VA-2016-01 | 37.440 | 0.440 | 0.205 | 0.470 | 0.235 | 1.069 | 1.148 | 1.108 | Mu2+ | 1 | |
| 35 | 05393 | MD-2017-06 | 38.161 | 0.425 | 0.188 | 0.413 | 0.194 | 0.971 | 1.032 | 1.001 | Mu2 | | |
| 29 | 06286 | ASSG02 | 38.204 | 0.424 | 0.187 | 0.409 | 0.169 | 0.964 | 0.903 | 0.934 | Mu2 | | |
| 31 | 05004 | Tingles | 38.194 | 0.425 | 0.187 | 0.432 | 0.225 | 1.017 | 1.201 | 1.109 | Mu2+ | 3 | |
| 37 | 05075 | MGS27-1520 | 38.035 | 0.428 | 0.191 | 0.433 | 0.189 | 1.012 | 0.990 | 1.001 | Mu2 | | |
| 36 | 05065 | MGS20-1430 | 38.148 | 0.426 | 0.188 | 0.410 | 0.160 | 0.964 | 0.849 | 0.906 | Mu2- | 3 | |
| 32 | 05063 | MGS18-1248 | 38.187 | 0.425 | 0.187 | 0.420 | 0.206 | 0.989 | 1.099 | 1.044 | Mu2 | 3 | |
| 25 | 05130 | DGS92-16 | 38.475 | 0.419 | 0.181 | 0.416 | 0.179 | 0.993 | 0.990 | 0.992 | Mu2 | | |
| 21 | 05309 | Qj31-20 | 38.543 | 0.418 | 0.179 | 0.435 | 0.202 | 1.042 | 1.127 | 1.085 | Mu2 | | |
| 19 | 05018 | Qj22-06 | 38.559 | 0.417 | 0.179 | 0.441 | 0.221 | 1.057 | 1.236 | 1.146 | Mu2+ | 3 | |
| 23 | 05020 | Qj42-07 | 38.525 | 0.418 | 0.179 | 0.430 | 0.214 | 1.028 | 1.195 | 1.111 | Mu2+ | 3,6 | |
| 22 | 05296 | Qj32-10 | 38.538 | 0.418 | 0.179 | 0.425 | 0.197 | 1.016 | 1.100 | 1.058 | Mu2 | 6 | |
| Four cores with only one <i>Mulinia</i> | | | | | | | | | | | | | |
| | 06275 | Zz82-86 | | | | | | | | | | Mu2+ | |
| | 06254 | Zh31-01 | | | | | | | | | | off trend | |
| | 06270 | Yh54-01 | | | | | | | | | | Mu2+ | |
| | 06253 | Xh54-01 | | | | | | | | | | Mu2 | |

1 evidence of age-mixing in results for *Mulinia* and *Mercenaria*

2 Combined D/L & quantitative data (Appendix C) indicate marginal quality results for all but ASP

3 large (>0.1) difference in deviations

4 two shells only

5 samples with high D/L values at depth in two adjacent cores in Eastville Paleochannel

6 6-h hydrolysis; D/L values converted (see Appendix B)

7 D/L values are between those of Mu2 and Mu3; assigned to Mu2.5

between 0.4 and 0.5 are associated with ASP D/L values in the other three taxa between 0.5 and 0.6; for GLU, the D/L values in all four genera are similar. These ranges of ASP and GLU D/L values for *Mercenaria* and *Spisula* are typical of those found in the Pleistocene shells from the island beaches and onshore Pleistocene units (clusters M2 and S2, respectively).

4.5. Relation between D/L clusters and local stratigraphic sequences

Although the broad regional framework of *Mulinia* D/L values in Fig. 8 is constrained by independent chronologic control at selected sites, it is important to compare AAR results with stratigraphic sequences to demonstrate how D/L values relate to named units at specific sites. These comparisons refer to results identified in Fig. 7, supplemented by the logs for offshore cores and related seismic stratigraphic information as presented in Appendix F.

4.5.1. East Lake Pit, Stetson Pit, CS80, and MLD-06, northeastern North Carolina

Results from these four sites (87–90, 92) in northeastern North Carolina (Fig. 9b) demonstrate the consistency of D/L values when “tested” within both superposed sequences and over a lateral extent of ~25 km, as well as providing a comparison with both OSL and coral U-series ages. Earliest studies of the Stetson Pit site include those by Cronin et al. (1981) and Szabo (1985), where a U-series age of ~70 ka was reported for a coral from an excavation at Stetson Pit. York et al. (1989) reported AAR data for *Mulinia* and *Mercenaria* from a split spoon core taken within ~1 km of the original Stetson Pit excavation, using the U-series results of Szabo (1985) as calibration for the shallowest aminozone found between 7 m and 11 m below sea level (York et al., 1989). York et al. (1989) referred to this as the Upper aminozone and identified Middle and Lower aminozones at depths of ~14 m and >17 m below sea level, respectively (York et al., 1989, Table 1). Only the RP AAR results for samples from the original York collection are discussed here, as these

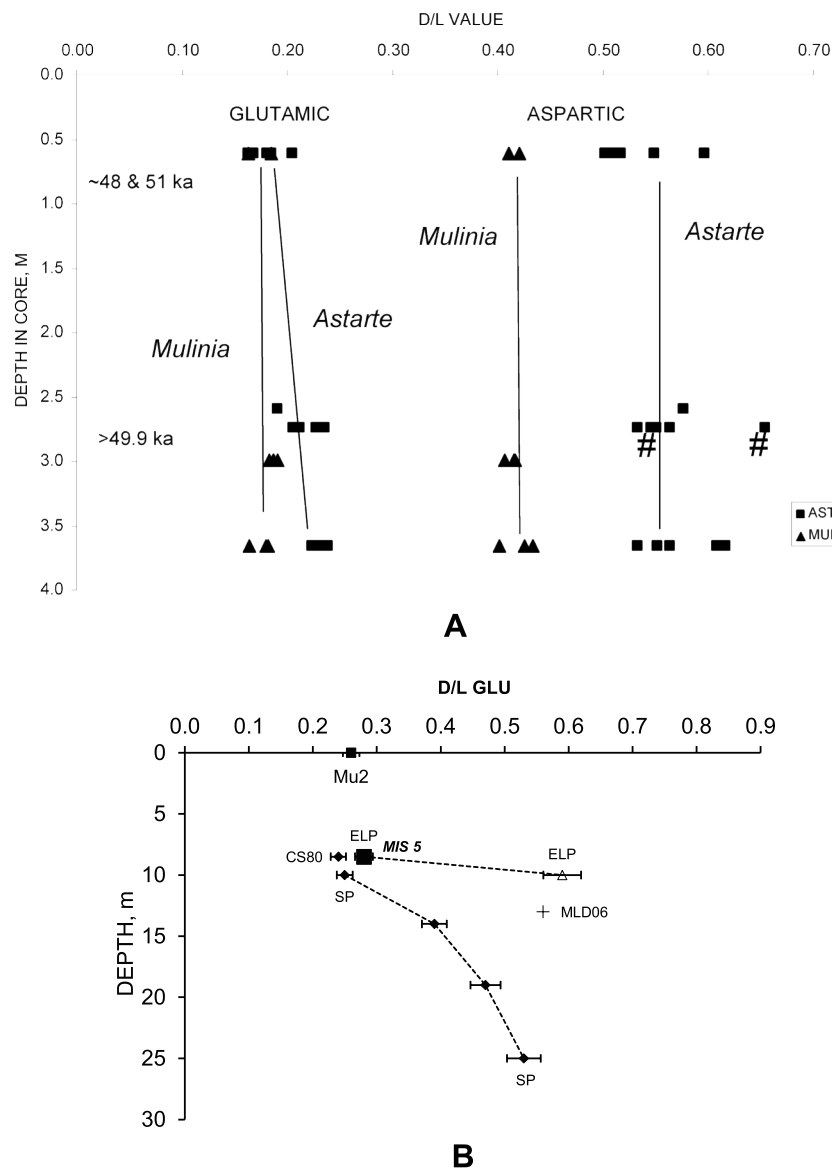


Fig. 9. a. D/L values for ASP and GLU in *Mulinia* and *Astarte* from core DGS92-16 (25), plotted vs. depth in core. ^{14}C calibrated age for two *Astarte* at 0.6 m and one *Astarte* at 2.7 m are listed to the left of the D/L trends in the figure. Two data points marked with # are for repeat analyses of the same shell, where a large difference in ASP D/L was observed. The slight trend of *Astarte* D/L GLU values vs depth is not apparent in the *Mulinia* results for either amino acid. The *Mulinia* results for DGS92-16 (cluster Mu2) are interpreted to represent an age of at least 50 ka based on the limiting ^{14}C ages for *Astarte* in this core. b. D/L GLU values for *Mulinia* from four northeastern North Carolina (Stetson and East Lake Pits, CS80 and MLD06) (sites 87–90, and 92) compared with aminozone Mu2 from Figs. 7 and 8. Only GLU values are plotted for clarity; D/L ASP values are consistent with the observations based on D/L GLU. D/L values are plotted vs. approximate depth below sea level. Lines connect data for multiple depths from Stetson Pit and East Lake Pit. The rectangle along the horizontal axis shows the range of Mu2 values for GLU (~0.26). East Lake Pit has two superposed clusters of results (Mu2 and Mu4), and Mu4 is found at a similar depth at MLD-06, ~1.5 km to the west. Mu2 is found at two sites to the east (Stetson Pit and CS80). The Stetson Pit section also reveals additional D/L clusters at depth, the lowermost one likely corresponding to the Mu4 cluster seen at MLD-06 and East Lake. D/L GLU values from East Lake Pit associated with MIS 5 OSL or U-series results are plotted as a solid square. These samples are from the same stratigraphic position as the Mu2 samples in the East Lake exposure (see Parham et al., 2013; Fig. 17), hence Mu2 at this site is assigned a calibrated age of ~80 ka to ~90 ka (MIS 5a or MIS 5c). This age assignment is consistent with a previous MIS 5a age assignment for the lowest D/L values observed at Stetson Pit (York et al., 1989). OSL data from Parham et al. (2013); U-series results are in Table 2b. See section 4.5.1 for discussion.

results can be compared directly with those for East Lake Pit and MLD-06 (Fig. 9b). At least four aminozones for this region are inferred from the collective RP results.

Two clusters of D/L values are recognized in superposition at East Lake Pit (Mu2 and Mu4), and Mu4 is found at the nearby (~1.5 km) MLD-06 site to the west. Mu2 at East Lake Pit is associated with both U-series and OSL results that collectively represent Marine Isotope Stage (MIS) 5, likely MIS 5a and/or MIS 5c, thereby serving as calibration for the Mu2 aminozone. Mu2 is found also at site CS80, to the east of Stetson Pit, demonstrating the regional extent of this aminozone. Mu3 and Mu4 are found at depth at Stetson Pit, representing middle to early Pleistocene (Wehmiller et al., 2010; 2012). In both the East Lake and Stetson Pit sections (and in other sections in the area – Wehmiller et al., 2010), increasing D/L values are found with increasing burial depth in superposed strata, a fundamental test of the reliability of the results. The Mu2 D/L values for these two sites are slightly higher than those for Delmarva sites (e.g., Fig. 8) because of the latitudinal temperature difference between the regions.

4.5.2. Maryland shelf cores and the identification of aminozones for units Q2 and Q1

For the Maryland shelf results, the sequence of D/L values observed in MGS cores 27–1520, 18–1230 and 18–1248 (37, 33, and 32) is related to the mapping by Toscano et al. (1989), who identified units Q2 and Q1 in superposition in cores 18–1230 and 18–1248, and the single unit Q2 in core 27–1520. Core logs with superimposed AAR data from Toscano et al. (1989) and Appendix B are found in Appendix F. The AAR results (Fig. 7) for Q2 in 27–1520 and 18–1248 cluster tightly as Mu2 (also with results for DGS92-16 (Fig. 9a), cited in section 4.3 and in Appendix F); D/L values for Q1 in both 18–1230 (Mu2.5) and 18–1248 (~Mu3) are significantly higher than in Q2, confirming the age differences in these cores observed by Toscano et al. (1989) for these two cores. Though in broad agreement, differences in the location of the seismic section and sediment cores make it difficult to compare with spatial precision the seismic interpretations of Brothers et al. (2020) and the core results of Toscano et al. (1989). *Spisula* data for the lowermost portions of 18–1230 and 18–1248 show scatter and evidence of contamination, suggesting shell alteration and/or age mixing. These two cores are critical for identification of superposed aminozones in the offshore, so this region of the shelf should be revisited to construct a more detailed

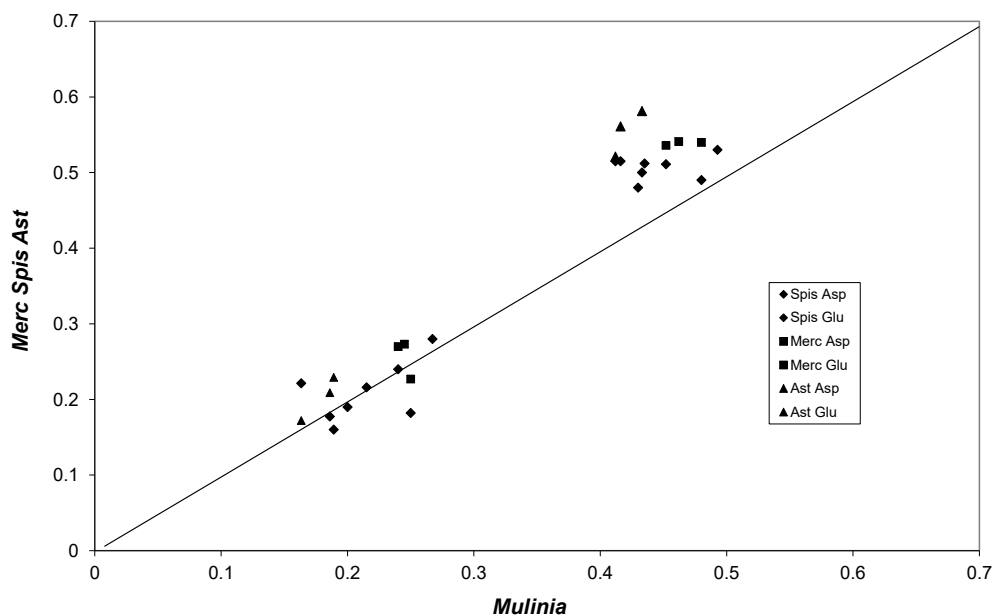


Fig. 10. D/L mean values for ASP and GLU in samples of *Mercenaria*, *Astarte*, and *Spisula* plotted against the corresponding values of ASP and GLU in coexisting *Mulinia*. Data from sites 25, 36, 37, 70, 75–77, 79, 83 and 88 are plotted, as these are the only ones with multiple coexisting samples of two or more of these taxa. These two groups of D/L values are equivalent to the M2 and S2 clusters in Fig. 6; D/L values for *Astarte* are more limited but are similar to the M1 and M2 clusters (Appendix B). The dashed line is the 1:1 relation for comparison. The relation shown here is consistent with the intra-generic racemization rates represented by the regressions in the captions for Figs. 6 and 7.

amino- and seismic stratigraphic sequence.

4.5.3. Southern Delmarva onshore and offshore aminozone correlations

The Mu2 *Mulinia* results from southern Delmarva sites KP (75) and Ch13 (70), reinforced with *Mercenaria* results (M2) from nearby sites CC (72) and EC-1 (73) (Appendix B; Fig. 6a), establish the range of D/L values for *Mixon's* (1985) Butlers Bluff member of the Nassawadox Formation. The D/L values for KP and Ch13 (southern end of Delmarva) are slightly higher than those in the Q2 unit in MGS cores 27–1520 (37) and 18–1248 (32) (Maryland shelf) because of the latitude - temperature difference between the two regions. D/L values for *Mulinia* and *Spisula* from cores offshore of Smith Island (76–79) (Appendices B and F) plot within the Mu2 and S2 clusters, confirming the interpretation of *Brothers et al.* (2020) that the Q2 unit is found in this offshore region. The *Spisula* results (cluster S2) from Smith and Wreck Islands (Fig. 6b) indicate the presence of a nearshore unit aminostratigraphically equivalent to Q2 offshore and the Nassawadox onshore. The cluster of Mu2 D/L values includes results representing the Wachapreague and Sinepuxent formations (see Fig. 4) (*Mixon, 1985; Ramsey, 2010*) along the eastern margin of Delmarva (sites 19–21, 23, 29, 31, 51, 55, 56, 64). Estimates of the age of the Sinepuxent/Wachapreague unit are based on multiple finite ^{14}C results from both shell and organic-rich sediment, in the range of 30–40 ka (*Finkelstein and Kearney, 1988; Owens and Denny, 1978*); *Raff et al.* (2018) reported ^{14}C ages for *Mulinia* and a bulk organic sample from “probable Wachapreague” of ~29 ka and >42.6 ka (infinite age), respectively, at ca. –10 m underlying Parramore Island; the former they recognize as improbable and associated with the common observation of Pleistocene shell carbonate yielding falsely young ages. Their >42.6 ka age and the similar >49 ka sample dated from Delaware shelf core DGS92-16 (25) (see Fig. 9a) provide good minimum-age constraints on the collective AAR results for the Sinepuxent/Wachapreague.

4.5.4. Southern Delmarva: aminozones of the Eastville and Exmore paleochannel fills

The combined Eyreville (69) - Cheriton East (94) and Exmore (66) cores represent filling units of the Eastville and Exmore paleochannels, respectively (*Colman and Mixon, 1988; Colman et al., 1990; Powars and Bruce, 1999; Browning et al., 2009*); these are important Pleistocene reference sections for the regional Delmarva stratigraphy. The Eyreville and Cheriton East results each appear as two overlapping but

superposed groups of D/L values (labeled Estville 1 and Estville 2 in Figs. 7 and 8); the Exmore results cluster around still higher D/L values but show a wide range, probably reflecting some sample alteration (Appendix B). There is a large range of L-SER/L-ASP in the Exmore samples (0.05–0.33), high values being indicative of alteration or contamination (*Kaufman, 2006*). Only five of these samples have L-SER/L-ASP values less than 0.1, values observed in most other *Mulinia* (App. B). The mean ASP and GLU D/L values of these five are 0.596 and 0.413, respectively, roughly 0.02 and 0.03 higher than the grand mean for all 14 Exmore samples. Given the fragile nature of the Exmore shells, even the highest D/L values from the Exmore samples are likely *minimum* values. The Exmore results overlap with those from the combined Omar/Lynch Heights formations (see Fig. 4) in southeastern Delaware (sites 13–15; *Ramsey, 2010; 2011*), implying similar ages.

The Eastville samples (from the Eyreville and Cheriton East cores) represent the Butlers Bluff and possibly the Stumptown members of the Nassawadox Formation (*Mixon, 1985; Fig. 18*), the latest stages of filling and transgression of the Eastville paleochannel. The Exmore samples represent a deeper (~30 m) portion of the unit that fills the Exmore paleochannel (*Powars, 2011*). The two apparent clusters of *Mulinia* D/L values for the Eastville samples are lower than the most reliable values for the corresponding *Mulinia* D/L values in the Exmore core (Fig. 7). This relation is consistent with the relative ages of these two paleochannels (*Colman and Mixon, 1988*). The lower D/L values from the Eastville cores (Estvle 1) plot within or the Mu2 cluster (Fig. 7), but distinctly higher D/L values (Mu2.5) (similar to those from the Q1 unit of MGS18-1230) are also seen (Estvle 2) (Figs. 7 and 8). D/L values for *Ensis* samples from the Eyreville core are also higher than any other *Ensis* results for the region (Appendix B), reinforcing the interpretation of the *Mulinia* data. Sites KP (75) and Ch13 (70), southwest of the Eyreville core site, yielded Mu2 (and M2) D/L values (Fig. 7). The combination of KP, Ch13, and Eastville results indicate that the filling of the Eastville paleochannel is recorded by deposits with both Mu2 and higher (Mu2.5) (~Q1) D/L values (Table 4). This aminostratigraphic sequence is consistent with the interpretation of *Mixon (1985)*, that the Eastville-Nassawadox-Wachapreague-Sinepuxent sequence represents paleochannel incision during a glacial-stage sea-level lowstand followed by deposition during interglacial transgression (Stumptown to Butlers Bluff), and then multiple phases of regressive deposition (Wachapreague-Sinepuxent). *Oertel and Foyle (1995, Fig. 9)* suggested two phases for the evolution of the Nassawadox, the earlier phase possibly being

represented by the Mu2.5 D/L cluster (Estvle 2 in Fig. 7). Numerical ages for the sequence of units related to the Eastville are proposed in section 5.

4.5.5. The aminostratigraphic relation of the Omar-Accomack spit to the Exmore and Persimmon Point paleochannels

The Persimmon Point paleochannel (McFarland and Beach, 2019; Brothers et al., 2020) underlies the northern portion of the landform mapped by Mixon (1985) as the Omar-Accomack (O-A) spit (Figs. 1–3). The O-A spit at its southern end overlies the Exmore paleochannel (Colman and Mixon, 1988; Colman et al., 1990). AAR results for O-A samples are limited to two sites (CW-4 and MF, 38 and 39) where *Mercenaria* results fall in the M4 cluster (Fig. 6a). *Mercenaria* D/L values in this range (ASP ~0.75, GLU ~ 0.50) correspond to equivalent *Mulinia* D/L values of ~0.75 and 0.55 (~cluster Mu4), respectively Figure 7. These equivalent *Mulinia* D/L values are substantially higher than those seen in the Exmore paleochannel fill (~0.60, ~0.40, respectively) (Fig. 7), indicating that the Persimmon Point paleochannel predates the Exmore, consistent with the relations of these two units in the offshore stratigraphy (Brothers et al., 2020).

4.6. Age-mixing, multiple apparent ages in offshore cores, and identification of the potential sources of Pleistocene-age beach shells

The offshore core results indicate that the Mu2 cluster (Figs. 7 and 8) represents the late Pleistocene unit Q2 mapped by Toscano et al. (1989) for the Maryland inner shelf and extended by Brothers et al. (2020) over the full region of the southern Delmarva inner shelf. Unit Q2 is particularly thick (~10 m) and exposed at the seafloor offshore of Smith and Wreck islands, and has been dissected and, in many locations, subsequently filled during Holocene ravinement and transgression. D/L values from cores in the Smith-Wreck region identify Q2 as a source for beach shells on these two islands (Figs. 7 and 8). Similarly, the results for the Pleistocene shells found on the beaches of Parramore, Cedar, and Metompkin islands can be linked to the Mu2 cluster and the equivalent Q2 unit through the intergeneric relation seen in Fig. 10. This is supported by the AAR data from cores penetrating Pleistocene sediments underlying Parramore and Cedar islands (sites 51, 55, 56, and 64), which Raff et al. (2018) and Shawler et al. (2019, 2020) infer to be former pre-Holocene barrier/beach deposits. This conclusion follows Oertel et al. (1989), who suggested the existence of a “barrier platform” underlying the southern Delmarva islands. The AAR results from both offshore and sub-barrier cores indicate that this platform is indeed of Pleistocene age, and equivalent to the regionally thick (0–20 m) and extensive unit Q2 (spanning at least 5100 km², over 160 km N–S) of Toscano et al. (1989) and Brothers et al. (2020).

Although most of our interpretation of the aminostratigraphy of the offshore cores is based on *Mulinia* data simply because of the abundance of this genus, the more limited AAR data for *Astarte*, *Mercenaria*, and *Spisula* from the offshore cores provide insights into either age mixing or possible age differences within these cores. Core DGS92-16 (25) is a particularly useful reference for comparison with other sites because AAR results for four taxa are available, along with paired ¹⁴C ages (Fig. 9a; core log in Appendix F). The results for *Astarte* (all samples analyzed were whole or nearly whole valves) from DGS 92-16 (25; ~23 m MSL) show a subtle trend of increasing D/L GLU values with depth (also for valine and alanine, Appendix B), although the ranges of D/L values for the three sampled depths all overlap and the ASP D/L values do not show this trend (Fig. 9) Two *Astarte* from ~0.6 m core depth have finite ¹⁴C ages (48.1 and 51.5 ka) while a deeper *Astarte* (~2.6 m) returned a ¹⁴C age of >49.9 ka (Table 2a). The D/L trend is not seen in the *Mulinia* data or in the more limited data for either *Spisula* or *Mercenaria* (all fragments) from this core (Fig. 9a; Appendix B, F), and one shallow (~0.6 m core depth) *Mercenaria* from DG92-16 has higher D/L values (M4), indicating that it has been reworked from an older unit. The DGS92-16 results for *Mercenaria* and *Spisula* fall within clusters M2, M4,

and S2. Where *Astarte* are found in other shelf cores, their D/L values fall within the range seen in DGS92-16 (25): 05292 (6); 05056 (30); 05065 (36); 05380 (28); 06254 (45); 06262 (47); and 06265 (52). The possibility of a slight and increasing age difference down-core at site DGS92-16 requires further detailed study, but this core demonstrates the value of multiple analyses whenever possible.

Mercenaria specimens have been obtained from eight Virginia or Maryland shelf cores in this study. These specimens are, with one exception, all fragments representing 50% or less of the shell (usually the robust hinge portion), providing evidence for possible transport. Sample JW2017-306, from Zz82-69 (48), was a complete valve and was subjected to multiple AAR analyses and also serial ¹⁴C analysis. This sample, and most of the other offshore *Mercenaria*, plot in the M2 cluster. Maryland shelf cores with *Mercenaria* include MGS18-1230 (33) and MGS18-1142 (34), with one sample from each core with D/L values equivalent to clusters M2 and M3, respectively. The M2 result is consistent with interpretations of Toscano et al. (1989); the M3 result confirms the original analysis (Toscano et al., 1989) but, based on the overall interpretation of this core, the M3 shell must be reworked from a nearby source unit (likely unit Q1). Core Uj35-03 (28) may have also sampled that source unit, as it contains *Mercenaria* representing three clusters (M1, M2, and M3), all found in a zone at the bottom of the core likely disturbed during coring or storage. In spite of this ambiguity, the AAR results identify a potential source unit at or near the core site.

The seismic stratigraphy of the shallow units in the Chincoteague Bight region of the northern Virginia barrier islands (Fig. 1a) indicates a complex paleodrainage history, suggesting extensive sediment reworking throughout multiple glacial-interglacial cycles (Brothers et al., 2020). This is supported by combined *Mulinia*-*Mercenaria* results for four cores (Zz82-68, -69, -71, and -92: 47, 48, 52, 49) from this area, which indicate sedimentary mixing of material of different ages. For detailed discussion, Appendix F contains four core logs (47–49 and 52) for expanded discussion of the relation between amino- and seismic stratigraphy in this region. For *Mercenaria*, only samples from Zz82-69 (48) and Zz82-92 (49) can be considered as possibly in place based on their physical condition and location within the core. This suggests that the erosion of an older unit in this area contributed shells through reworking. Samples from Zz82-71 (52) have D/L values intermediate between M2 and M3; three analyses of separate portions of the one *Mercenaria* shell demonstrate the magnitude of intra-sample variability, potentially indicative of alteration and serving as reminder about this issue for all analyzed samples, particularly reworked specimens with a complex taphonomic history. Even if all the M3 *Mercenaria* fragments in these cores are not in place, their D/L values serve to identify a source unit in the area, a unit that is also recognized onshore at sites 40, 44, 81–85 and that was likely present on the shelf at one time. The *Mercenaria* D/L results from DGS92-16 and Zz82-69 are shown in Fig. 11, which includes data for onshore samples from clusters M2, M3, and M4. This comparison demonstrates that the both DGS92-16 and Zz82-69 have shell fragments with D/L values comparable to these “old” M3 and M4 aminozones. Similar to *Mercenaria*, AAR analysis of *Mulinia* from cores Zz82-68 (47) and Zz82-69 (48) in this region show a wide range of D/L values that span all of clusters Mu2 and Mu3, suggesting a mixing of samples with a wide range of ages (Appendix B; Fig. 7).

Although the beach collections discussed here do not represent a statistically rigorous geographic distribution of results, several generalizations are warranted. Notably, they represent a wide range of erosional systems. The two southernmost islands, Smith and Wreck, are highly dynamic, experience rapid geomorphic change, and in places, migrate rapidly landward over a shallow platform of backbarrier deposits (Deaton et al., 2017). All analyzed *Mercenaria* from these islands are Holocene, whereas all analyzed *Spisula* are Pleistocene (Table 3). These results require that sediment for these islands is sourced from two units, representing the different habitats of these two taxa and with very different ages. The Wreck collection site lies on a migrating spit that became emergent only in 2012, while the Smith collection site is on a

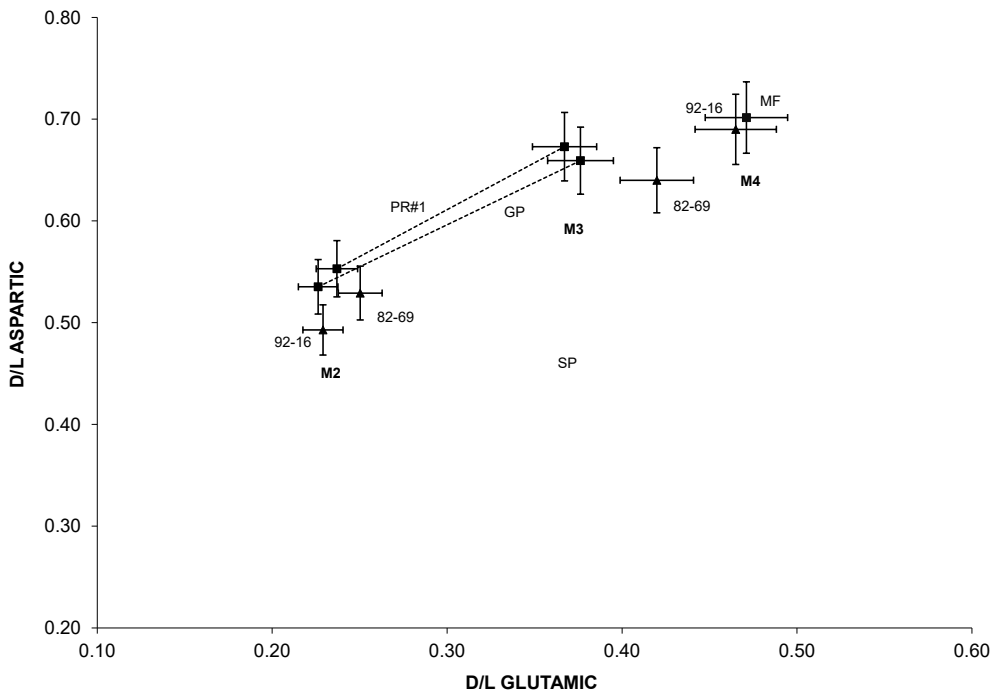


Fig. 11. D/L ASP and GLU in *Mercenaria* from onshore sites Gomez (GP), PR#1, and MF (81–85, 39) compared with *Mercenaria* data from offshore cores DGS92-16 (25) and Zz82-69 (48). Note axes do not include the origin. The results for GP (M2 and M3) are consistent with the stratigraphic superposition of these samples. The dashed lines connect results for two aminozones seen at both GP and PR#1. The results from PR#1 are consistent with the two units at GP and demonstrate age mixing at the PR#1 site, as inferred from prior IE and GC data. The MF results imply a still greater age (cluster M4). Both DGS92-16 and Zz82-69 have *Mercenaria* samples with M2 and higher D/L values (M3 or M4), the latter in samples that are interpreted to have been reworked from an older source unit. Age mixing in Zz82-69 is also evident in the *Mulinia* results (section 4.6). Beach shell results also fall in cluster M2 (Fig. 6a).

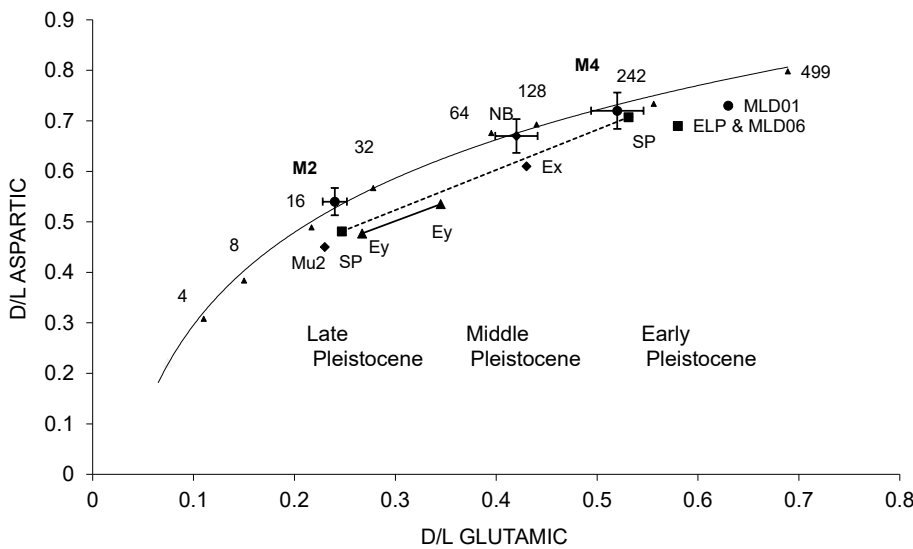


Fig. 12. Numerical age modeling using the elevated temperature intragenetic kinetic pathway of Kaufman (2006) for reference. Co-varying D/L ASP and D/L GLU values from Kaufman (2006) are plotted for different times, as listed above the kinetic curve (e.g., 2, 4, 8, 16 days at 110°). Decreasing incremental changes in D/L values with increasing time along this isothermal curve represent the overall slowing of racemization rates with increasing extent of racemization. Age differences for samples in the present study are inferred from this covariance curve, assuming all samples have the same effective temperature; modeling suggests that age estimates derived from this approach must be assigned a range of at least 10% because of this assumption (e.g., Wehmiller et al., 2000, 2012). Holocene samples are not plotted in Fig. 12 because their history does not include the cooler effective temperatures associated with Pleistocene samples. Mean *Mercenaria* D/L values for specific sites are represented by the M2, M3, and M4 data points as follows: M2, CC (72) and GP(81–84); M3, NB(53, 54); and M4, MF(39). Mean *Mulinia* D/L values for specific sites are represented by Mu2, Mu2.5, Mu3, and Mu4 as follows: (Mu2), KP (75), Ch-13 (70); Eyreville core (69) (two depths, Mu2

and Mu2.5, connected by the solid line); Exmore (66) (Mu3) (highest five values), and Stetson Pit (89, 90) (two depths, Mu2 and Mu4, connected by the dashed line); *Rangia* (Rn), two clusters for this genus from northern Chesapeake Bay (8–11). The two SP clusters represent the Stetson Pit stratigraphic section that spans the interval from late Pleistocene (MIS 5) to early Pleistocene (York et al., 1989; Wehmiller et al., 2010; 2012).

portion of the island that has migrated landward more than 500 m in the past two decades, accelerating during the years immediately prior to sample collection (as observed by Deaton et al. (2017) and from Google Earth time-lapse images). In contrast, northern Parramore is “anchored” on a Pleistocene headland (Raff et al., 2018), erosion of which, on both the shoreface and through inlet incision, provides Pleistocene-age *Mercenaria* (~40% of samples on the Parramore beach are Pleistocene in age) and *Spisula* (~90% of samples are Pleistocene in age). The percentages of Pleistocene shells decrease north of Parramore, where Cedar, Metompkin, Assawoman, and Wallops islands comprise the “arc of erosion” of Chincoteague Bight (Leatherman et al., 1982; Oertel et al.,

2008; McBride et al., 2015; Fenster et al., 2016; Deaton et al., 2017). Pleistocene-aged shells are essentially absent from the beaches of these islands except at the southern end of Metompkin Island. Spatial changes in the distribution of Pleistocene beach shells from these islands is consistent with the variable depths to subsurface Pleistocene units in this coastal segment (Finkelstein and Ferland, 1987; Byrnes, 1988; Shawler et al., 2020).

Storms are the likely cause of many of the major transport “events” that would bring shelly material to the beaches through runup and overwash. At least seven major named storms impacted the Delmarva Islands between 1990 and 2012, as summarized by McBride et al. (2015):

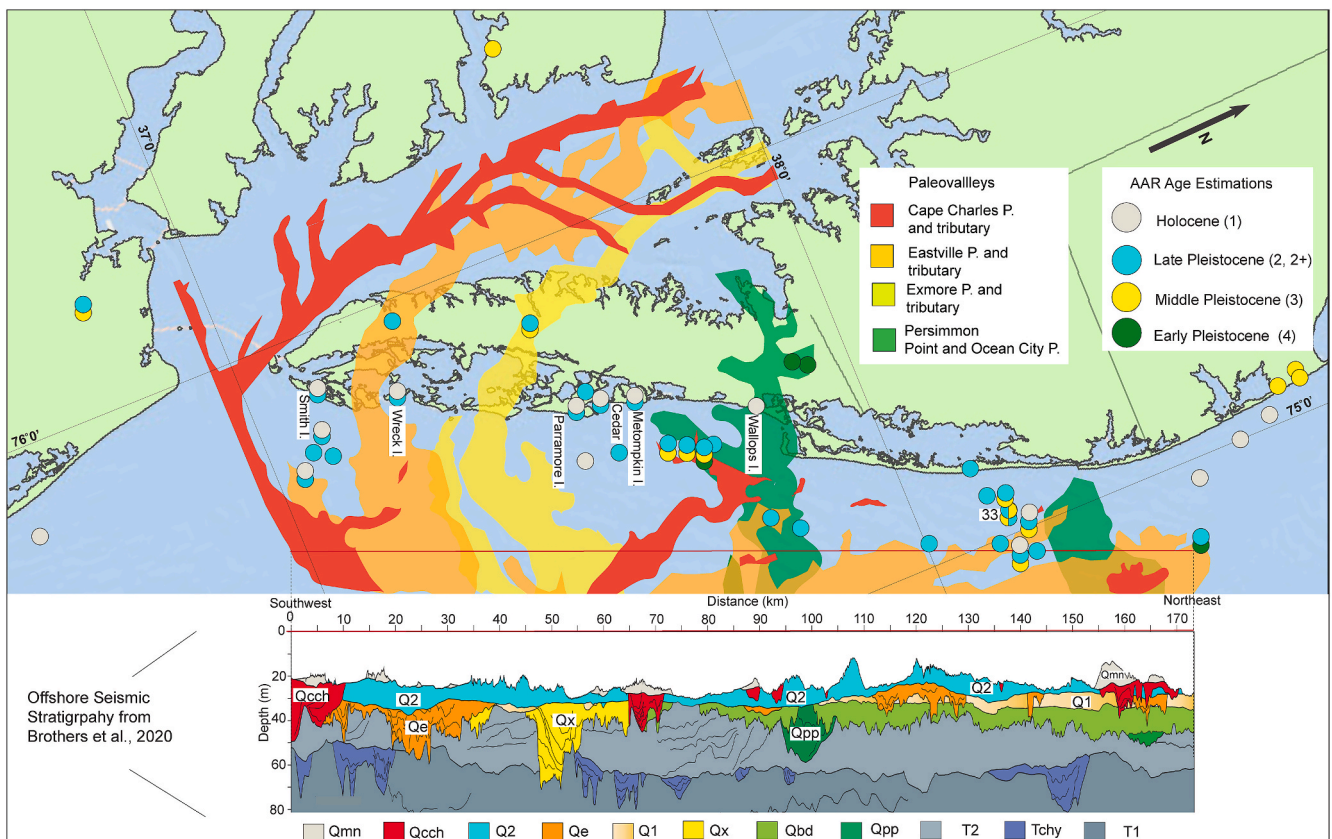


Fig. 13. Summary of regional aminostratigraphy for Delmarva onshore, beach, barrier island, and offshore results. Map of the Delmarva Peninsula showing collection sites (dots), paleochannels (polygons, see Fig. 3 for references) and offshore geologic cross section. Stratigraphy and collection sites represent the Delmarva region from Cape Charles VA to the Maryland-Delaware border (Fig. 1a). Stratigraphic units mentioned in the text are as follows: Qmn = marine nearshore, Holocene unit; Qcch = Fill of the Cape Charles Paleochannel; Q2 = Late Pleistocene estuarine and marine sediments that are not channel fill; Qe = Fill of the Eastville Paleochannel; Q1 = Middle Pleistocene estuarine and marine sediments that are not channel fill; Qx = Fill of the Exmore Paleochannel; Qpp = Fill of the Persimmon Point Paleochannel. For a complete offshore stratigraphic description see Brothers et al. (2020). Sites 1–12, 26, 27, 80, 85, 87–93 not plotted. Color coding is used to identify Holocene and late, middle, and early Pleistocene aminozones. Multiple colors for a single site represent multiple ages, either because of age mixing or because multiple units are found in superposition. The designations 2, 2+, 3, and 4 refer to *Mulinia* (Mu2 through Mu4) clusters, but color coding also represents data for other genera. Onshore, late Pleistocene is found in central and southern Delmarva; middle Pleistocene aminozones are found in the Eastville and Exmore paleochannels where they underlie the Delmarva Peninsula. The early Pleistocene is identified in the northern part of the Omar-Accomack spit, overlying the Persimmon Point paleochannel. The light blue (late Pleistocene) aminozone is found in offshore unit Q2 and in numerous beach and sub-barrier sites. At least one core (33) on the Maryland shelf sampled Q2 and underlying Q1, interpreted as middle Pleistocene in age.

Table 2). Boyajian and Thayer (1995) described the storm transport of large quantities of articulated, living shells to southern New Jersey beaches in a single storm event; this mechanism might be invoked for the Pleistocene shells of the Delmarva islands if the shells had remained articulated, protected, and well-preserved in their host unit until storm-transported and disarticulated at the time of accumulation. The regionally extensive unit Q2 likely serves as that host unit.

5. Discussion: aminozone age estimates

5.1. What time interval is represented by the M2/S2/Mu2 regional aminozone?

Age estimates for Pleistocene units of the mid-Atlantic coastal plain (other than by AAR) are based on either U-series, radiocarbon, or optically-stimulated luminescence (OSL) methods. Detailed site-specific comparisons of multiple methods are rarely available because sample collections are made by different workers and because of the ephemeral nature of most exposures (Lamothe et al., 1998). The age estimates for the Pleistocene beach and offshore shells that represent the M2/S2/Mu2 clusters (and the equivalent offshore Q2 unit) based on both ^{14}C and AAR are critical to the understanding of the late Quaternary relative

sea-level history for the region. Several studies (Mallinson et al., 2008; Scott et al., 2010; Parham et al., 2013), using optically stimulated luminescence (OSL) geochronology, indicate that sediments interpreted as marine in origin were deposited during MIS 3 and are preserved as emergent units at several locations in northeastern North Carolina and southern Delmarva. These age estimates are fundamental components of discussions of ice-volume chronology, sea-level history, and isostatic adjustment (e.g., DeJong et al., 2015; Pico et al., 2017; Creveling et al., 2017; Miller and Andrews 2019). The conceptual model proposed by Scott et al. (2010) and employed by DeJong et al. (2015) identifies two intervals for relative submergence of the mid-Atlantic land surface at roughly 55 ka (early MIS 3) and 70–80 ka (MIS 5a). Only the latter (older) age interval is supported by U-series coral ages from SE Virginia and NE North Carolina (Wehmiller et al., 2004). Our age estimates from paired ^{14}C -AAR analyses must be evaluated in the context of these two possibilities.

The strongest argument in favor of the MIS 5a age assignment for the M2/S2/Mu2 aminozone is the equivalence of most of the offshore AAR results with those from onshore samples that are stratigraphically associated with corals whose U-series ages in the ~75–85 ka range (Figs. 7, 8 and 9b). The combined ^{14}C -AAR results for *Astarte* with “infinite” (or near infinite) ^{14}C ages (sites 6, 25, 28, 30 and 36) do not

rule out the possibility of at least some core samples (all at water depths of at least ~ -20 m – Table 1) dating to ~ 55 –60 ka. Nevertheless, these ^{14}C -AAR results provide a minimum age for associated *Spisula*, *Mercenaria*, and *Mulinia* in these and other offshore cores, thereby demonstrating that many of the “finite” (i.e., 30–45ka) ^{14}C ages on these other taxa must be incorrect (Colman et al., 1989; Pigati et al., 2007; Busschers et al., 2014; Rojas and Martinez, 2016), *Spisula* apparently being particularly vulnerable (Nadeau et al., 2001). The contrast in D/L values between the outer (chalky) and inner (robust) layers of LY92-15 (site 60) (Appendix B, C) demonstrates the effect of shell alteration on D/L values, and similar effects are likely for shell radiocarbon results, although in this particular case the shell yielded a “clean” infinite (>44 ka) ^{14}C result when carefully leached prior to analysis. The likelihood of partial contamination of carbonates with atmospheric carbon is also supported by serial ^{14}C analysis of *Mercenaria* sample JW2017-306 (site 48). Apparent ages differ by more than 5000 years over the sample transect (43.7 ka to 48.8 ka) (Table 2), several orders of magnitude longer than the lifespan of a single organism. Notably, none of the ^{14}C analyses achieve the “infinite” age expected from the paired D/L values for this sample. Nonetheless, this analysis provides further evidence that low-level carbon contamination likely affects many of the shell radiocarbon ages reported here. Shell-bearing units formed during either MIS 3 or MIS 5 would have been sub-aerially exposed during later phases of low sea level, hence vulnerable to diagenetic carbon exchange. The results for Pleistocene *Spisula*, plotted in Fig. 6b can be interpreted to represent incremental additions of inorganic [modern?] carbon, but with no addition of L-amino acids, thereby resulting in falsely young ^{14}C ages with no concurrent decrease in D/L values as compared with the “true” values (those represented by the results for on-shore Pleistocene samples). The relative serine abundance in the ^{14}C -dated samples also does not indicate any significant amino acid contamination (Appendix B). Among the different taxa analyzed here for ^{14}C , only the *Astarte* yielded results near or at the laboratory detection limits of ~ 50 ka (Table 2).

The younger age option (~ 55 ka) for the M2/S2/Mu2 aminozone is within the range of OSL ages obtained in the three major studies of emergent deposits (elevations: -5 to $+8$ m) in the region (Mallinson et al., 2008; Scott et al., 2010; Parham et al., 2013). These units apparently lack shells at the OSL collection sites, hence no direct comparison with AAR methods has occurred. Mallinson et al. (2008) reported OSL ages of 65–80 ka and 40–60 ka for the Sedgefield and Poquoson members, respectively, of the Tabb formation in northeastern North Carolina. Scott et al. (2010), studying sites in southeastern Virginia, reported OSL ages of 39–44 ka for the Poquoson and 33–36 ka for the Sedgefield members. They also report OSL ages for the Wachapreague Formation (39–47 ka) and for the Butler’s Bluff Formation (69 ka) from samples collected on the southern Delmarva peninsula west of Smith Island and near the Kiptopeake site (75). Similarly, in northeastern North Carolina, Parham et al. (2013) reported a range of OSL ages from ~ 35 to ~ 65 ka for samples collected within $\sim \pm 5$ m of present sea level. The OSL ages each have uncertainties of at least 5 ka, but the collective mean value of the OSL results falls somewhere between 45 and 50 ka. The 69 ka OSL age for the Butler’s Bluff Formation on the Delmarva Peninsula can be interpreted as “late MIS 5a” and is consistent with the AAR age estimate for samples from nearby sites; however, this result was rejected by Scott et al. (2010) based on geochemical evidence. Although AAR data are available for shells from many sites proximal to those with OSL results (Wehmiller et al., 2010; Parham et al., 2013; Wehmiller, 2013a), unambiguous comparison of AAR and OSL results is possible at only one site, East Lake Pit (87) as summarized in Fig. 9b. Conversely, OSL, AAR, and U-series results for samples from Moyock Sand Pit (NC) – the only other site with AAR, U-Th, and OSL results – are contradictory, with the OSL results indicating MIS 3 (~ 50 ka, Parham et al., 2013), younger than the MIS 5a ages derived from U-series and AAR (Wehmiller et al., 2010), but these results might be explained by differences in sampling sites within the

excavation. Indirect comparisons of OSL and AAR results are found in Parham et al. (2013, Tables 3 and 4): AAR age estimates listed as 70 to 90 ka have D/L values that fall within the Mu2 cluster reported here and agree with at least some OSL ages for samples in the same region.

Although the number of U-series calibrated AAR results for the M2/S2/Mu2 (Q2) aminozone is small, we conclude that this aminozone represents deposition during all or part of MIS 5 because: 1) the abundance of MIS 5 U-series results (and associated AAR results) in the NC-VA area; 2) the limiting ^{14}C results from the offshore cores; and 3) the consistency of this aminozone at ~ 50 sites (e.g., Table 4, Figs. 7 and 8) over a broad latitude region and within individual, local stratigraphic sequences. The age-resolution capability of AAR within the time-frame 40–100 ka is dependent on many factors, temperature history being the most important (e.g., Wehmiller, 1982: app A). (Miller et al., 1997, 1999) presented an excellent example of racemization (epimerization) over the past ~ 100 kyr in independently dated eggshell samples from Australia, showing that MIS 3 (30–60 ka) can be distinguished from MIS 5 (both 80 ka and 120 ka) but that scatter within the MIS 3 results prevents unambiguous age resolution within the MIS 3 interval. Similarly, D/L values for mollusks from MIS 3 (~ 50 ka) uplifted terrace deposits in Southern California can be resolved from those for MIS 5 samples (Wehmiller, 2013a, and references therein). Mangerud et al. (2008), addressing the question of finite ^{14}C ages, observed a clear trend of D/L vs ^{14}C age within the 30–50 ka range, but we do not see this trend (Fig. 5). These various independent observations imply that it should be possible to resolve MIS 3 (30–60 ka) from MIS 5 (80–130 ka) ages using the AAR results presented here. If MIS 3 deposits are present in the study area, they may only be represented by the limited number ($n = 3$) of aminozone Mu2-results, but even in these few cases the difference in D/L values between Mu2 and Mu2-results is small compared with what would be predicted from the Miller et al. (1999) study. Two of the Mu2-results are for offshore cores (sites 36 and 58) at elevations > 10 m below sea level, and one (site 55) is from a sub-barrier core that sampled the Mu2 unit in nearby cores (51, 56, and 64), suggesting a local example of the inherent variability in these results.

5.2. Contrasting age models for the delmarva Quaternary record: “long” versus “short” chronologies

The interpretation of regional aminostratigraphy and the relative history of Delmarva paleochannels are closely related. The AAR results presented here are relevant to the ages of the Eastville, Exmore, and Persimmon Point paleochannels, but the focus of most prior paleochannel age discussions has been on the Exmore. The time of formation of Exmore paleochannel was interpreted by Colman et al. (1990) to be either MIS 8 or 12, with the paleochannel fill occurring during either MIS 7 or MIS 11, the older ages favored by Colman et al. (1990) based on a body of stratigraphic and geomorphic evidence. This uncertainty reflects contradictory age estimates (by AAR and U-series) for coral and mollusk samples from the Omar-Accomack region (MF, 39) on Delmarva and the Norris Bridge site (53, 54) on the western shore of Chesapeake Bay, as reviewed by Mixon et al. (1982: Figs. 4, 5), Szabo (1985), Wehmiller et al. (1988), and Wehmiller (2013a). The original mollusk AAR data for these sites were grouped in a “mid-Pleistocene” aminozone (~ 400 ka); the U-series coral results assigned ages of 187 ± 20 ka to Norris Bridge (53) and $340 + 137/-66$ ka to the Matthews Field (39) site from the Omar-Accomack Spit (Figs. 1–3). Mixon et al. (1982) and Szabo (1985) interpreted the 340 ka age as a maximum age and concluded that the 187 ka result was the correct age for both samples, conforming to Mixon’s interpretation that the MF and NB sites were correlative and synchronous. The new RP data instead indicate that MF is older than NB (see Fig. 6a), consistent with the age difference implied by the U-series results and even some subtle differences in original AAR data (Wehmiller et al., 1988). The contrast between the MIS 7 and MIS 11 age estimates for the Exmore paleochannel fill is an example of conflicts between “short” (less than 200 kyr) and “long” (up to ~ 1000 kyr)

chronologies for the Quaternary record in the mid-Atlantic (York et al., 1989; Wehmiller, 2013a). The depositional model proposed by Scott et al. (2010) assigns the Exmore paleochannel to MIS 6, significantly younger than either of the optional ages proposed by Colman et al. (1990). The AAR age estimate (M4) for sites CW-4 and MF (38 and 39) constrains the age of stratigraphically older Persimmon Point paleochannel (McFarland and Beach, 2019).

Using an independent approach for interpreting the age implications of the RP data from these sites, we suggest that the 187 and 340 ka U-series ages for the Norris Bridge and Mathews Field sites are both minimum ages and that shell samples from the two sites are distinctly different in age (Clusters M3 and M4, Fig. 6a). This approach is outlined in Fig. 12, which uses the covariance of ASP and GLU D/L values from elevated laboratory kinetic experiments (Kaufman, 2006) to quantify the relative age differences represented by incremental increases in D/L values for known time intervals. This empirical approach does not invoke any specific kinetic model for estimating ages (e.g., review by Clarke and Murray-Wallace, 2006), similar to the “model-free” approach of Tomiak et al. (2013). Wehmiller et al. (2010, section 7.2) used this same approach to estimate relative age differences represented by different clusters of D/L values observed in Pleistocene *Mulinia* samples from cores in the Albemarle Embayment, North Carolina. For clarity, Fig. 12 includes only results for the M2 and M4 *Mercenaria* clusters (plus the D/L values for NB), the Mu2, Exmore, and Eastville *Mulinia* clusters, and selected results from the long section at Stetson Pit NC. For reference, Fig. 12 shows the lowest and highest D/L values for the Stetson Pit superposed section (89, 90); Appendix B; Figs. 7 and 8), as these values represent a majority of the Quaternary section in NC (York et al., 1989; Wehmiller et al., 2010; 2012); the higher (older) Stetson Pit D/L values represent an age approximately 10 times greater than the lower (younger) values. The mean ASP and GLU D/L Exmore values of 0.61 and 0.43, as compared with the Mu2 *Mulinia* values from the Exmore region (0.45 and 0.21, respectively) represent more than a four-fold increase in age when compared with the Kaufman (2006) covariance curve. If the Mu2 aminozone represents all or part of MIS 5 (i.e., 80 to 130 ka), then the Exmore results are interpreted to represent between 320 and 520 ka using the minimum four-fold factor. The two Eastville clusters plot slightly to significantly above the Mu2 cluster, suggesting an approximate two-fold age difference, but with both being younger than the Exmore age estimate. Browning et al. (2009) reported $^{87}\text{Sr}/^{86}\text{Sr}$ age estimates from shell carbonate samples in this same Eyreville depth interval of between 240 and 740 ka. Although the Sr-isotope results span a large age range, they all imply an age greater than MIS 5, hence the combined AAR and Sr ages indicate that units representing MIS 5 and MIS 7 or MIS 9 are preserved on the basal flanks of the Eastville paleovalley, supporting the model of Oertel and Foyle (1995) for the multi-phase evolution of southern Delmarva. Fig. 12 also shows the ASP and GLU values for *Mercenaria* from specific sites within the M2, M3, and M4 clusters to compare results for sites with associated U-series data (GP, NB, MF; 81–84, 53/54, and 39). The covarying trends for *Mercenaria* and *Mulinia* are parallel with those for the heating experiment data, with offsets caused by genus-specific differences in relative kinetics (e.g., Figs. 6 and 7). The estimated age for the M4 group (sites MF and CW-4 (39, 38) is approximately 8–10 times that of the M2 group, or roughly 600 to 1200 ka, while the age of the NB site is approximately 4–5 times that of the M2 group (~320–600 ka). The MF and CW-4 ages are consistent with Sr-isotope calibrated AAR age estimates from the Albemarle Embayment of North Carolina (Wehmiller et al., 2012). One sample with nearly racemic D/L values (D/L GLU ~0.9; Appendix B) from the underlying Neogene Yorktown Formation at the CWW site (41; Belknap, 1979; Belknap and Wehmiller, 1980) is estimated by this approach to be 3–4x older than the M4 group, or approximately 3000 ka. Although this modeling approach yields age estimates with relatively large uncertainties because it assumes equivalent effective temperatures for all samples (see Wehmiller et al., 2012 for discussion), the collective AAR results support a mid-Pleistocene age for the formation of the

Exmore paleochannel. Similarly, we assign an early Pleistocene age to the Persimmon Point paleochannel based on local stratigraphy and the AAR results for sites 38 and 39 (Mixon, 1985; McFarland and Beach, 2019). The Exmore *Mulinia* D/L values are greater than those seen in the Q1 unit (Maryland shelf sites 32, 33), consistent with the Q1-Exmore relation mapped in the offshore by Brothers et al. (2020). Because no offshore cores penetrated the units identified by Brothers et al. (2020) as either Eastville- or Exmore-correlative, the relation between the offshore Q1 D/L values and the onshore Exmore D/L values is a fundamental link in the regional aminostratigraphy.

Age estimates for the Eastville-Exmore paleochannel system can also be inferred from AAR data for *Rangia* from Quaternary units in central and northern Chesapeake Bay (Fig. 1). Genau et al. (1994) discussed limited *Rangia* results from a vibracore on Taylors Island, Md (23), results that are re-evaluated here in light of new data and a better understanding of the relation of the Taylors Island samples to the underlying paleochannels. The *Rangia* results are in two clusters of RP D/L values (Appendix B), plotted in Fig. 6a, similar to the M2 and M3 clusters observed for *Mercenaria*. The *Rangia* cluster with higher D/L values is observed at Norris Bridge (53), Poplar Creek Bluff (27), Taylors Island (26), and Edgewood (8–10). The latter two sites represent units that fill paleochannels within the central and northern Chesapeake Bay (Colman and Mixon, 1988; Dunbar et al., 2001). A *Rangia* cluster with lower D/L values is also observed in a separate paleochannel in the northern Chesapeake (Hughes, 1991; Dunbar et al., 2001), a cluster also apparent in the GC data obtained by Belknap (1979, Fig. 40) for a subsurface unit at Worton Point, Maryland (12). The Taylors Island results are interpreted to represent the latest stage of filling of the Exmore paleochannel, which underlies the Taylors Island region (Colman and Mixon, 1988; Genau et al., 1994; DeJong et al., 2015). This interpretation contradicts that of Genau et al. (1994), but is based on a re-evaluation of the original GC data for the Taylors Island samples, the actual relation of the Taylors Island collection site to the subsurface paleochannels (Jacobs, 1980; Colman and Halka, 1989), and the regional consistency of all the RP *Rangia* results presented here. We suggest that cluster of higher *Rangia* D/L values represents a post-Exmore paleochannel flooding “event” in the central and northern Chesapeake. The age difference between the two *Rangia* clusters can be estimated using the model presented in Fig. 12: if the lower and higher D/L *Rangia* clusters represent the units that fill the Eastville and Exmore paleochannels, respectively, then the age of the older cluster is estimated to be approximately 4 times older than that of the younger cluster. This age range is consistent with that inferred from *Mulinia* data for samples that can be linked directly to the Exmore paleochannel fill.

The modeling approach seen in Fig. 12 provides quantitative insight into the possible age range represented the Mu2 cluster. For example, in the region between 37.5° and 37.8° N (Fig. 8), the *Mulinia* ASP and GLU values range from 0.41 to 0.47 (ASP) and 0.18 to 0.24 (GLU), within the Mu2 cluster. Assuming that no factors other than age differences are responsible for these ranges, the samples with the higher D/L values are estimated to be about 1.5x older than those with the lower D/L values. This range is consistent with Mu2 likely representing all of MIS 5 (75 ka to 130 ka).

5.3. Synthesis

The sites from this study and their associated aminozones or data clusters derived from Figs. 6 and 7 and Table 4 are listed in Table 5 (an expanded version of Table 5 is in Appendix G). We assign the results from all sites in this paper to broadly defined age ranges: either Holocene, late, middle, or early Pleistocene. Based on paired ^{14}C -AAR analysis, direct association, or intergeneric relations, clusters M1, S1, and Mu1 represent Holocene ages; based on associated U-series results and limiting ^{14}C ages, clusters M2, S2 and Mu2 represent the late Pleistocene (MIS 5). Clusters M3 and Mu3 are interpreted to represent middle Pleistocene (~200–500 ka), and clusters M4 and Mu4 likely represent

Table 5

AAR data clusters and age estimates. Sites with map reference # (Table 1) are grouped from Holocene through early Pleistocene. For the *Mulinia* (Mu) clusters, deviations from the latitude regressions are summarized in Table 4. If the deviations are significant, then the results are labeled either as Mu2+, Mu2.5, or Mu2-. In several cases multiple ages are found at a site, either because of age-mixing or because of two units in stratigraphic superposition. Age estimates are based on the associated AAR clusters and their independent calibrations. Stratigraphic units are identified where an unambiguous assignment can be made.

| Site # | Type of Collection | Isotopic ages | Ast** | Merc | Mul | Spis | Ran** | Offshore seismic unit | Onshore lithostratigraphic unit | Stratigraphic age; comments |
|--|----------------------|---------------------------|-------|---------|--------|------|-------|------------------------------------|---------------------------------|-----------------------------|
| Holocene fill and shallow shelf deposits; mix of Holocene and late Pleistocene shells | | | | | | | | | | |
| 17 | Offshore core | | | | Mu1 | S1 | | Shoal? | | Hol |
| 24 | Offshore core | | | | Mu1 | | | Shoal? | | Hol |
| 80 | Offshore core | Multiple Holocene | A1 | M1 | | S1 | | Shoal | | Hol |
| 16 | Offshore core | 14C ages | | M1 | | | | Shoal? | | Hol |
| 42 | Beach | | | M1 | | | | | Beach | Hol |
| 46 | Beach | | | M1 | | | | | Beach | Hol |
| 67 | Offshore core | | | | | S1 | | Shoal? | | Hol |
| 60 | Beach | Some reworked Pleistocene | | M1 | | S2 | | | Beach | Hol and Late P mixed |
| 59 | Beach | | | M1 | | S1 | | | Beach | Hol and Late P mixed |
| 57 | Beach | 14C ages | | M1 | | | | | Beach | Hol and Late P mixed |
| 50 | Beach | | | M2 | | | | | | |
| | | | | M1 | | | | | Beach | Hol and Late P mixed |
| | | | | M2 | | | | | | |
| 71 | Beach | | | M1 | | S2 | | | Beach | Hol and Late P mixed |
| 74 | Beach | | | M1 | | S2 | | | Beach | Hol and Late P mixed |
| 86 | Offshore core | | | | Mu2 | S1 | | Shoal? | | Hol and Late P mixed |
| 61 | Beach | | | M1 | | | | | Beach | Hol and Late P mixed |
| | | | | M2 | | | | | | |
| 62 | Beach | | | M1 | | S1 | | | Beach | Hol and Late P mixed |
| | | | | M2 | | S2 | | | | |
| MIS 2 incision; Cape Charles paleovalley; offshore unconformity 10 | | | | | | | | | | |
| Late Pleistocene shelf, sub-barrier, paleovalley fill, and onshore units | | | | | | | | | | |
| 21 | Inland core | | | | Mu2 | | | | Sinepuxent | Late P |
| 12 | Inland core | | | | | | ~ M2 | | Paleochannel fill | Late P |
| 19 | Inland core | | | | Mu2+ | | | | Sinepuxent | Late P |
| 23 | Inland core | | | | [Mu2+] | | | | Sinepuxent | Late P |
| 30 | Offshore core | 51.6 ka 14C | A2 | | | S2 | | Q2 | | Late P |
| 34 | Offshore core | 37.4 ka 14C | | M3 (r) | | S1 | | Q2 | | Late P |
| | | | | | | S2 | | | | |
| 36 | Offshore core | 48.5 ka 14C | A2 | | Mu2- | S2 | | Q2 | | Late P |
| 37 | Offshore core | | A2 | | Mu2 | S2 | | Q2 | | Late P |
| 8 | Excavation/ Exposure | | | | | | ~ M2 | | Paleochannel fill | Late P |
| 11 | Inland core | | | | | | ~ M2 | | Paleochannel fill | Late P |
| 25 | Offshore core | 46.3 to >49.9 ka 14C | A2 | M2 (M3) | Mu2 | S2 | | probable Q2 | | Late P |
| 9 | Excavation/ Exposure | | | | | | ~ M2 | | Paleochannel fill | Late P |
| 1 | Offshore core | | | | | S2 | | MIS 3 or 5: Uptegrove et al., 2012 | | Late P |
| 2 | Offshore core | | | | | S2 | | MIS 3 or 5: Uptegrove et al., 2012 | | Late P |
| 3 | Offshore core | | | | | S2 | | MIS 3 or 5: Uptegrove et al., 2012 | | Late P |
| 4 | Offshore core | | | | | S2 | | MIS 3 or 5: Uptegrove et al., 2012 | | Late P |
| 22 | Inland core | | | | [Mu2] | | | | Sinepuxent | Late P |
| 35 | Offshore core | | | | Mu2 | | | probable Q2 | | Late P |
| 68 | Inland core | | | M2 | | | | | Nassawadox | Late P |
| 70 | Inland core | | | M2 | Mu2+ | | | | Nassawadox | Late P |
| 63 | Inland core | | | M2 | | | | | Nassawadox | Late P |
| 65 | Inland core*** | | | | {Mu2} | | | | Wachapreague | Late P |
| 72 | Inland core | | | M2 | | | | | Nassawadox | Late P |
| 73 | Inland core | | | M2 | | | | | Nassawadox | Late P |
| 83 | Excavation/ Exposure | | | | [Mu2+] | S2 | | | Sedgefield | Late P |
| 7 | Offshore core | | A2 | | | | | NJ shelf | | Late P |
| 75 | Inland core*** | | | M2 | Mu2 | S2 | | | Nassawadox | Late P |
| 45 | Offshore core | | A2 | | [Mu2?] | S2 | | Q2 likely only 1 Mu1 | | Late P |
| 47 | Offshore core | | A2 | M2 | Mu2+ | | | Q2 base or older; mixing | | Late P |

(continued on next page)

Table 5 (continued)

| Site # | Type of Collection | Isotopic ages | Ast** | Merc | Mul | Spis | Ran** | Offshore seismic unit | Onshore lithostratigraphic unit | Stratigraphic age; comments |
|--|-----------------------------|----------------|-------|------|---------|------|-------|---|---------------------------------|---|
| 48 | Offshore core | 46.6 ka 14C | | M2 | Mu2+ | | | Q2 base or older; mixing | | Late P |
| 52 | Offshore core | | A2 | M2 | | S2 | | Qbd or Qpp; mixing/lag deposit | | Late P |
| 43 | Offshore core | | | | [Mu2+] | S2 | | Q2 likely | | Late P |
| 79 | Offshore core | 6.65 ka 14C | | M1 | Mu2 | | | Holocene over Q2 | | Late P; altered Q2 samples? |
| 78 | Offshore core | | | | Mu2 | | | Qmn Qcch | | Late P; lag deposit in Holocene? |
| 76 | Offshore core | | | M1 | Mu2 | S2 | | Q2 definite | | Late P |
| 77 | Offshore core | | | | [Mu2+] | S2 | | Q2 likely | | Late P |
| 49 | Offshore core | | | M2 | Mu2 | | | Q2 with reworked sample (Qpp lower in core) | | Late P |
| | | | | M3? | | | | | | |
| 58 | Offshore core | | | M2 | Mu2- | | | Q2 unlikely at the depth of Mu2 data; Mixing? | | Late P |
| 64 | Barrier island core | 29; >42 ka 14C | | | Mu2 | | | | Wachapreague | Late P |
| 29 | Barrier island core | | | | Mu2 | | | | Sinepuxent | Late P |
| 51 | Barrier island core | | | | Mu2 | | | | Wachapreague | Late P |
| 55 | Barrier island core | | | | Mu2- | | | | Wachapreague | Late P |
| 56 | Barrier island core | | | | Mu2 | | | | Wachapreague | Late P |
| 88 | Inland core | >39.7 ka 14C | | M2 | Mu2 | S2 | | | Sedgefield? | Late P |
| 91 | Inland core | | | | Mu2 | | | | Sedgefield? | Late P |
| 81 | Excavation/ Exposure | MIS 5 U-Th | | M2 | | S2 | | | Sedgefield | Late P |
| 28 | Offshore core | 44.8 ka 14C | A2 | M1 | | | | Q2? | mixing | Late P? mixing |
| | | | | M2 | | | | | | |
| | | | | M3 | | | | | | |
| Sections with Late Pleistocene over older Pleistocene units: Maryland and New Jersey shelves; superposed sections in VA and NC; and Eastville Paleochannel fill | | | | | | | | | | |
| 33 | Offshore core | | | M1 | Mu2 | S2? | | Q1; Q2 | | Late and late middle P |
| | | | | | Mu2.5 | | | | | |
| 32 | Offshore core | | | | Mu2 Mu3 | S2 | | Q1 (?); Q2 | | Late and late middle P; Q1 uncertain because of limited seismic control |
| 5 | Offshore core | | | M4+ | | S2 | | NJ shelf | | Late over early P |
| 6 | Offshore core | >52 ka 14C | A2 | M4+ | | S2 | | NJ shelf | | Late over early P |
| 85 | Excavation/ Exposure | | | M2 | | S2 | | | Pungo Ridge | Late and middle P mixed |
| | | | | M3 | | | | | | |
| 84 | Excavation/ Exposure | | | M2 | | S2 | | | Sedgefield | Late and middle P |
| | | | | M3 | | | | | | |
| 89 | Inland core*** | | | | Mu2 Mu3 | | | | multiple | Late to Early P |
| | | | | | Mu4 | | | | | |
| 90 | Inland core*** | | | | Mu2 Mu3 | | | | multiple | Late to Early P |
| | | | | | Mu4 | | | | | |
| 87 | Excavation/ Exposure | MIS 5 U-Th | | | Mu2 Mu4 | | | | multiple | Late and Early P |
| 69 | Inland core | | | | Mu2+; | | | | Nassawadox/ Stumptown | Late middle & late P |
| | Eastville Paleochannel fill | | | | Mu2.5 | | | | | |
| 94 | Inland core | | | | Mu2; | | | | Nassawadox/ Stumptown | Late middle & late P |
| | Eastville Paleochannel fill | | | | Mu2.5 | | | | | |
| Incision of Eastville paleovalley (~MIS 6) and creation of offshore unconformity 8 | | | | | | | | | | |
| Middle to Early Pleistocene paleovalley fill and onshore units | | | | | | | | | | |
| 27 | Excavation/ Exposure | | | | | | ~ M2 | | Paleochannel fill | Middle P |
| 26 | Inland core | | | | | | ~ M3 | | Paleochannel fill | Middle P |
| 10 | Inland core | | | | | | ~ M3 | | Paleochannel fill | Middle P |
| 15 | Inland core | | | | Mu3 | | | | Omar | Middle P |
| 13 | Inland core | | | | Mu3 | | | | Omar | Middle P |
| 14 | Inland core | | | | Mu3 | | | | Omar | Middle P |
| 51 | Excavation/ Exposure | | | | | | ~ M3 | | Shirley | Middle P |
| 82 | Excavation/ Exposure | | | M3 | | | | | Sedgefield | Middle P |
| 66 | Inland core | | | | Mu3 | | | | Exmore paleochannel fill | Middle P |
| Incision of Exmore paleovalley (~MIS 6) and creation of offshore unconformity 6 | | | | | | | | | | |
| 53 | Excavation/ Exposure | | | M3/ | | | | | Shirley | Early/middle P |
| | | | | M4 | | | | | | |
| 40 | Inland core | | | M3/ | | | | | Accomack Mbr, Omar | Early/middle P |
| | | | | M4 | | | | | | |

(continued on next page)

Table 5 (continued)

| Site # | Type of Collection | Isotopic ages | Ast** | Merc | Mul | Spis | Ran** | Offshore seismic unit | Onshore lithostratigraphic unit | Stratigraphic age; comments |
|--------|--------------------|---------------|-------|-----------|--|------|-------|-----------------------|---------------------------------|-----------------------------|
| 44 | Inland core | | | M3/ M4 | | | | | Accomack Mbr, Omar | Early/middle P |
| 39 | Inland core | | | M4 | | | | | Accomack Mbr, Omar | Early P |
| 38 | Inland core | | | M4 | | | | | Accomack Mbr, Omar | Early P |
| 93 | Inland core | | | | Mu4 | | | | | Early P |
| 92 | Inland core | | | | Mu4 | | | | | Early P |
| 41 | Inland core | | | | <i>Incision of Persimmon Point paleovalley and creation of offshore unconformity 4</i> | | | M4+ | Yorktown | Neogene |

* Uncalibrated.

** Rangia & Astarte ~ Mercenaria.

*** IE data also.

[] uncertain because of limited or scattered results.

multiple ages within the middle and early Pleistocene (~500 ka to ~1000 ka). Cluster Mu2.5 is distinct from both Mu2/2+ and Mu3 and is significant because it represents the offshore Q1 unit and an older unit within the Eastville paleochannel fill. The three major Pleistocene aminozones identified here (M2-S2-Mu2; M3-Mu3; M4-Mu4) are broadly correlative with the three major aminozones (AZ2, AZ3, and AZ4) described by Wehmiller et al. (2010; 2012) for the Albemarle Embayment, eastern North Carolina, also representing late, middle, and early Pleistocene, respectively.

If multiple zones are listed in Table 5, then either age mixing or superposition is implied. Brackets imply that the zone designation is based on taxa other than *Mulinia*. A plus (+) or minus (-) sign is listed if the D/L values are thought to be above or below the “typical” aminozone value (see Table 4). In some cases, the relation between an aminozone and the associated seismic unit is unambiguous, but in cases where samples were collected at an unconformity, they could represent either or both the unit above or below the unconformity. In general, Mu2 corresponds to offshore stratigraphic unit Q2; Mu3 corresponds stratigraphic unit Q1 in the two cores from the Maryland shelf (32, 33, Table 5; Fig. 7). The distribution of these late, middle, and early Pleistocene aminozones is summarized in Fig. 13, which uses color-coded symbols for the AAR results to link the offshore seismic stratigraphy of Brothers et al. (2020) to the onshore, sub-barrier, and beach sample chronology established here. Fig. 13 demonstrates the frequent occurrence of late Pleistocene shell material (all or part of MIS 5) on the shelf, on beaches, beneath barrier islands, and in onshore units. Samples of middle and early Pleistocene age samples are recognized in several subsurface sections in NC, VA, and DE including the Exmore paleochannel, an important stratigraphic feature in the history of the Delmarva peninsula. Middle Pleistocene (pre-MIS 5) samples are found on the mid-Atlantic shelf at a limited number of sites, likely reworked but identifying the presence of these older unit(s) on the mid-Atlantic shelf.

6. Conclusions

6.1. Implications for AAR methods, modeling, and sampling strategies

Because multiple taxa are needed for a comprehensive study such as this, the comparability of results between taxa must be understood. Some amino acids appear more reliable in some taxa than in others, either because of the relative abundance of those amino acids or because of the inherent age-resolution capability within the D/L interval in question. Although the focus of the present study is on results obtained using the reverse-phase (RP) AAR method, we conclude this newer method has reinforced or confirmed conclusions based on earlier GC or IE methods (e.g., Toscano and York, 1992; Toscano, 1992). D/L values for aspartic acid (ASP), abundant in all the taxa studied, are generally useful for distinction between Holocene and late Pleistocene samples

(and even within the Holocene), but the declining rate of racemization of ASP makes this amino acid less useful in older samples, except at low-resolution. D/L values for glutamic acid (GLU), also usually abundant, also successfully resolve Holocene and late Pleistocene samples and become more useful as a tool for defining aminozones within the middle Pleistocene. Results for other amino acids can be used to “refine” interpretations based on ASP and GLU results.

The taxa used in this study vary in their utility for several reasons. The small and generally thin-shelled *Mulinia* are the most abundant in offshore cores but are potentially most susceptible to diagenetic alteration or contamination. Hence, multiple analyses must be conducted to determine the most representative D/L value for a specific unit based on this genus. Because of the abundance of *Mulinia* results, we have been able to recognize the regionally extensive Mu2 aminozone, interpreted as MIS 5, that represents offshore unit Q2, which is nearly continuous on the Delmarva shelf, with correlative units south of the mouth of Chesapeake Bay in North Carolina. Conversely, robust *Mercenaria* samples provide the opportunity to investigate the chemical integrity of the shell with multiple AAR analyses, but intra-sample variability for this genus is a more significant issue, especially when subsamples as small as ~5 mg are taken from these large (~100 g or more) shells. One conclusion from this and other studies (Wehmiller et al., 1995; 2015) is that both *Mercenaria* and similarly large *Spisula* can survive reworking, hence any aminostratigraphic studies based on these or other taxa must consider this process. Results from onshore site 85 and offshore sites 25, 28, 49, and 48 demonstrate that the modern age-mixing processes observed at beach and shelf sites have also occurred during deposition and erosion of offshore units during the Pleistocene. Results from the Chincoteague Bight region demonstrate that Interpretation of AAR data from dynamic coastal environments often requires iterative evaluation of subtle factors such as mixing, sample alteration, and detailed understanding of core stratigraphy.

In a few cases the new RP results have led to a reinterpretation of local or regional aminostratigraphic relations. Important examples include the original results for *Rangia* samples from the Taylors Island site, central Chesapeake Bay (26), and an alternative approach to the interpretation of both relative and numerical ages of the critical Mathews Field and Norris Bridge sites (39 and 53/54). This new interpretation is internally consistent with current knowledge about the relative ages of the major Quaternary paleochannels underlying the Delmarva Peninsula.

6.2. Reliability of ^{14}C ages for Pleistocene mollusks

The reliability of ^{14}C ages obtained on Pleistocene mollusk carbonate has been debated for almost as long as the ^{14}C method has been available. The present study contributes some insight into this discussion, as it has employed paired ^{14}C -AAR analyses of individual shells to compare

age interpretations based on the two methods. The principal conclusion is that ^{14}C ages within the range $\sim 28\text{--}\sim 45$ ka obtained on samples of *Mercenaria* or *Spisula* from either beach or offshore sites are anomalously young. In all cases, the D/L values from these paired ^{14}C -AAR analyses fall within the range of D/L values observed for samples from onshore emergent sites, some of which are independently “calibrated” as being ~ 80 ka (MIS 5a) in age.

Several *Astarte* samples analyzed in this study have returned “infinite” or “near infinite” ^{14}C ages, and this is the only genus in our study to yield ^{14}C results that consistently approach the detection limit of the method. Many of the paired *Astarte* results constrain the interpretation of either AAR or ^{14}C data in other cores, often confirming that some ^{14}C ages of other mollusk samples are incorrect, as those apparently younger samples are stratigraphically older than the *Astarte* samples. The inherent “geochemical robustness” of *Astarte* deserves further study, as this species may prove to be a preferential target for future ^{14}C dating of Pleistocene materials.

6.3. Regional aminozones and age assignments

Within the study area, four broadly defined aminozones are recognized, corresponding to the Holocene, late, middle, and early Pleistocene. The aminozones are numbered according to the genus in which they are identified and assigned ages based on correlations between taxa and/or local geochronologic control. Each of these aminozones is recognized at numerous individual sites, and each of them is also recognized in stratigraphic superposition at one or more sites, affirming the consistency of the AAR results. The late Pleistocene aminozone (M2-S2-Mu2) is observed at almost all sampling locations (offshore, onshore, beach, and sub-barrier) and is associated with the nearly continuous Q2 unit on the inner shelf. This unit likely acts as the source of both sediment and Pleistocene shells found on the modern beaches. ^{14}C ages for Q2 shells range from ~ 30 ka to >52 ka, but AAR results indicate that these must all be minimum ages. Although the sampling strategies for the beach samples have been rather biased, we find an abundance of Pleistocene shells on beaches from North Parramore to Smith Island, likely reflecting the presence of a Pleistocene ridge (former barrier-island or regressive coastal deposits) underlying these barriers. In particular, Pleistocene *Mercenaria* and *Spisula* are found in relatively high abundance near modern tidal inlets (e.g., Wachapreague and Metompkin inlets) which can erode into underlying Pleistocene deposits, or along the highly dynamic southern Virginia barrier islands (Wreck, Smith). Further north, this remnant Pleistocene high has probably been eroded on the shoreface as the barrier islands of the Chincoteague Bight migrated landward, resulting in a dearth of Pleistocene shells on these beaches. Only an integrated study of shelf, beach, and even onshore samples would recognize the geographic variability of the processes involved in barrier island evolution. Ideally, a systematic sampling effort of multiple taxa on all the islands at a single time (or pre- and post-storm) would enhance our insights into the spatial distribution of the sources of the Pleistocene beach shells. Although logistically challenging and requiring hundreds of AAR analyses, such a study would be a significant and unique contribution to the understanding of shoreface sediment dynamics. The utility of the AAR method derives from its ability to obtain large numbers of analyses, either from individual sites or from mappable stratigraphic units, thereby helping to identify diagenetic and taphonomic factors that likely affect all geochemical dating methods.

The middle Pleistocene aminozone (M3 and Mu3) is not represented by a large number of sites, and further study would likely result in subdividing this zone into multiple ages (e.g., the superposed section at Stetson Pit, NC). M3 results are recognized in onshore sites on the west shore of Chesapeake Bay and also in probable reworked samples from the Chincoteague Bight, an area of complexly cut and filled seismic sequences indicating multiple episodes of erosion and potential reworking. Aminozones Mu2 and Mu3 are found in superposition in two

Maryland shelf cores, representing units Q2 and Q1, respectively, and confirming the original observations of Toscano et al. (1989), Toscano (1992), and Toscano and York (1992). The relation of these Mu3 units to the Exmore paleochannel and the seismic stratigraphic framework of Brothers et al. (2020), combined with AAR age modeling, confirms a mid-Pleistocene (MIS 12 or older) age for the formation of the Exmore paleochannel. The AAR age estimate for the stratigraphically younger Eastville paleochannel is enigmatic but definitely consistent with the relative ages of the Exmore-Eastville paleochannel pair. The MIS 12 and MIS 6 age estimates support the model (Colman et al., 1990) that the Delmarva Peninsula had significant episodes of southward advance during major interglacials MIS 11 and MIS 5, respectively. These age estimates for the Exmore and Eastville are substantially greater than the MIS 6 and MIS 5b ages proposed by Scott et al. (2010) based on OSL geochronology. Where this sequence is recognized on the inner shelf (Brothers et al., 2020), in the subsurface of the southern Delmarva Peninsula and the central-northern Chesapeake Bay (Colman and Mixon, 1988), AAR results are consistent with local stratigraphic relations. AAR age modeling indicates that aminozone M4 represents an early Pleistocene (≥ 800 ka) age; this aminozone is younger than the Persimmon Point paleochannel based on local age and elevation information. Collectively, the AAR results imply that the Delmarva paleochannel system developed over at least the past ~ 1000 ka. Although the numerical ages derived from AAR results have significant uncertainties because of inherent modeling assumptions, the proposed ages and the regional AAR dataset are stratigraphically consistent and form a hypothesis for testing with additional chronologic tools (Brothers et al., 2020). The duration of the Delmarva record is similar to that seen in other long Quaternary coastal records, such as the nearby Albemarle Embayment (Culver et al., 2008; 2011; 2016), the Coorong Coastal Plain of Australia (Blakemore et al., 2015; Murray-Wallace, 2018), and the Wanganui Basin, New Zealand (Bowen et al., 1998).

6.4. Broader implications for regional sea-level history

The combined ^{14}C -AAR chronology for onshore, offshore, and beach samples and their host units presented here provides insights into late Pleistocene relative sea-level changes along the US mid-Atlantic coast. This history has important implications for models of isostatic adjustment and global ice volume during the interval between the last interglacial and the present. The geochronology of this time interval is challenging because it is generally at or beyond the limit of ^{14}C and the resolving power of AAR is limited by the inherent vulnerability of the method to geochemical and thermal factors. The AAR data, constrained by limiting ^{14}C and U-series ages, define the regionally extensive “Q2” aminozone, with onshore and offshore equivalents, that is dominated by “late last interglacial” (MIS 5a) samples, with some older samples reworked into the Q2 unit. While the existence of this aminozone does not negate the possibility of younger (MIS 3) deposits in the region, we expect to have encountered evidence of these younger units in the large AAR dataset presented here. Without the paired ^{14}C -AAR approach, results from either of these methods could be misleading or otherwise rejected without supporting evidence, so it is important that future investigations of MIS 3 ice-volume/sea-level histories include this combined approach if at all possible. The presence of this widespread last interglacial unit over a broad latitude and elevation range needs to be incorporated into current models of glacial-isostatic adjustment in response late Pleistocene ice volume and relative sea-level change.

Author statement

J. F. Wehmiller: Conceptualization, methodology, validation, formal analysis, investigation, data curation, writing- original draft; writing – review and editing, visualization, funding; L.L. Brothers: Conceptualization, methodology, validation, formal analysis, investigation, writing – review; and editing, visualization; K. W. Ramsey: Conceptualization,

methodology, formal analysis, resources, data curation, writing – review and editing, visualization, supervision, project administration, funding acquisition; D. S. Foster: Formal analysis, investigation; C. R. Mattheus: Investigation, resources, data curation, visualization; C. J. Hein: Resources, writing-review and editing; J.L. Shawler: Resources, writing-review and editing.

Declaration of competing interest

The authors declare that they have no known competing financial interests or personal relationships that could have appeared to influence the work reported in this paper.

Acknowledgments

This project has built upon early work by Daniel Belknap, June Mirecki, Linda York and Brian Boutin, whose graduate research at the University of Delaware in the 1970's and 1980's formed the basis for many of the more recent investigations reported here. Later work by Linda York and Marguerite Toscano established a stratigraphic framework for the mid-Atlantic shelf and an important collection of samples, many of which were used in the early phases of this study. Additionally, Linda York's 1991 "discovery" of Pleistocene shells on Parramore Island became the catalyst for subsequent studies of age mixing on Atlantic coast beaches. We thank Robert Thieler (US Geological Survey [USGS]) and colleagues for shell collections made on Smith, Wreck, and Metompkin Islands, and for other logistical support; Art Trembanis (Univ. of Delaware) for shell collections from Cedar and Metompkin Islands; the Cheriton East core samples were provided by Thomas Cronin (USGS), who along with Robert Poirier (USGS) provided samples of the Eyreville Core. Peter Parham (East Carolina Univ.) assisted with the collection of the East Lake (North Carolina) samples. Katherine Whitacre, Jordan Bright, and Darrell Kaufman (Northern Arizona University) provided all the RP analyses reported here. William Thompson, Woods Hole Oceanographic Institution, provided the U-series results for East Lake Pit. The support of Leslie Skibinski and Greg Dietl, Paleontological Research Institution (Ithaca, NY) and the NOSAMS Facility (Woods Hole MA) is also acknowledged. Thomas Cronin and Daniel Muhs (both USGS) reviewed an earlier draft of the manuscript; Steven Colman and Colin Murray-Wallace provided critical and very helpful reviews of the journal submission. Helpful discussions with David Krantz and Darrin Lowery are also acknowledged.

This project was funded through a cooperative agreement with the Bureau of Ocean Energy Management of the U.S. Department of the Interior, Offshore Sand Resources for Coastal Resilience and Restoration Planning: M14AC00003 and M16AC00001. We thank J. Waldner (BOEM) for support and encouragement during this project. We also thank S. Howard and K. Luciano, South Carolina Geological Survey, and numerous colleagues in both the Mid-Atlantic and Southeast Atlantic BOEM ASAP projects, active from 2015 through 2019. This paper is contribution #3999 of the Virginia Institute of Marine Science, William & Mary. Partial support was also provided to Hein by the Mid-Atlantic Sea Grant program (NOAA) award numbers R/71856G and R/71856H and a Virginia Sea Grant (NOAA) Fellowship award NA18OAR4170083 supported Shawler. JFW acknowledges support from the University of Delaware Retired Faculty Research Program.

We dedicate this paper to the memory of David Q. Bowen, an inspiring leader in the field of Quaternary science and advocate for the importance of land-sea correlations. In 1988 DQ joined a group from the University of Delaware for a tour of the Delmarva-Chesapeake region; not surprisingly, the trip was filled with lively discussion and thoughtful questions.

Any use of trade, firm or product names is for descriptive purposes only and does not imply endorsement by the U.S. Government.

Appendices A, B, C, D, E, F, and G. Supplementary data

Supplementary data to this article can be found online at <https://doi.org/10.1016/j.quageo.2021.101177>.

References

- Belknap, D.F., 1979. Application of Amino Acid Geochronology to Stratigraphy of Late Cenozoic Marine Units of the Atlantic Coastal Plain [Ph.D. Thesis]. Newark, University of Delaware, p. 348.
- Belknap, D.F., Wehmiller, J.F., 1980. Amino acid racemization in Quaternary mollusks: examples from Delaware, Maryland, and Virginia. In: Hare, P.E., Hoering, T.C., King Jr., K. (Eds.), *Biogeochemistry of Amino Acids*. John Wiley, New York, pp. 401–414.
- Bowen, D.Q., Pillans, B., Sykes, G.A., Beu, A.G., Edwards, A.R., Kamp, P.J.J., Hull, A.G., 1998. Amino acid geochronology of Pleistocene marine sediments in the Wanganui Basin: a New Zealand framework for correlation and dating. *J. Geol. Soc.* 155, 439–446.
- Blakemore, A.G., Murray-Wallace, C.V., Westaway, K.E., Lachlan, T.J., 2015. Aminostratigraphy and sea-level history of the Pleistocene Bridgewater formation, mount Gambier region, southern Australia. *Aust. J. Earth Sci.* 62, 151–169.
- Boyajian, A.G., Thayer, C.W., 1995. Clam calamity: a recent supratidal storm-deposit as an analog for fossil shell beds. *Palaos* 10, 484–489.
- Bronk Ramsey, C., 2009. Bayesian analysis of radiocarbon dates. *Radiocarbon* 51, 337–360. <https://doi.org/10.1017/S0033822200033865>.
- Brothers, L.L., Foster, D.S., Pendleton, E.A., Baldwin, Wayne E., 2020. Seismic stratigraphic framework of the continental shelf offshore Delmarva, U.S.A.: Implications for Mid-Atlantic Bight evolution since the Pliocene. *Mar. Geol.* 428, 106287.
- Browning, J.V., Miller, K.G., McLaughlin Jr., P.P., Edwards, L.E., Kulpecz, A.A., Powars, D.S., Wade, B.S., Feigenson, M.D., Wright, J.D., 2009. Integrated sequence stratigraphy of the postimpact sediments from the Eyreville core holes, Chesapeake Bay impact structure inner basin. In: Gohn, G.S., Koerber, C., Miller, K.G., Reimold, W.U. (Eds.), *The ICDP-USGS Deep Drilling Project in the Chesapeake Bay Impact Structure: Results from the Eyreville Core Holes*, vol. 458. Geological Society of America Special Paper, pp. 775–810. [https://doi.org/10.1130/2009.2458\(33\)](https://doi.org/10.1130/2009.2458(33)).
- Bureau of Ocean Energy Management Atlantic Sand Assessment: <https://www.boem.gov/marine-minerals/atlantic-sand-assessment-project-asap>, <https://www.boem.gov/marine-minerals/building-national-offshore-sand-inventory>.
- Busschers, F.S., Wesselingh, F.P., Kars, R.H., Verluisj-Helder, M., Wallinga, J., Bosch, J. H.A., Timmer, J., Nierop, K.G.J., Meijer, T., Bunnik, F.P.M., De Wolf, H., 2014. Radiocarbon dating of late Pleistocene marine shells from the southern North Sea. *Radiocarbon* 56 (3), 1151–1166.
- Byrnes, M.R., 1988. Holocene Geology and Migration of a Low-Profile Barrier Island System, Metompkin Island, Virginia. Doctor of Philosophy (PhD), Dissertation. Ocean/Earth/Atmos Sciences, Old Dominion University. <https://doi.org/10.25777/qh0t-n783>. https://digitalcommons.odu.edu/ocean_etds/113.
- Chen, Z.-Q., Hobbs III, C.H., Wehmiller, J.F., Kimball, S.M., 1995. Late Quaternary Paleochannel Systems on the Continental Shelf, South of the Chesapeake Bay entrance. *J. Coast Res.* 11, 605–614.
- Cheng, H., Edwards, R.L., Shen, C.-C., Polyak, V.J., Asmerom, Y., Woodhead, J., Hellstrom, J., Wang, Y., Kong, X., Spötl, C., Wang, X., Alexander, E.C., 2013. Improvements in ^{230}Th and ^{234}U half-life values, and U–Th isotopic measurements by multi-collector inductively coupled plasma mass spectrometry. *Earth Planet Sci. Lett.* 371–372, 82–91.
- Clarke, S.J., Murray-Wallace, C.V., 2006. Mathematical expressions used in amino acid racemization geochronology—A review. *Quat. Geochronol.* 1, 261–278.
- Colman, S.M., Mixon, R.B., 1988. The record of major Quaternary sea-level changes in a large Coastal Plain estuary, Chesapeake Bay, eastern United States. *Palaogeography, Palaeoclimatology, Palaeoecology* 68, 99–116.
- Colman, S.M., Halka, J.P., 1989. Map Showing Quaternary Geology of the Southern Maryland Part of the Chesapeake Bay. U. S. Geological Survey Miscellaneous Field Studies Map MF-1948-C.
- Colman, S.M., Mixon, R.B., Ruben, M., Bloom, A.L., Johnson, G.H., 1989. Comment on "Late Pleistocene barrier island sequence along the southern Delmarva Peninsula: Implications for middle Wisconsin sea levels. *Geology* 17, 84–85.
- Colman, S.M., Halka, J.P., Hobbs III, C.H., Mixon, R.B., Foster, D.S., 1990. Ancient channels of the Susquehanna River beneath Chesapeake Bay and the Delmarva Peninsula. *Geol. Soc. Am. Bull.* 102, 1268–1279.
- Creveling, J.R., Mitrovica, J.X., Clark, P.U., Waelbroeck, C., 2017. Predicted bounds on peak global mean sea level during marine isotope stages 5a and 5c. *Quat. Sci. Rev.* 163, 193–208.
- Cronin, Thomas, Szabo, Barney, Ager, Thomas, Hazel, Joseph, Owens, James, et al., 1981. Quaternary climates and sea levels of the U. S. Atlantic Coastal Plain. *Science* 211, 233–240.
- Culver, S.J., Farrell, K.M., Mallinson, D.J., Horton, B.P., Willard, D.A., Thieler, E.R., Riggs, S.R., Snyder, S.W., Wehmiller, J.F., Bernhardt, C.E., Hillier, C., 2008. Micropaleontologic record of late Pliocene and quaternary paleoenvironments in the northern Albemarle Embayment, North Carolina, U.S.A. *Palaogeogr. Palaeoclimatol. Palaeoecol.* 264, 54–77.
- Culver, S.J., Farrell, K.M., Mallinson, D.J., Willard, D.A., Horton, B.P., Riggs, S.R., Thieler, E.R., Wehmiller, J.F., Parham, P., Snyder, S.W., Hillier, C., 2011. Micropaleontologic record of quaternary paleoenvironments in the central

- Albemarle Embayment, North Carolina, U.S.A. *Palaeogeogr. Palaeoclimatol. Palaeoecol.* 305, 227–249.
- Culver, S.J., Farrell, K.M., Mallinson, D.J., Willard, D.A., Horton, B.P., Riggs, S.R., Thieler, E.R., Wehmiller, J.F., Parham, P., Moore, J.P., Snyder, S.W., Hillier, C., 2016. Micropaleontologic record of Pliocene and Quaternary paleoenvironments in the southern Albemarle Embayment, North Carolina, U.S.A. *Palaeogeogr. Palaeoclimatol. Palaeoecol.* 457, 360–379.
- Darby, D.A., 1983. Sedimentology, diagenesis, and stratigraphy of Pleistocene coastal deposits in southeastern Virginia. Fifteenth Annual Virginia Geologic Field Conference.
- Darby, D.A., Evans Jr., A.E., 1992. Provenance of Quaternary beach deposits, Virginia and North Carolina. In: Wehmiller, J.F., Fletcher, C.H. (Eds.), *Quaternary Coasts of the United States: Lacustrine and Marine Systems*, Society of Economic Paleontologists and Mineralogists, vol. 48. Special Publication, pp. 113–119.
- Davies, D.J., Powell, E.N., Stanton Jr., R.J., 1989. Taphonomic signature as a function of environmental process: shells and shell beds in a hurricane-influenced inlet on the Texas coast. *Palaeogeogr. Palaeoclimatol. Palaeoecol.* 72, 317–356.
- Deaton, C.D., Hein, C.J., Kirwan, M.L., 2017. Barrier island migration dominates ecogeomorphic feedbacks and drives salt marsh loss along the Virginia Atlantic Coast, USA. *Geology* 45, 123–126.
- DeJong, B.D., Bierman, P.R., Newell, W.L., Rittenour, T.M., Mahan, S.A., Balco, G., Road, D.H., 2015. Pleistocene relative sea levels in the Chesapeake Bay region and their implications for the next century. *GSA Today (Geol. Soc. Am.)* 25, 4–9.
- Dunbar, J.B., Wakeley, L.D., Miller, S.P., Swartzel, S.M., 2001. Geology without borders: A conceptual model for Aberdeen Proving Ground. In: Ehlen, J., Harmon, R.S. (Eds.), *The Environmental Legacy of Military Operations*: Boulder, Colorado, vol. 14. Geological Society of America Reviews in Engineering Geology, pp. 191–202.
- Fenster, M.S., Dolan, R., Jones Smith, J., 2016. Grain-size distributions and coastal morphodynamics along the southern Maryland and Virginia barrier islands. *Sedimentology* 63, 809–823.
- Finkelstein, K., 1992. Stratigraphy and preservation potential of sediments from adjacent Holocene and Pleistocene barrier-island systems, Cape Charles Virginia. In: Wehmiller, J.F., Fletcher, C.H. (Eds.), *Quaternary Coasts of the United States: Lacustrine and Marine Systems*, vol. 48. Society of Economic Paleontologists and Mineralogists Special Publication, pp. 129–140.
- Finkelstein, K., Ferland, M.A., 1987. Back-barrier response to sea-level rise, Eastern Shore of Virginia. In: Nummedal, D., Pilkey, O.H., Howard, J. (Eds.), *Sea-Level Fluctuations and Coastal Evolution*. SEPM (Society for Sedimentary Geology), pp. 145–155. <https://doi.org/10.2110/pec.87.41.0145>.
- Finkelstein, Kenneth, Kearney, Michael, 1988. Late Pleistocene barrier-island sequence along the southern Delmarva Peninsula: Implications for middle Wisconsin sea levels. *Geology* 16, 41–45.
- Finkelstein, Kenneth, Kearney, Michael, 1989. Reply to comments “Late Pleistocene barrier island sequence along the southern Delmarva Peninsula: Implications for middle Wisconsin sea levels”. *Geology* 17, 86–88.
- French, H.M., Demitroff, M., Strelitskiy, D., Forman, S.L., Gozdzik, J., Konishchev, V.N., Rogov, V.V., Lebedeva-Verba, M.P., 2009. Evidence for Late-Pleistocene permafrost in the Pine Barrens, southern New Jersey. *Earth's Cryosphere* 3, 17–28.
- Frey, R.W., Dorjes, J., 1988. Fair- and foul-weather shell accumulations on a Georgia Beach. *Palaios* 3, 561–576.
- Genau, R.B., Madsen, J.A., McGeary, S., Wehmiller, J.F., 1994. Seismic reflection identification of Susquehanna River paleochannels on the mid-Atlantic coastal plain. *Quaternary Research* 42, 166–175.
- Groot, J.J., Ramsey, K.W., Wehmiller, J.F., 1990. Ages of the Bethany, Beverdam, and Omar Formations of southern Delaware. Delaware Geological Survey Report of Investigations 47, 1–19.
- Heaton, T.J., Köhler, P., Butzin, M., Bard, E., Riemer, R.W., Austin, W.E.N., Bronk Ramsey, C., Grootes, P.M., Hughen, K.A., Kromer, B., Reimer, P.J., Adkins, J., Burke, A., Cook, M.S., Olsen, J., Skinner, L.C., 2020. Marine 20 – The marine radiocarbon age calibration curve (0–55,000 CALBP). *Radiocarbon* 62 (4), 779–820. <https://doi.org/10.1017/RDC.2020.68>.
- Hobbs III, C.H., 2004. Geological history of Chesapeake Bay, USA. *Quat. Sci. Rev.* 23, 641–661.
- Hughes, W.B., 1991. Application of marine seismic profiling to a ground water contamination study, Aberdeen Proving Ground, Maryland. *Ground Water Monit. Remed.* 11, 97–102.
- Jacobs, J.M., 1980. Stratigraphy and Lithology of Quaternary Landforms on the Eastern Coast of the Chesapeake Bay. MS Thesis. University of Delaware, Newark DE USA, pp. 1–84.
- Kaufman, D.S., 2006. Temperature sensitivity of aspartic and glutamic acid racemization in the foraminifera *Pulleniatina*. *Quat. Geochronol.* 1, 188–207.
- Kaufman, D.S., Manley, W.F., 1998. A new procedure for determining DL amino acid ratios in fossils using reverse phase liquid chromatography. *Quat. Sci. Rev.* 17, 987–1000.
- Kidwell, S.M., Best, M.M.R., Kaufman, D.S., 2005. Taphonomic trade-offs in tropical marine death assemblages: Differential time-averaging, shell loss, and probable bias in siliciclastic vs. carbonate facies. *Geology* 33, 729–732.
- Kowalewski, M., Goodfriend, G.A., Flessa, K.W., 1998. The high-resolution estimates of temporal mixing in shell beds: the evils and virtues of time-averaging. *Paleobiology* 24, 287–304.
- Kowalewski, M., Avila Serrano, G.E., Flessa, K.W., Goodfriend, G.A., 2000. Dead delta's former productivity: Two trillion shells at the mouth of the Colorado River. *Geology* 28, 1059–1062.
- Kowalewski, M., Casebolt, S., Hua, Q., Whitacre, K.E., Kaufman, D.S., Kosnik, M.A., 2018. One fossil record, multiple time resolutions: Disparate time-averaging of echinoids and mollusks on a Holocene carbonate platform. *Geology* 46, 51–54.
- Krantz, D.E., Hobbs III, C.H., Wikel, G.L., 2016. Atlantic Coast and Inner Shelf. In: Bailey, C.M., Sherwood, W.C., Eaton, L.S., Powars, D.S. (Eds.), *Geology of Virginia: Martinsville, Virginia*, Virginia Museum of Natural History, pp. 341–380.
- Lamothe, M., Wehmiller, J.F., Noller, J.S., 1998. Comparison of Approaches to Dating Atlantic Coastal Plain Sediments. Virginia Beach, vol. A. <http://udspace.udel.edu/handle/19716/13228>.
- Leatherman, S.P., Rice, T.E., Goldsmith, V., 1982. Virginia Barrier Island Configuration: A Reappraisal. *Science* 215, 285–287.
- Leupke, G., 1990. Economic Heavy Minerals in Sediments from an Offshore Area East of Cape Charles, Virginia, pp. 1–10. U. S. Geological Survey Open File Report 90-451.
- Litwin, R.J., Smoot, J.P., Pavich, M.J., Markewich, H.W., Brook, G., Durika, N.J., 2013. 100,000-year-long terrestrial record of millennial-scale linkage between eastern North American mid-latitude paleovegetation shifts and Greenland ice-core oxygen isotope trends. *Quaternary Research* 80, 291–315.
- Mallinson, D., Burdette, K., Mahan, S., Brook, G., 2008. Optically stimulated luminescence age controls on late Pleistocene and Holocene coastal lithosomes, North Carolina, USA. *Quaternary Research* 69, 97–109.
- Mallinson, D.J., Culver, S.J., Riggs, S.R., Thieler, E.R., Foster, D., Wehmiller, J., Farrell, K.M., Pierson, J., 2010. Regional seismic stratigraphy and controls on the Quaternary evolution of the Cape Hatteras region of the Atlantic passive margin, USA. *Mar. Geol.* 268, 16–33.
- Mangerud, J., Kaufman, D., Hansen, J., Svendsen, J.I., 2008. Ice-free conditions in Novaya Zemlya 35,000–30,000 cal years B. P. as indicated by radiocarbon ages and amino acid racemization evidence from marine molluscs. *Polar Res.* 27, 187–208.
- Martin, R.E., Wehmiller, J.F., Harris, M.S., Liddell, W.D., 1996. Comparative taphonomy of bivalves and foraminifera from Holocene tidal flat sediments, Bahia la Choya, Sonora, Mexico (Northern Gulf of California): Taphonomic Grades and Temporal Resolution. *Paleobiology* 22, 80–90.
- Mattheus, C.R., Ramsey, K.W., Tomlinson, J.L., 2020a. Geologic Map of Offshore Delaware: Delaware Geological Survey Geologic Map Series No. 25 scale 1:40,000.
- Mattheus, C.R., Ramsey, K.W., Tomlinson, J.L., 2020b. The evolution of coastal-plain incised valleys over multiple glacio-eustatic cycles: Insights from the inner continental shelf of Delaware, U.S.A. *J. Sediment. Res.* 90 (11), 1510–1526. <https://doi.org/10.2110/jsr.2020.69>.
- McBride, R.A., Fenster, M.S., Seminack, C.T., Richardson, T.M., Sepanik, J.M., Hanley, J. T., Bundick, J.A., Tedder, E., 2015. Holocene barrier-island geology and morphodynamics of the Maryland and Virginia open-ocean coasts: Fenwick, Assateague, Chincoteague, Wallops, Cedar, and Paramore Islands. In: Brezinski, D.K., Halka, J.P., Ott Jr., R.A. (Eds.), *Tripping from the Fall Line: Field Excursions for the GSA Annual Meeting*, Baltimore 2015, pp. 309–423.
- McFarland, E.R., Beach, T.A., 2019. Hydrogeologic framework of the Virginia Eastern Shore: U.S. Geological Survey Scientific Investigations Report 2019–5093 13. <https://doi.org/10.3133/sir20195093>, 26.
- McLaughlin, P.P., Miller, K.G., Browning, J.V., Ramsey, K.W., Benson, R.N., Tomlinson, J.L., Sugarman, P.J., 2008. Stratigraphy and Correlation of the Oligocene to Pleistocene Section at Bethany Beach, Delaware. *Delaware Geol. Surv. Rep. Invest.* 75, 1–47.
- Miller, G.H., Andrews, J.T., 2019. Hudson Bay was not deglaciated during MIS-3. *Quat. Sci. Rev.* 225, 105944.
- Miller, G.H., Magee, J.W., Jull, A.J.T., 1997. Low-latitude glacial cooling in the Southern Hemisphere from amino-acid racemization in emu eggshells. *Nature* 35, 241–244.
- Miller, G.H., Magee, J.W., Johnson, B.J., Fogel, M.L., Spooner, N.A., McCulloch, M.T., Ayliffe, L.K., 1999. Pleistocene extinction of *Genyornis newtoni*: human impact on Australian megafauna. *Science* 283, 205–208.
- Miller, K.G., Sugarman, P.J., Browning, J.V., Sheridan, R.E., Kulhanek, D.K., Monteverde, D.H., Wehmiller, J.F., Lombardi, C., Feigenson, M.D., 2013a. Pleistocene sequence stratigraphy of the shallow continental shelf, offshore New Jersey: Constraints of Integrated Ocean Drilling Program Leg 313 core holes. *Geosphere* 9, 74–95.
- Miller, G.H., Kaufman, D.S., Clarke, S.J., 2013b. Amino acid dating. In: Elias, S.A., Mock, C.J. (Eds.), *Encyclopedia of Quaternary Science*, second ed. Elsevier, Waltham, MA, pp. 37–48.
- Mirecki, J.E., Wehmiller, J.F., Skinner, A., 1995. Geochronology of Quaternary coastal units, southeastern Virginia. *J. Coast Res.* 11, 1135–1144.
- Mixon, R.B., 1985. Stratigraphic and Geomorphic Framework of Uppermost Cenozoic Deposits in the Southern Delmarva Peninsula, Virginia and Maryland. *U.S. Geological Survey Professional Paper 1067-G*, p. 53. <https://pubs.er.usgs.gov/publication/pp1067G>.
- Mixon, R.B., Szabo, B.J., Owens, J.P., 1982. Uranium-series Dating of Mollusks and Corals, and Age of Pleistocene Deposits, Chesapeake Bay Area, Virginia and Maryland. U. S. Geological Survey Professional Paper 1067-E, p. 18. <https://pubs.usgs.gov/pp/1067e/report.pdf>.
- Mixon, R.B., Berquist Jr., C.R., Newell, W.L., Johnson, G.H., Powars, D.S., Schindler, J.S., Rader, E.K., 1989. Geologic Map and Generalized Cross Sections of the Coastal Plain and Adjacent Parts of the Piedmont. U. S. Geological Survey Miscellaneous Investigations series, Virginia. Map I-2033.
- Muhs, D.R., Simmons, K.R., Schumann, R.R., Groves, L.T., DeVogel, S.B., Minor, S.A., Laurel, D., 2014. Coastal tectonics on the eastern margin of the Pacific Rim: late Quaternary sea-level history and uplift rates, Channel Islands National Park, California, USA. *Quat. Sci. Rev.* 105, 209–238.
- Muhs, D.R., Pigati, J.S., Schumann, R.R., Skipp, G.L., Porat, N., DeVogel, S.B., 2018. Quaternary sea-level history and the origin of the northernmost coastal aeolianites in the Americas: Channel Islands National Park, California, USA. *Palaeogeogr. Palaeoclimatol. Palaeoecol.* 491, 38–76.

- Murray-Wallace, C.V., Ferland, M.A., Roy, P.S., Sollar, A., 1996. Unravelling patterns of reworking in lowstand shelf deposits using amino acid racemization and radiocarbon dating. *Quat. Sci. Rev.* 15, 685–697.
- Murray-Wallace, C.V., 2018. Quaternary History of the Coorong Coastal Plain, Southern Australia: an Archive of Environmental and Global Sea-Level Changes. Springer, Cham, p. 229.
- Nadeau, M.-J., Grootes, P.M., Voelker, A., Bruhn, F., Duhr, A., Oriwall, A., 2001. Carbonate ^{14}C background: does it have multiple personalities? *Radiocarbon* 43, 169–176.
- Nicholas, W.A., Chivas, A.R., Murray-Wallace, C.V., Fink, D., 2011. Prompt transgression and gradual salinization of the Black Sea during the early Holocene constrained by amino acid racemization and radiocarbon dating. *Quat. Sci. Rev.* 20, 3769–3790.
- Oertel, G.F., Foyle, A.M., 1995. Drainage Displacement by Sea-Level Fluctuation at the Outer Margin of the Chesapeake Seaway. *J. Coast Res.* 11, 583–604.
- Oertel, G.F., Kearney, M.S., Leatherman, S.P., Woo, H.-J., 1989. Anatomy of a barrier platform: outer barrier lagoon, southern Delmarva Peninsula, Virginia. *Mar. Geol.* 88, 303–318.
- Oertel, G.F., Allen, T.R., Foyle, A.M., 2008. The influence of drainage hierarchy on pathways of barrier retreat: an example from Chincoteague Bight, Virginia USA. *SE. Geol.* 45, 179–201.
- Olszewski, T.D., Kaufman, D.S., 2015. Tracing burial history and sediment recycling in a shallow estuarine setting (Copano Bay, Texas) using postmortem ages of the bivalve *Mulinia lateralis*. *Palaios* 30, 224–237.
- O'Neal, M.L., Wehmiller, J.F., Newell, W.L., 2000. Amino acid geochronology of Quaternary coastal terraces on the northern margin of Delaware Bay, southern New Jersey, USA. In: Goodfriend, G.A., Collins, M.J., Fogel, M.L., Macko, S.A., Wehmiller, J.F. (Eds.), *Perspectives in Amino Acid and Protein Geochemistry*. Oxford University Press, Oxford, pp. 301–319.
- Owens, J.P., Denny, C.S., 1978. *Geologic Map of Worcester County Maryland*. Maryland Geological Survey, Baltimore. <https://jscholarship.library.jhu.edu/handle/1774.2/34631>.
- Parham, P.R., Riggs, S.R., Culver, S.J., Mallinson, D.J., Rink, W.J., Burdette, K., 2013. Quaternary coastal lithofacies, sequence development and stratigraphy in a passive margin setting, North Carolina and Virginia, USA. *Sedimentology* 60, 503–547.
- Pendleton, E.A., Ackerman, S.D., Baldwin, W.E., Danforth, W.W., Foster, D.S., Thieler, E. R., Brothers, L.L., 2015. High-resolution Geophysical Data Collected along the Delmarva Peninsula, 2014, USGS Field Activity 2014-002-FA (Ver. 3.0, December 2015). U.S. Geological Survey data release. <https://doi.org/10.5066/F5067MW5062F5060>. Available online:
- Pico, T., Creveling, J.R., Mitrovica, J.X., 2017. Sea level records from the U. S. mid-Atlantic constrain Laurentide ice sheet extent during marine isotope stage 3. *Nat. Commun.* 8, 15612. <https://doi.org/10.1038/ncomms15612>.
- Pigati, J.S., Quade, J., Wilson, J., Jull, A.J.T., Lifton, N.A., 2007. Development of low-background vacuum extraction and graphitization system for ^{14}C dating of old (40–60 ka) samples. *Quat. Int.* 166, 4–14.
- Potter, E.-K., Lambeck, K., 2004. Reconciliation of sea-level observations in the Western North Atlantic during the last glacial cycle. *Earth Planet Sci. Lett.* 217, 171–181.
- Powars, D.S., 2011. Middle and late Pleistocene geology of the Eastern Shore of Virginia and relationship to the Chesapeake Bay impact structure with impact debris core display. In: 41st Virginia Geological Field Conference, Wachapreague, Virginia, October 29–30, 2011, pp. 15–35.
- Powars, D.S., Bruce, T.S., 1999. The Effects of the Chesapeake Bay Impact Crater on the Geological Framework and Correlation of Hydrogeologic Units of the Lower York-James Peninsula. U.S. Geological Survey Professional Paper, Virginia, p. 82, 1612.
- Powell, E.N., Logan, A., Stanton Jr., R.J., Davies, D.J., Hare, P.E., 1989. Estimating time-since-death from the free amino acid content of the mollusk shell: a measure of time averaging in modern death assemblages? Description of the technique. *Palaios* 4, 16–31.
- PSDS: Program for the Study of Developed Shorelines. <http://beachnourishment.wcu.edu/>.
- Raff, J.L., Shawler, J.L., Ciarletta, D.J., Hein, E.A., Lorenzo-Trueba, J., Hein, C.J., 2018. Insights into barrier-island stability derived from transgressive/regressive state changes of Parramore Island, Virginia. *Mar. Geol.* 403, 1–19. <https://doi.org/10.1016/j.margeo.2018.04.007>.
- Ramsey, K.W., 2010. Stratigraphy, correlation, and depositional environments of the Middle to Late Pleistocene interglacial deposits of southern Delaware. Delaware Geological Survey Report of Investigations 76, 1–43.
- Ramsey, K.W., 2011. Geologic Map of the Fairmount and Rehoboth Beach Quadrangles. Delaware: Delaware Geological Survey Geologic Map Series No. 16 scale 1:24,000.
- Ramsey, K.W., Tomlinson, J.L., 2012. Geologic Map of the Bethany Beach and Assawoman Bay Quadrangles. Delaware: Delaware Geological Survey Geologic Map Series No. 18 scale 1:24,000.
- Reusser, L.J., Bierman, P.R., Pavich, M.J., Zen, E.-an, Larsen, J., Finkel, R., 2004. Rapid late Pleistocene incision of Atlantic passive margin river gorges. *Science* 305, 499–502.
- Riggs, S.R., York, L.L., Wehmiller, J.F., Snyder, S.W., 1992. Depositional patterns resulting from high-frequency Quaternary sea-level fluctuations in northeastern North Carolina. In: Fletcher III, C.H., Wehmiller, J.F. (Eds.), *Quaternary Coasts of the United States: Marine and Lacustrine Systems*, vol. 48. Society of Economic Paleontologists and Mineralogists Special Publication, pp. 155–160.
- Rojas, A., Martínez, S., 2016. Marine isotope stage 3 (MIS3) versus Marine isotope stage 5 (MIS5) fossiliferous marine deposits from Uruguay. In: Gasparini, G.M., et al. (Eds.), *Marine Isotope Stage 3 in Southern South America, 60 Ka B.P. – 30 Ka B.P.* Springer Earth System Sciences. https://doi.org/10.1007/978-3-319-40000-6_14.
- Rojas, A., Martínez, S., 2020. The Fossil, the Dead, the Living: Beach Death Assemblages and Molluscan Biogeography of the Uruguayan Coast. In: Martínez, S., Rojas, A., Cabrera, F. (Eds.), *Actualistic Taphonomy in South America, Topics in Geobiology*, vol. 48. Springer, Cham. https://doi.org/10.1007/978-3-030-20625-3_2.
- Ryan, D.D., Lachlan, T.J., Murray-Wallace, C.V., Price, D.M., 2020. The utility of single foraminifera amino acid racemization analysis for the relative dating of Quaternary beach barriers and identification of reworked sediment. *Quat. Geochronol.* 60, 101103.
- Scott, T.W., Swift, D.J.P., Whittecar, G.R., Brook, G.A., 2010. Glacioisostatic influences on Virginia's late Pleistocene coastal plain deposits. *Geomorphology* 116, 175–188.
- Shawler, J.L., Ciarletta, D.J., Lorenzo-Trueba, J., Hein, C.J., 2019. Drowned foredune ridges as evidence of pre-historic barrier-island state changes. In: *Coastal Sediments '19, Proceedings of the 12th International Symposium on Coastal Engineering and Science of Coastal Sediment Processes*.
- Shawler, J.L., Ciarletta, D.J., Connell, J.E., Boggs, B.Q., Lorenzo-Trueba, J., Hein, C.J., 2020. Relative influence of antecedent topography and sea-level rise on barrier-island migration. *Sedimentology*. <https://doi.org/10.1111/sed.12798>.
- Sheridan, R.E., Ashley, G.M., Miller, K.G., Waldner, J.S., Hall, D.W., Uptegrove, J., 2000. Offshore-onshore correlation of upper Pleistocene strata, New Jersey coastal plain to continental shelf and slope. *Sediment. Geol.* 134, 197–207.
- Simonson, A.E., Lockwood, R., Wehmiller, J.F., 2013. Three approaches to radiocarbon calibration of amino acid racemization in *Mulinia lateralis* from the Holocene of the Chesapeake Bay, USA. *Quat. Geochronol.* 16, 62–72.
- Sweeney, E.M., Pendleton, E.A., Ackerman, S.D., Andrews, B.D., Baldwin, W.E., Danforth, W.W., Foster, D.S., Thieler, E.R., Brothers, L.L., 2015. High-resolution Geophysical Data Collected along the Delmarva Peninsula 2015, U.S. Geological Survey Field Activity 2015-001-FA (Ver. 3.0, May 2016). U.S. Geological Survey data release p. <https://doi.org/10.5066/F5067P5055KK5063>. Available online:
- Szabo, B.J., 1985. Uranium-series dating of fossil corals from marine sediments of southeastern United States Atlantic Coastal Plain. *Geol. Soc. Am. Bull.* 96, 398–406.
- Thompson, W.G., Spiegelman, M.W., Goldstein, S.L., Speed, R.C., 2003. An open-system model for U-series age determinations of fossil corals. *Earth Planet Sci. Lett.* 210, 365–381.
- Tomiač, P.J., Penkman, K.E.H., Hendy, E.J., Demarchi, B., Murrells, S., Davis, S.A., McCullagh, P., Collins, M.J., 2013. Testing the limitations of artificial protein degradation kinetics using known-age massive *Porites* coral skeletons. *Quat. Geochronol.* 16, 87–109.
- Toscano, M.A., 1989. Comment on "Late Pleistocene barrier island sequence along the southern Delmarva Peninsula: Implications for middle Wisconsin sea levels. *Geology* 17, 85–86.
- Toscano, M.A., 1992. Record of Oxygen Isotope Stage 5 on the Maryland inner shelf Atlantic Coastal Plain – A post-transgressive highstand regime. In: Wehmiller, J.F., Fletcher, C.H. (Eds.), *Quaternary Coasts of the United States: Lacustrine and Marine Systems*, vol. 48. Society of Economic Paleontologists and Mineralogists Special Publication, pp. 89–99.
- Toscano, M.A., York, L.L., 1992. Quaternary stratigraphy and sea-level history of the U. S. middle Atlantic coastal plain. *Quat. Sci. Rev.* 11, 301–328.
- Toscano, M.A., Kerhin, R.T., York, L.L., Cronin, T.M., Williams, S.J., 1989. Quaternary Stratigraphy of the Inner Continental Shelf of Maryland, vol. 50. Maryland Geological Survey Report of Investigations No., p. 116
- Uptegrove, J., Waldner, J.S., Stanford, S.D., Monteverde, D.H., Sheridan, R.E., Hall, D. W., 2012. *Geology of the New Jersey Offshore in the Vicinity of Barnegat Inlet and Long Beach Island*. New Jersey Geological and Water Survey Geologic Map Series GMS 12-3. <https://www.nj.gov/dep/njgs/pricelst/gms/gms12-3.pdf>.
- Wehmiller, J.F., 1977. Amino acid studies of the Del Mar, California midden site: apparent rate constants, ground temperature models, and chronological implications. *Earth Planet Sci. Lett.* 37, 184–196.
- Wehmiller, J.F., 1982. A review of amino acid racemization studies in Quaternary mollusks: stratigraphic and chronologic applications in coastal and interglacial sites, Pacific and Atlantic coasts, United States, United Kingdom, Baffin Island, and Tropical Islands. *Quat. Sci. Rev.* 1, 83–120.
- Wehmiller, J.F., 1984. Interlaboratory comparison of amino acid enantiomeric ratios in fossil Pleistocene mollusks. *Quaternary Research* 22, 109–120.
- Wehmiller, J.F., 2013a. United States Quaternary coastal sequences and molluscan racemization geochronology - what have they meant for each other for the past 45 years? *Quat. Geochronol.* 16, 3–20.
- Wehmiller, J.F., 2013b. Interlaboratory comparison of amino acid enantiomeric ratios in Pleistocene fossils. *Quat. Geochronol.* 16, 173–182.
- Wehmiller, J.F., Miller, G.H., 2000. Aminostratigraphic dating methods in Quaternary geology. In: Noller, J.S., Sowers, J.M., Lettis, W.R. (Eds.), *Quaternary Geochronology, Methods and Applications*, vol. 4. American Geophysical Union Reference Shelf, pp. 187–222.
- Wehmiller, J.F., Pellerito, V., 2015. An evolving database for Quaternary aminostratigraphy. *GeoResJ* 6, 115–123. <http://www.sciencedirect.com/science/article/pii/S2214242815000170>.
- Wehmiller, J.F., Belknap, D.F., Boutin, B.S., Mirecki, J.E., Rahaim, S.D., York, L.L., 1988. A review of the aminostratigraphy of Quaternary mollusks from United States Atlantic Coastal Plain sites. In: Easterbrook, D.L. (Ed.), *Dating Quaternary Sediments*, vol. 227. Geological Society of America Special Paper, pp. 69–110.
- Wehmiller, J.F., York, L.L., Bart, M.L., 1995. Amino acid racemization geochronology of reworked Quaternary mollusks on US Atlantic coast beaches: Implications for chronostratigraphy, taphonomy, and coastal sediment transport. *Mar. Geol.* 124, 303–337.
- Wehmiller, J.F., Stecher III, H.A., York, L.L., Friedman, I., 2000. The thermal environment of fossils: effective ground temperatures (1994-1998) at aminostratigraphic sites, U.S. Atlantic coastal plain. In: Goodfriend, G.A., Collins, M. J., Fogel, M.L., Macko, S.A., Wehmiller, J.F. (Eds.), *Perspectives on Amino Acid and Protein Geochemistry*, pp. 219–250 (Oxford).

- Wehmiller, J.F., Simmons, K.R., Cheng, H., Edwards, R.L., Martin-McNaughton, J., York, L.L., Krantz, D.E., Shen, C.-C., 2004. Uranium-series coral ages from the US Atlantic Coastal Plain: the "80 ka problem" revisited. *Quat. Int.* 120, 3–14.
- Wehmiller, J.F., Thieler, E.R., Miller, D., Pellerito, V., Bakeman Keeney, V., Riggs, S.R., Culver, S., Mallinson, D., Farrell, K.M., York, L.L., Pierson, J., Parham, P.R., 2010. Aminostratigraphy of surface and subsurface Quaternary sediments, North Carolina coastal plain, USA. *Quat. Geochronol.* 5, 459–492. <https://doi.org/10.1016/j.quageo.2009.10.005>.
- Wehmiller, J.F., Harris, W.B., Boutin, B.S., Farrell, K.M.F., 2012. Calibration of amino acid racemization (AAR) kinetics in United States mid-Atlantic Coastal Plain Quaternary mollusks using $^{87}\text{Sr}/^{86}\text{Sr}$ analyses: Evaluation of kinetic models and estimation of regional Late Pleistocene temperature history. *Quat. Geochronol.* 7, 21–36.
- Wehmiller, J.F., York, L.L., Pellerito, V., Thieler, E.R., 2015. Racemization-inferred Age Distribution of Mollusks in the US Atlantic Margin Coastal System. Geological Society of America Annual Meeting, Baltimore. Available at: <https://gsa.confex.com/gsa/2015AM/webprogram/Paper263915.html>.
- Wehmiller, J.F., Brothers, L., Foster, D.S., Ramsey, K.W., 2019a. Southern Delmarva barrier island beaches: linking offshore and onshore units using racemization geochronology to infer sediment sources during shoreline migration. In: Paper 13-5, Geological Society of America, SE Sectional Meeting, Charleston SC. <https://gsa.confex.com/gsa/2019SE/webprogram/Paper326646.html>.
- Wehmiller, J.F., Ramsey, K.W., Howard, S., Mattheus, C.R., Harris, M.S., Luciano, K., 2019b. New Perspectives on US Atlantic Coastal Plain Aminostratigraphy Gleaned from Extensive Analyses of Shell Specimens from Inner Continental Shelf Vibracores. Geological Society of America, SE Sectional Meeting, Charleston SC. Paper 39-1. <https://gsa.confex.com/gsa/2019SE/webprogram/Paper326300.html>.
- Westaway, R., 2009. Calibration of decomposition of serine to alanine in *Bithynia* opercula as a quantitative dating technique for Middle and Late Pleistocene sites in Britain. *Quat. Geochronol.* 4, 241–259.
- Williams, C.P., 1999. Late Pleistocene and Holocene Stratigraphy of the Delaware Inner Continental Shelf. MS Thesis. University of Delaware, Newark, p. 175.
- York, L.L., 1990. Aminostratigraphy of U. S. Atlantic Coast Pleistocene Deposits: Maryland Continental Shelf and North and South Carolina Coastal Plain. Ph D thesis. Univ. of Delaware, Newark, p. 580.
- York, L.L., Wehmiller, J.F., Cronin, T.M., Ager, T.A., 1989. Stetson Pit, Dare County, North Carolina: an integrated chronologic, faunal, and floral record of subsurface coastal Quaternary sediments. *Palaeogeogr. Palaeoclimatol. Palaeoecol.* 72, 115–132.